IN-1340
NASA CR–72577
November 1969

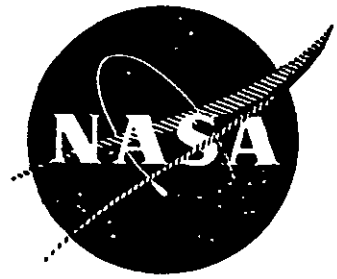

CAVITY REACTOR CRITICAL EXPERIMENT
VOLUME V
(Complete Co-Axial Flow Mockup)

Get DRA

G. D. Pincock and P. L. Chase

Prepared for
NATIONAL AERONAUTICS AND SPACE ADMINISTRATION
Contract C-67747-A

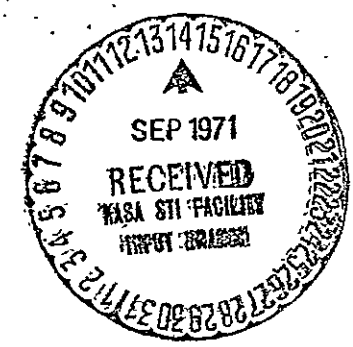

IDAHO NUCLEAR CORPORATION
National Reactor Testing Station
Idaho Falls, Idaho

PRINTED IN USA

IN-1340
NASA CR-72577
Issued: November 1969
Limited Distribution

CAVITY REACTOR CRITICAL EXPERIMENT
VOLUME V
(Complete Co-Axial Flow Mockup)

BY

G. D. Pincock and P. L. Chase

Prepared for

NATIONAL AERONAUTICS AND SPACE ADMINISTRATION

Contract C-67747-A

Technical Management
NASA-Lewis Research Center
Cleveland, Ohio

Nuclear Systems Division
Robert E. Hyland, Project Manager

Space Nuclear Propulsion Office
Capt. C. E. Franklin, USAF

IDAHO NUCLEAR CORPORATION
A Jointly Owned Subsidiary of
AEROJET GENERAL CORPORATION
ALLIED CHEMICAL CORPORATION
PHILLIPS PETROLEUM COMPANY

U. S. Atomic Energy Commission Research and Development Report
Issued Under Contract AT(10-1)-1230
Idaho Operations Office

ABSTRACT

The previous experiments of the cylindrical (coaxial flow) cavity reactor concept were aimed principally at studying specific parameters, i.e.,

Critical masses (Volume 1 report)

Adequacy of foil fuel mockup vs a gas core (Volume 2)

Effects of cavity liner materials, hydrogen, fuel in the reflector and core fuel shape (Volume 3)

Waves and control methods (Volume 4)

This volume, Number 5, studies a complete mockup of a system containing most of the above engineering design considerations.

Approved: J. F. Kunze

J. F. Kunze, Branch Manager
Operations & Analysis

TABLE OF CONTENTS

TABLE OF CONTENTS
(Continued)

TABLES

FIGURES

FIGURES
(Cont'd)

FIGURES
(Cont'd)

1.0 SUMMARY

A detailed mockup of the coaxial flowing gas cavity reactor was performed with the critical experiment assembly. The hydrogen coolant was simulated with polystyrene (CH) and polyethylene (CH_2) and thin solid sheets of uranium were used to mockup the gaseous fuel. The fuel and hydrogen varied both radially and axially to mockup the calculated distribution of these materials in a hot, operating system. The cavity wall was lined with stainless steel, 0.04 meanfree absorption paths thick, to simulate the cavity containment vessel and there was an annulus of fuel containing 823 grams of U^{235} in the radial reflector.

The critical mass in the core was 44.9 kg of uranium, with the exhaust nozzle tank filled with D_2O plugging the exhaust hole of the reactor. The core average fuel worth was $0.250 \pm 0.017\%\Delta k/kg$. The worth of polyethylene was measured within the active core and coolant regions and it was found that this material had a positive worth out to a radius of about 35 cm from the core center in the heavily loaded core regions and then became negative from there to the cavity wall. Near the exhaust nozzle end of the core where the fuel density was the lowest, the hydrogenous material was of negative worth throughout the core and propellant regions. Therefore, the expected mixing of coolant and fuel near the active core boundary in the operating cavity reactor system will have a negative effect on reactivity if the active core boundary remains constant. On the other hand, any expansion of the fuel is a positive reactivity effect (References 1 and 4).

The exhaust nozzle tank was removed and measured to be worth $0.456\%\Delta k$ which represents about 1.8 kg of uranium in the cavity. The exhaust nozzle tank had an appreciable effect in the reflector regions. Its removal reduced the thermal neutron flux in the reflector per unit reactor power by about 17%. The core region flux is affected to a lesser extent when removing the exhaust nozzle tank, since the total reactor power production was conserved.

2.0 INTRODUCTION

Although previous critical experiments attempted to mockup to some extent a flowing gas reactor (Reference 2, Section 8.0) a detailed mockup was not made of a cylindrical shaped, coaxial-flow cavity reactor. It was the purpose of this experiment to simulate, as closely as possible, the complex configuration including mixing of fuel and hydrogen in the outer regions of the active core and varying the fuel and hydrogen densities both radially and axially. The earlier measurements were made with a beryllium heat shield in the radial reflector; however, this experiment contained uranium in the reflector to reduce the core critical mass. There was not a beryllium heat shield in the reflector. Thus, the effect was a substantial reduction in the total fuel loading for the cavity region compared to the earlier configuration.

3.0 DESCRIPTION OF REACTOR

The changes required for this mockup experiment were all within the cavity region as compared to Configuration 9 discussed in Reference 1, Section 12.0. The annulus of MTR type fuel plates was left in the radial reflector. This annulus contained 823.2 grams of U^{235} and was positioned

19 cm from the wet surface of the cavity wall as shown in Reference 1, Section 3. The stainless steel liner was also left on the cavity wall and ends of the cavity. This liner was 0.0965 cm thick and weighed 83 kg.

The core support structure was removed from the reactor and modified back to the original configuration (Reference 3, Section 7) that was used prior to the wave experiments. After the modification was completed, the assembly weighed 53.41 kg including the bolts used to hold the assembly in place in the reactor. This compares with 53.75 kg as reported in Reference 3, p. 138.

Hydrogen was placed in the reactor in the form of polyethylene (CH_2) and foamed polystyrene (CH). The same material was used for this experiment as was used for the variable hydrogen reactor reported in Reference 2, Section 8. Figure 3.1 shows the layout of the initial core configuration and Figure 3.2 specifies the relative fuel and hydrogen densities desired for the mockup. Subsequent discussion will show what changes were required in order to produce a critical reactor. Pre-analysis of the initially planned configuration significantly over predicted the multiplication factor. These changes will be described in detail as the initial loading is discussed.

The foamed polystyrene formed the base support structure for the hydrogenous material across the gap between the active core and cavity wall. The polystyrene was cut into a "swiss cheese" configuration so as to give the desired hydrogen density over Region 3. The higher densities for Regions 1, 2, and 4 were achieved by adding sheets of polyethylene and dispersing it uniformally over the hydrogen region. The material masses for these regions are given in Table 3.1.

The predicted total core uranium loading was 40 kg. The fuel was distributed through the several zones according to Table 3.2 so as to give the desired concentrations. The individual fuel elements were loaded according to Figures 3.3 to 3.6. The location of the various fuel elements in each of the fuel zones is specified in Figure 3.7.

In addition to the amount of aluminum in the core support structure mentioned earlier, there were 216 fuel elements weighing 110.4 kg, 208 lids weighing 6.16 kg and 4640 fuel spacers weighing 16.05 kg. All of this material was type 1100 aluminum. The support structure was also this same type aluminum except for 15.15 kg of type 6061 aluminum in a support ring at the back end of the cavity where the structure bolted to the reactor tank.

All other reactor components were the same as has been used on other cavity reactor experiments described in References 1 to 4.

TABLE 3.1

Hydrogen Concentrations in Complete Mockup of Flowing Gas Power Reactor

Region	CH_2 (gm)	CH (gm)	Region Volume (cm^3)	Hydrogen atoms	Hydrogen Density (atoms/cm^3)	Required Density (atoms/cm^3)
1	13038	3725	4.326×10^5	1.292×10^{27}	2.987×10^{21}	3.0×10^{21}
2	1942	4282	4.882×10^5	3.649×10^{26}	0.747×10^{21}	0.75×10^{21}
3	0	3168	3.761×10^5	1.465×10^{26}	0.390×10^{21}	0.40×10^{21}
4	440	3725	4.326×10^5	2.101×10^{26}	0.486×10^{21}	0.50×10^{21}
5	0	352	1.628×10^5	1.628×10^{25}	0.100×10^{21}	0.10×10^{21}
6	0	856	2.646×10^5	3.959×10^{25}	0.150×10^{21}	0.15×10^{21}
Zone						
2A	30.5	0	2.646×10^5	2.619×10^{24}	0.099×10^{20}	0.100×10^{20}
3 & 3A	33.1	0	1.900×10^5	2.842×10^{24}	0.150×10^{20}	0.150×10^{20}
4	14.5	0	0.543×10^5	1.245×10^{24}	0.229×10^{20}	0.230×10^{20}
4A	7.9	0	0.339×10^5	0.678×10^{24}	0.200×10^{20}	0.200×10^{20}

TABLE 3.2

Core Loading from the Estimated 40 kg Critical Mass

Zone	Fuel Fraction	Relative Fuel Density	Fuel Mass (kg)	Number Elements	Fuel Density g/cm^3	Number of Fuel Sheets
1	0.477	1.000	19.07	208	0.0541	7278
2, 2A	0.358	0.752	14.34	208	0.0406	5475
3	0.056	0.465	2.22	52	0.0252	849
3A	0.077	0.561	3.09	60	0.0304	1180
4	0.018	0.245	0.72	52	0.0133	274
4A	0.014	0.305	0.56	40	0.0165	212
	1.000		40.00			15268

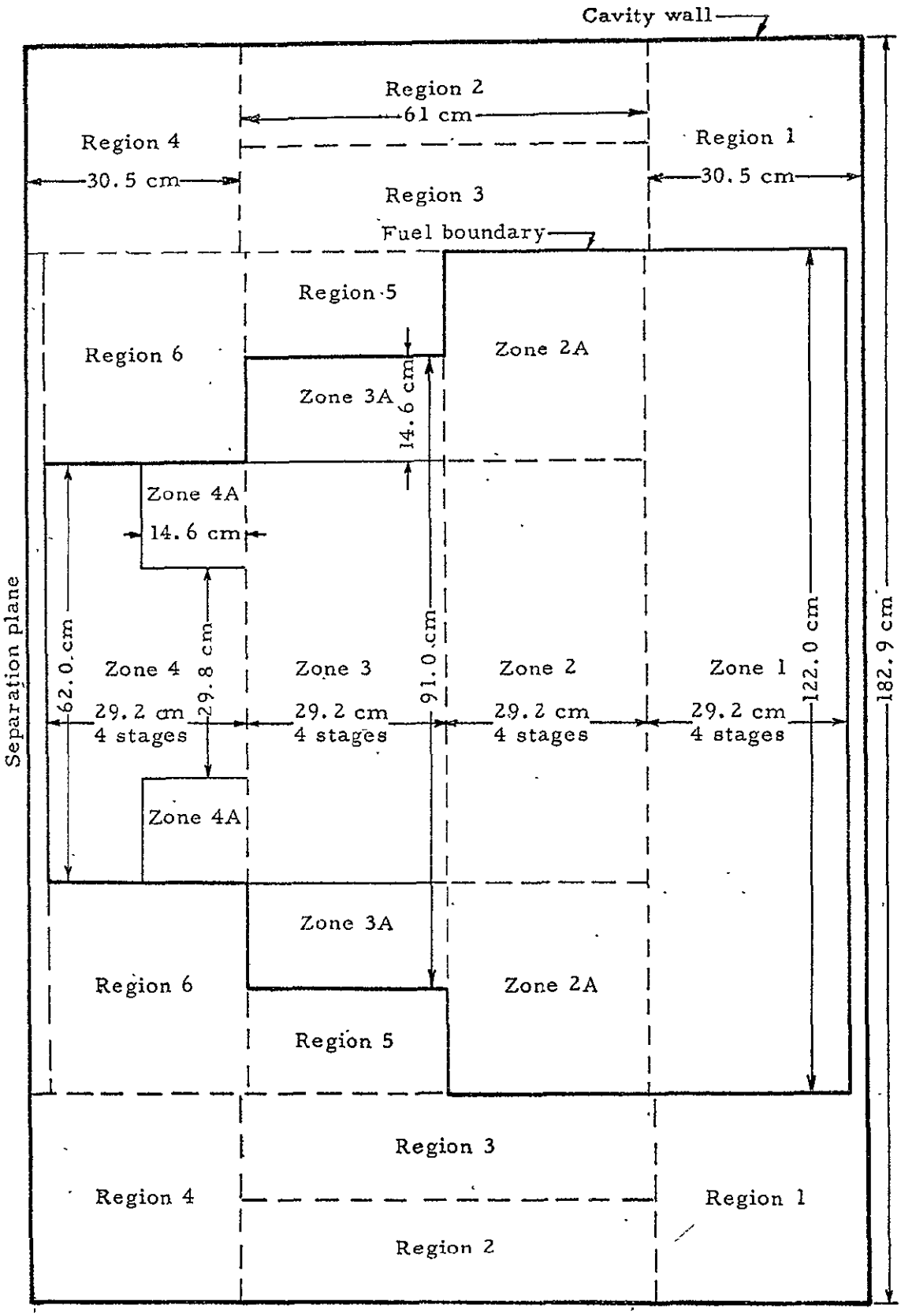

Fig. 3.1 Cavity region layout for variable hydrogen, variable fuel density core

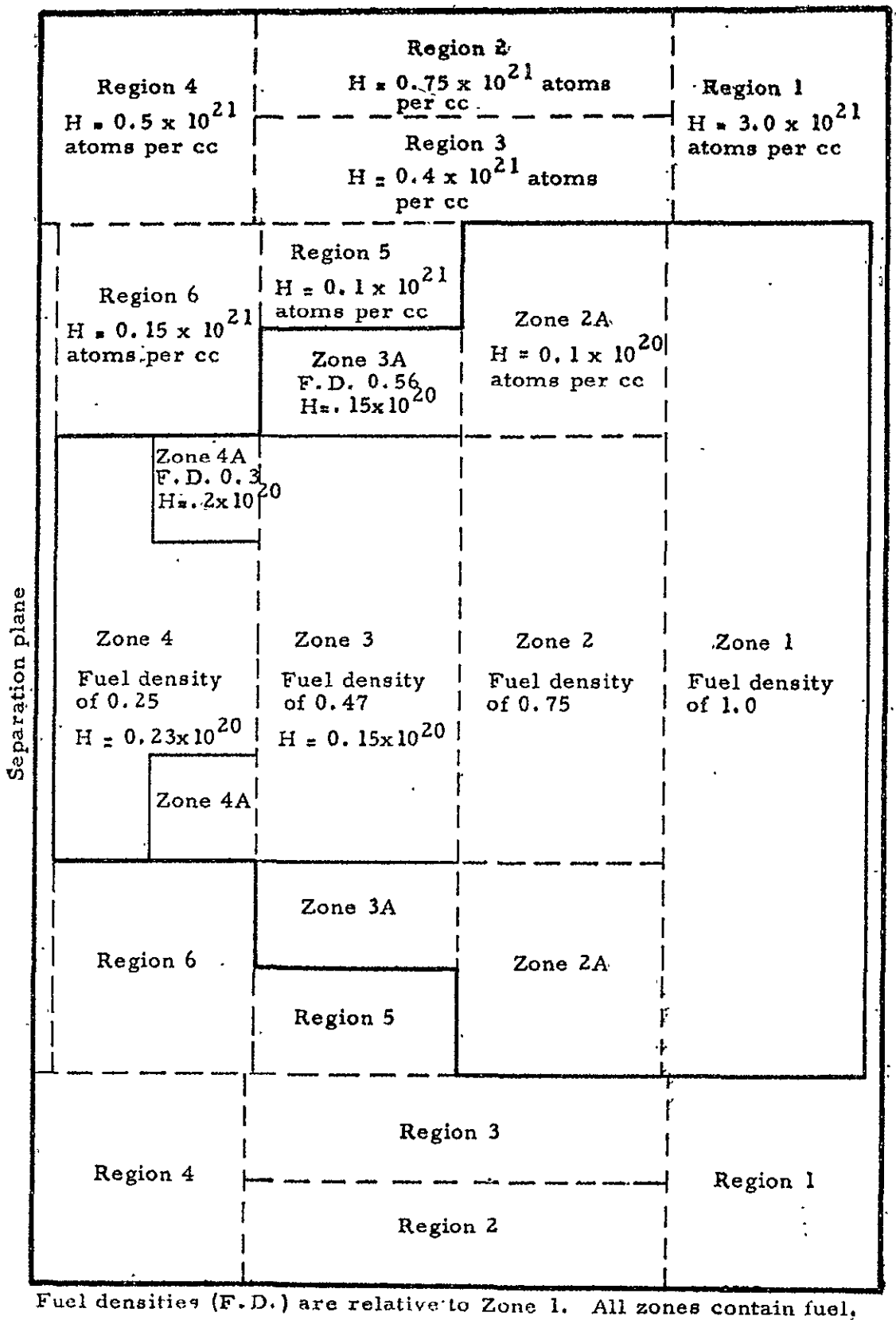

Fig. 3.2 Hydrogen and fuel density specifications for the variable hydrogen variable fuel density core.

TYPE 1 Fuel Element

1	2	3	4	5	6	7	8	9	10	11	12	13	14	15	16	Stage number
1	2	3	1	2	3	1	2	3	1	2	3	1	2	3	1	Fuel orientation
9	9	9	9	7	7	7	7	0	0	0	0	0	0	0	0	Number of fuel sheets per stage

TYPE 2 Fuel Element

1	2	3	4	5	6	7	8	9	10	11	12	13	14	15	16	Stage number
2	3	1	2	3	1	2	3	1	2	3	1	2	3	1	2	Fuel orientation
9	9	9	9	7	7	7	6	0	0	0	0	0	0	0	0	Number of fuel sheets per stage

TYPE 3 Fuel Element

1	2	3	4	5	6	7	8	9	10	11	12	13	14	15	16	Stage number
3	1	2	3	1	2	3	1	2	3	1	2	3	1	2	3	Fuel orientation
8	8	8	9	6	6	6	6	0	0	0	0	0	0	0	0	Number of fuel sheets per stage

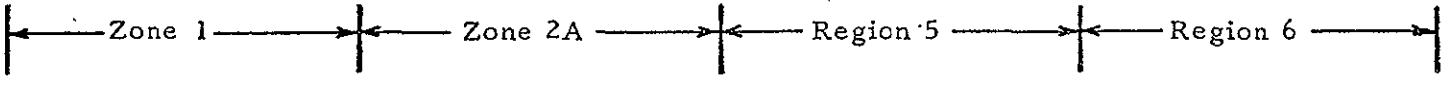

The following number and types of fuel elements will be required of the above loading:

Zones	Type 1	Type 2	Type 3	Totals
1, 2A	32	32	32	96

Fig. 3.3 Fuel element loading recipe over Zones 1 and 2A in outer core radius

TYPE 1 fuel element

1	2	3	4	5	6	7	8	9	10	11	12	13	14	15	16	Stage number
1	2	3	1	2	3	1	2	3	1	2	3	1	2	3	1	Fuel orientation
9	9	9	9	7	7	7	7	5	5	5	5	0	0	0	0	Number of fuel sheets per stage

TYPE 2 fuel element

1	2	3	4	5	6	7	8	9	10	11	12	13	14	15	16	Stage number
2	3	1	2	3	1	2	3	1	2	3	1	2	3	1	2	Fuel orientation
9	9	9	9	7	7	7	6	4	5	5	5	0	0	0	0	Number of fuel sheets per stage

TYPE 3 fuel element

1	2	3	4	5	6	7	8	9	10	11	12	13	14	15	16	Stage number
3	1	2	3	1	2	3	1	2	3	1	2	3	1	2	3	Fuel orientation
8	8	8	9	6	6	6	6	5	5	5	5	0	0	0	0	Number of fuel sheets per stage

Zone 1 — Zone 2A — Zone 3A — Region 6

The following number and types of fuel elements will be required of the above loading:

Zones	Type 1	Type 2	Type 3	Totals
1, 2A, 3A	20	20	20	60

Fig. 3.4 Fuel element loading recipe for Zones 1, 2A, and 3A

TYPE 1 fuel element

1	2	3	4	5	6	7	8	9	10	11	12	13	14	15	16	Stage number
1	2	3	1	2	3	1	2	3	1	2	3	1	2	3	1	Fuel orientation
9	9	9	9	7	7	7	7	5	4	4	4	3	3	2	2	Number of fuel sheets per stage

TYPE 2 fuel element

1	2	3	4	5	6	7	8	9	10	11	12	13	14	15	16	Stage number
2	3	1	2	3	1	2	3	1	2	3	1	2	3	1	2	Fuel orientation
9	9	9	9	7	7	7	6	4	4	4	4	3	3	2	2	Number of fuel sheets per stage

TYPE 3 fuel element

1	2	3	4	5	6	7	8	9	10	11	12	13	14	15	16	Stage number
3	1	2	3	1	2	3	1	2	3	1	2	3	1	2	3	Fuel orientation
8	8	8	9	6	6	6	6	4	4	4	4	2	2	3	2	Number of fuel sheets per stage

The following number and types of fuel elements will be required of the above loading:

Zones	Type 1	Type 2	Type 3	Totals
1, 2, 3, 4A, 4	13	13	14	40

Fig. 3.5 Fuel element loading recipe for Zones 1, 2, 3, 4A and 4

TYPE 1 fuel element

1	2	3	4	5	6	7	8	9	10	11	12	13	14	15	16
1	2	3	1	2	3	1	2	3	1	2	3	1	2	3	1
9	9	9	9	7	7	7	7	5	4	4	4	2	2	2	2

Stage number
Fuel orientation
Number of fuel sheets per stage

TYPE 2 fuel element

1	2	3	4	5	6	7	8	9	10	11	12	13	14	15	16
2	3	1	2	3	1	2	3	1	2	3	1	2	3	1	2
9	9	9	9	7	7	7	6	4	4	4	4	2	2	2	2

Stage number
Fuel orientation
Number of fuel sheets per stage

TYPE 3 fuel element

1	2	3	4	5	6	7	8	9	10	11	12	13	14	15	16
3	1	2	3	1	2	3	1	2	3	1	2	3	1	2	3
8	8	8	9	6	6	6	6	4	4	4	4	2	2	3	2

Stage number
Fuel orientation
Number of fuel sheets per stage

Zone 1 — Zone 2 — Zone 3 — Zone 4

The following number and types of fuel elements will be required of the above loading:

Zones	Type 1	Type 2	Type 3	Totals
1, 2, 3, 4	4	4	4	12

Fig. 3.6 Fuel element loading recipe for Zones 1, 2, 3, and 4, the inner most radius

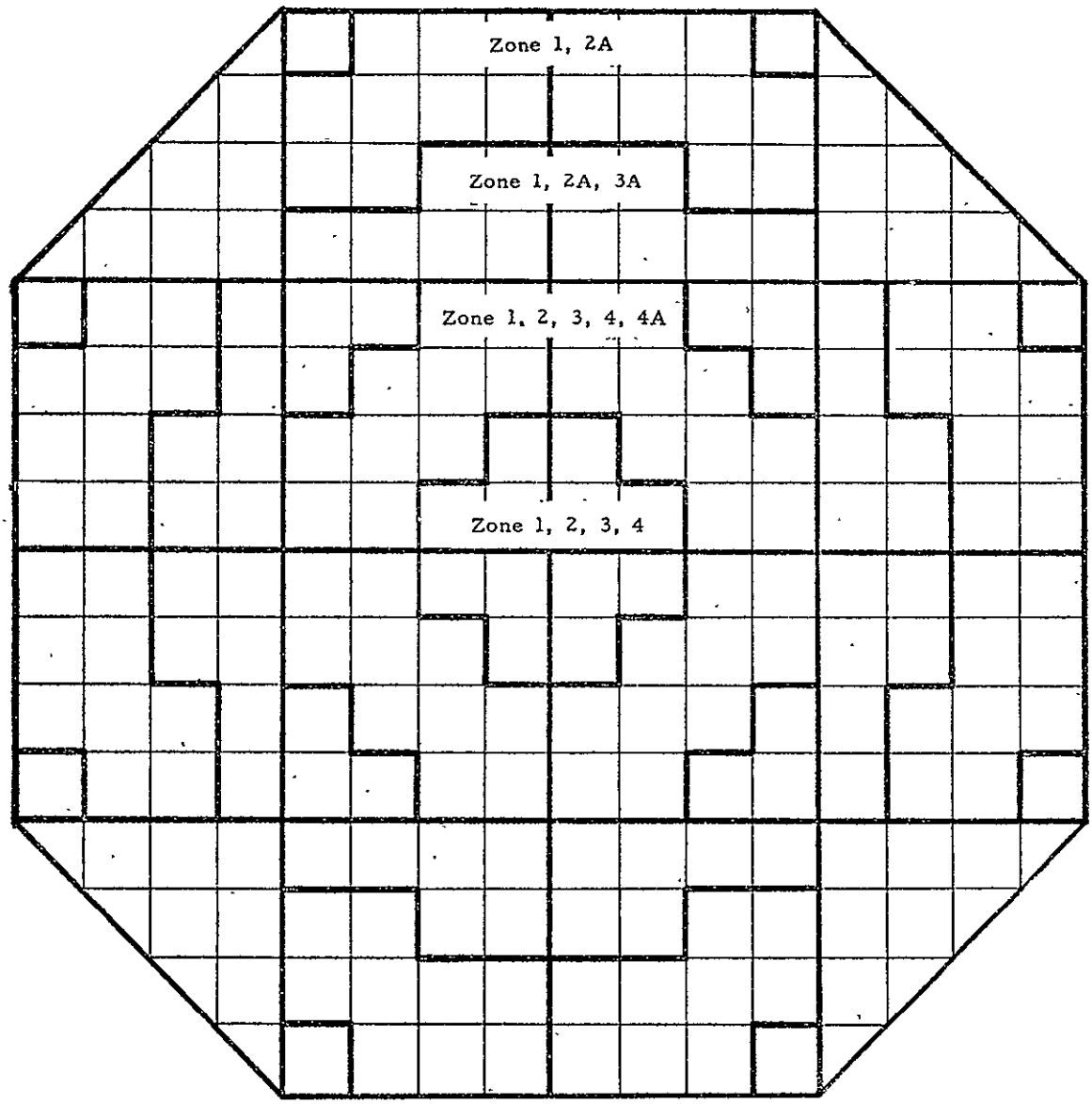

Fig. 3.7 Cross section view of core as separation plane showing the location of the fueled zones in the active core

4.0 TEST PROCEDURES

Control rod worths were measured by making rod "bumps." This required leveling the reactor on an infinite period with the actuators (if more than one was used) at an equally inserted position. The rods were then equally withdrawn to produce a reactor period. This period was measured and converted to reactivity from the standard inhour equation. One dollar was equal to 0.765%Δk. From previously measured rod worth curves given in Tables 4.1 and 4.2, the fraction of the total worth of the actuators (or actuator) was obtained. Each actuator contained three poison rods (boron carbide as described in Reference 4, Section 2). The control rods penetrated the end reflector opposite the separation plane and the actuators had both shim and scram functions. Exact location of the rods can be seen in Reference 1, Section 3.0. All k-excess, rod, and material worths are evaluated and reported in %Δk, with the delayed neutron fraction being 0.765%, (includes γ, n production in D_2O).

All power distribution measurements were made with catcher foils as described in Reference 4, p. 23. These foils were normally exposed in the cavity region only where the power was generated. Since there was an annulus of fuel in the radial reflector, some catcher foils were also exposed there to measure the fission power produced in the annulus. Where cadmium ratios were measured, the foils were covered with 0.0508 cm (0.020 inch) thick cadmium.

Flux measurements were made with bare and cadmium covered gold foils. The foils were nominally 0.000508 cm (0.0002 inch) thick and 1.429 cm in diameter. The gold foils were counted on a 256-channel gamma ray analyzer and the 0.41 Mev peak was converted to disintegrations per minute at reactor shutdown by using the constants given in Reference 4, p. 25. Where both bare and cadmium covered gold was available at the same points in the reactor, the data were reduced to cadmium ratios and thermal neutron flux from the equations given in Reference 4, p. 69 and Reference 3, p. 49, 50.

In order to specify locations in the reactor, a radial and an axial reference point was established. The axial point chosen was the inner or wet surface of the outer containment tank at the end of the reactor containing the control rods. This point was 90.1 cm from the inner surface of the cavity wall. The radial reference point was the radial center of the reactor. Unless otherwise specified, all foil positions will be given with respect to these two points.

TABLE 4.1

Actuator No. 6 - Tabular Rod Worth Curve

Ratiometer Reading

	0	100	200	300	400	500	600	700	800	900
0	100.00	100.00	97.15	94.30	91.45	88.63	85.80	82.98	80.16	77.38
1000	74.65	71.97	69.36	66.80	64.32	61.91	59.55	57.26	55.05	52.88
2000	50.76	48.71	46.72	44.79	42.92	41.11	39.36	37.66	36.02	34.43
3000	32.89	31.41	29.97	28.58	27.25	25.97	24.73	23.54	22.40	21.29
4000	20.23	19.22	18.24	17.31	16.41	15.56	14.74	13.96	13.21	12.51
5000	11.83	11.18	10.57	9.99	9.42	8.89	8.39	7.90	7.45	7.02
6000	6.62	6.24	5.87	5.52	5.19	4.88	4.58	4.29	4.03	3.78
7000	3.54	3.31	3.09	2.89	2.70	2.51	2.33	2.16	2.00	1.84
8000	1.69	1.55	1.42	1.29	1.17	1.05	.94	.83	.74	.64
9000	.56	.48	.40	.33	.26	.20	.14	.09	.04	0

Ratiometer Reading

	0	100	200	300	400	500	600	700	800	900
0	0	0	2.85	2.85	2.84	2.83	2.83	2.82	2.82	2.78
1000	2.73	2.68	2.61	2.56	2.48	2.41	2.36	2.29	2.21	2.17
2000	2.12	2.05	1.99	1.93	1.87	1.81	1.75	1.70	1.64	1.59
3000	1.54	1.48	1.44	1.39	1.33	1.28	1.24	1.19	1.14	1.11
4000	1.06	1.01	.98	.93	.90	.85	.82	.78	.75	.70
5000	.68	.65	.61	.58	.57	.53	.50	.49	.45	.43
6000	.40	.38	.37	.35	.33	.31	.30	.29	.26	.25
7000	.23	.23	.22	.20	.19	.19	.18	.17	.16	.16
8000	.15	.14	.13	.13	.12	.12	.11	.11	.09	.10
9000	.08	.08	.08	.07	.07	.06	.06	.05	.05	.04

TABLE 4.2

Tabular Rod Worth - 7 Actuators

Ratiometer Reading	0	100	200	300	400	500	600	700	800	900
0	100.00	100.00	96.54	93.16	89.86	86.64	83.50	80.43	77.74	74.52
1000	71.68	68.92	66.23	63.62	61.08	58.61	56.22	53.90	51.64	49.45
2000	47.34	45.29	43.30	41.38	39.52	37.72	35.99	34.32	32.71	31.16
3000	29.66	28.21	26.82	25.48	24.19	22.95	21.77	20.63	19.53	18.48
4000	17.48	16.52	15.60	14.72	13.88	13.08	12.32	11.59	10.89	10.23
5000	9.59	8.99	8.42	7.87	7.34	6.85	6.38	5.93	5.50	5.10
6000	4.72	4.35	4.01	3.68	3.38	3.08	2.81	2.55	2.30	2.08
7000	1.86	1.66	1.47	1.30	1.14	.99	.85	.73	.62	.52
8000	.43	.35	.28	.22	.18	.14	.11	.09	.08	.08

	0	100	200	300	400	500	600	700	800	900
0	0	0	3.46	3.38	3.30	3.22	3.14	3.07	2.99	2.92
1000	2.84	2.76	2.69	2.61	2.54	2.47	2.39	2.32	2.26	2.19
2000	2.11	2.05	1.99	1.92	1.86	1.80	1.73	1.67	1.61	1.55
3000	1.50	1.45	1.39	1.34	1.27	1.24	1.18	1.14	1.10	1.05
4000	1.00	.96	.92	.88	.84	.80	.76	.73	.70	.66
5000	.64	.60	.57	.55	.53	.49	.47	.45	.43	.40
6000	.38	.37	.34	.33	.30	.30	.27	.26	.25	.22
7000	.22	.20	.19	.17	.16	.15	.14	.12	.11	.10
8000	.09	.08	.07	.06	.04	.04	.03	.02	.01	.00

5.0 INITIAL LOADING

Initial loading of the mockup began on January 16, 1969. As each increment of fuel was added to the reactor, count rate data were taken both with the control rods fully inserted and fully withdrawn. Three counting channels were used and the results are given in Table 5.1. The average inverse multiplication from the three channels is shown in Figure 5.1. It will be noted that after nine increments the core was loaded with the expected critical mass of 40 kg but it was subcritical by an indicated 5%Δk. At this point, measurements were taken to determine the approximate worth of the polyethylene (CH_2), and polystyrene (CH) which occupied the space between the active core and the cavity wall. Based on the subcritical data corrected for the difference between indicated subcriticality and known rod worths (factor of 1.235), this sector of hydrogenous material (0.51 kg of hydrogen) was worth about -1.7%Δk which extrapolates to a total worth of the CH and CH_2 in this annulus of -11.5%Δk. An equivalent amount of hydrogen in the form of CH_2 was then placed only in the outer three inches next to the cavity but in the same axial and azimuthal region where the sector of CH and CH_2 had been removed. This material was worth about -0.9%Δk showing a factor of two in worth as was expected from previous measurements. There was nothing unusual about these results so it was concluded that the error in critical mass was due primarily to the lack of information on fuel worth in the variable fuel density core.

After consulting with the NASA representative, it was decided to place fuel in portions of Regions 5 and 6, thus extending Zones 3A and 4A. The extensions agreed upon are shown in Figure 5.2. The hydrogen density in the form of foamed polystyrene (CH) was maintained, at this point, at the levels specified for Regions 5 and 6. The fuel loading in Region 5 which is specified as Zone 3A extension was the same as for Zone 3A. Likewise, the fuel density in the extension of Zone 4A was the same as for Zone 4A. This fuel was added in several increments as shown in Table 5.1. In increment 14, 60 sheets of fuel (157.2 grams) were added to the reactor as shown in Figures 5.3 and 5.4. Actually five sheets of fuel were added to stage 9 in 12 fuel elements in the positions shown in the above figures for increment 14. The next step (increment 15) was to add five sheets of fuel per stage over three stages in 12 fuel elements as shown in Figures 5.3 and 5.4. A total of 180 sheets of fuel or 471.6 grams was placed in a 1/4 sector of the core. The inverse multiplication data showed a worth of about 0.79%Δk/kg for fuel in this region. Increment 16 was an addition of fuel in Region 6 over a 1/4 sector of the core. Increment 17 completed the addition of fuel in Region 6 which represented the extension to Zone 4A. A total of 225 sheets or 589.5 grams of uranium was placed in the reactor and multiplication increased about 0.86%Δk which gives a uranium worth of 1.47%Δk/kg.

Increment 18 completed the 1/4 sector which was started in Increments 14 and 15 by adding 2 additional stages to the outer row of fuel elements and a single stage to the next row in from the outside. There were 171 sheets of fuel (448.0 grams) placed in the reactor with an increase in multiplication of 0.43%Δk. This gave a fuel worth of 0.96%Δk/kg. The next two increments completed the extension of Zone 3A into Region 5 by adding the remaining 3/4 sector. The addition of 1245 sheets of fuel (3261.9

grams) was worth about 2.8%Δk which results in a uranium worth of 0.86%Δk/kg.

The reactor was still subcritical at this point. The fuel element loading had changed considerably in the outer portion of the core and the total loading had increased to 17151 sheets or 44.9 kg of uranium. The changes in fuel element loading can be seen in Figures 5.5 to 5.8. The other fuel elements were unchanged from the original loading. Table 5.2 summarizes the new core loading.

The next step taken to increase multiplication was to insert the 30.5 cm diameter exhaust nozzle tank filled with D_2O in the center of the movable tank (end reflector). The inverse multiplication data changed from 0.0108 to 0.0082, on the average, with the control rods withdrawn. The final change which produced a critical assembly was the removal of 4.233 kg of CH_2 from Region 1. This was done in two increments and the final k-excess was 0.168%Δk. Since additional k-excess was needed to efficiently operate the reactor, 817 grams of additional CH_2 were removed from Region 1 thus increasing k-excess to 0.368%Δk. The CH_2 was, therefore, worth -0.246%Δk/kg.

The above change in Region 1 reduced the hydrogen concentration in this region from 3.0×10^{21} to 2.0×10^{21} atoms/cm^3.

TABLE 5.1

Inverse Multiplication

Mockup of Flowing Gas Reactor

Increment	Sheets	Channel 1 CPM	Channel 1 CRo/CR	Channel 2 CPM	Channel 2 CRo/CR	Channel 3 CPM	Channel 3 CRo/CR	Average CRo/CR	Rod Positions
0	0	203	1.000	168	1.000	151	1.000	1.000	In
0	0	230	1.000	188	1.000	175	1.000	1.000	Out
1	2285	465	0.437	382	0.440	361	0.418	0.432	In
1	2285	565	0.407	478	0.393	447	0.391	0.397	Out
2	3083	567	0.358	466	0.361	436	0.346	0.355	In
2	3083	698	0.330	587	0.320	545	0.321	0.324	Out
3	4849	772	0.263	627	0.268	601	0.251	0.261	In
3	4849	1007	0.228	835	0.225	785	0.223	0.225	Out
	New CRo	199		165		148			In
		225		184		172			Out
4	7106	1082	0.188	872	0.193	837	0.180	0.187	In
4	7106	1482	0.152	1229	0.150	1138	0.151	0.151	Out
5	9116	1364	0.146	1077	0.153	1001	0.148	0.149	In
5	9116	2024	0.111	1633	0.113	1546	0.111	0.112	Out
6	10625	1581	0.126	1287	0.128	1207	0.123	0.126	In
6	10625	2548	0.088	2030	0.091	1930	0.089	0.089	Out
7	12119	1817	0.110	1480	0.111	1404	0.105	0.109	In
7	12119	3124	0.072	2520	0.073	2460	0.070	0.072	Out
8	13633	2076	0.096	1693	0.097	1609	0.092	0.095	In
8	13633	3883	0.058	3126	0.059	2948	0.058	0.058	Out
9	15268	2379	0.084	2000	0.083	1813	0.082	0.083	In
9	15268	4774	0.047	3999	0.046	3621	0.048	0.048	Out
Removed last two increments of fuel loading and removed "A" sector of CH_2 and CH at top of cavity.									
10	12119	2190	0.091	1783	0.093	1662	0.089	0.091	In
10	12119	3926	0.057	3193	0.058	2958	0.058	0.058	Out
11	13633	2505	0.079	2098	0.079	1932	0.077	0.078	In
11	13633	5056	0.045	4120	0.045	3835	0.045	0.045	Out

TABLE 5.I

(Continued)

Increment	Sheets	Channel 1 CPM	Channel 1 CRo/CR	Channel 2 CPM	Channel 2 CRo/CR	Channel 3 CPM	Channel 3 CRo/CR	Average CRo/CR	Rod Positions
12	15268	2994	0.066	2474	0.067	2230	0.066	0.066	In
12	15268	6726	0.033	5445	0.034	5001	0.034	0.034	Out
Placed 3479 gm CH_2 in outer 3 in. of top sector									
13	15268	2673	0.074	2164	0.076	2066	0.072	0.074	In
13	15268	5574	0.041	4545	0.041	4188	0.042	0.041	Out
Removed CH_2; re-installed CH_2, CH assembly, added 60 sheets of fuel									
14	15328	2399	0.083	1944	0.085	1877	0.079	0.079	In
14	15328	4893	0.047	3977	0.047	3701	0.047	0.047	Out
Completed 1/4 sector extension of Zone 3A, 180 sheets added									
15	15508	2498	0.080	2053	0.083	1918	0.077	0.077	In
15	15508	5110	0.044	4296	0.043	3893	0.044	0.044	Out
Added 1/4 sector extension of Zone 4A, 58 sheets									
16	15566	2555	0.078	2129	0.078	1943	0.076	0.077	In
16	15566	5381	0.042	4441	0.041	4071	0.042	0.042	Out
Added 3/4 sector extension of Zone 4A, 167 sheets									
17	15733	2716	0.073	2247	0.073	2072	0.071	0.072	In
17	15733	6046	0.037	5047	0.036	4648	0.037	0.037	Out
Complete 1/4 sector of extension of Zone 3A, 171 sheets									
18	15904	2885	0.069	2423	0.068	2190	0.068	0.068	In
18	15904	6733	0.033	5502	0.033	5087	0.034	0.0335	Out
	New CRo	194		161		155			In
		219		179		181			Out
Added 1/4 sector of extension of Zone 3A, 413 sheets									
19	16317	3193	0.061	2712	0.059	2635	0.059	0.060	In
19	16317	8587	0.026	7298	0.025	6997	0.026	0.026	Out
Added 180° sector of extension of Zone 3A, 832 sheets									

TABLE 5.1

(Continued)

Increment	Sheets	Channel 1 CPM	Channel 1 CRo/CR	Channel 2 CPM	Channel 2 CRo/CR	Channel 3 CPM	Channel 3 CRo/CR	Average CRo/CR	Rod Positions
20	17151	4242	0.0457	3575	0.0450	3355	0.0462	0.0456	In
20	17151	18596	0.0118	15578	0.0103	14844	0.0104	0.0108	Out
Placed 30.5 cm diameter tank in end reflector									
21	17151	4598	0.0422	3837	0.0420	3672	0.0422	0.0421	In
21	17151	26938	0.0081	23396	0.0080	21452	0.0084	0.0082	Out
Removed 1704 gm CH_2 from Region 1									
22	17151	5033	0.0385	4368	0.0369	3838	0.0404	0.0386	In
22	17151	51725	0.0042	42904	0.0042	38057	0.0048	0.0048	Out
Removed 2529 gm of CH_2 from Region 1									
23	17151	5976	0.0325	5047	0.0319	4540	0.0341	0.0328	In
23	17151	Critical with 0.1675%Δk k-excess							Out

TABLE 5.2

Core Loading After Modification to Regions 5 and 6

Zone	Fuel Fraction	Relative Fuel Density	Fuel Mass (kg)	Fuel Density g/cm^3	No. of Fuel Elements	Number of Fuel Sheets*
1	0.424	1.000	19.07	0.0541	208	7278
2 & 2A	0.319	0.752	14.34	0.0406	208	5475
3	0.050	0.465	2.22	0.0252	52	849
3A	0.069	0.561	3.09	0.0304	60	1180
3A ext.	0.096	0.584	4.32	0.0316	96	1648
4	0.016	0.245	0.72	0.0133	52	274
4A	0.012	0.305	0.56	0.0165	40	212
4A ext	0.014	0.326	0.61	0.0176	60	235
	1.000		44.93			17151

*Each fuel sheet has an average weight of 2.62 gm of uranium metal (93.2%U-235, 1.0% U-234, 5.4% U-238 and 0.4% U-236).

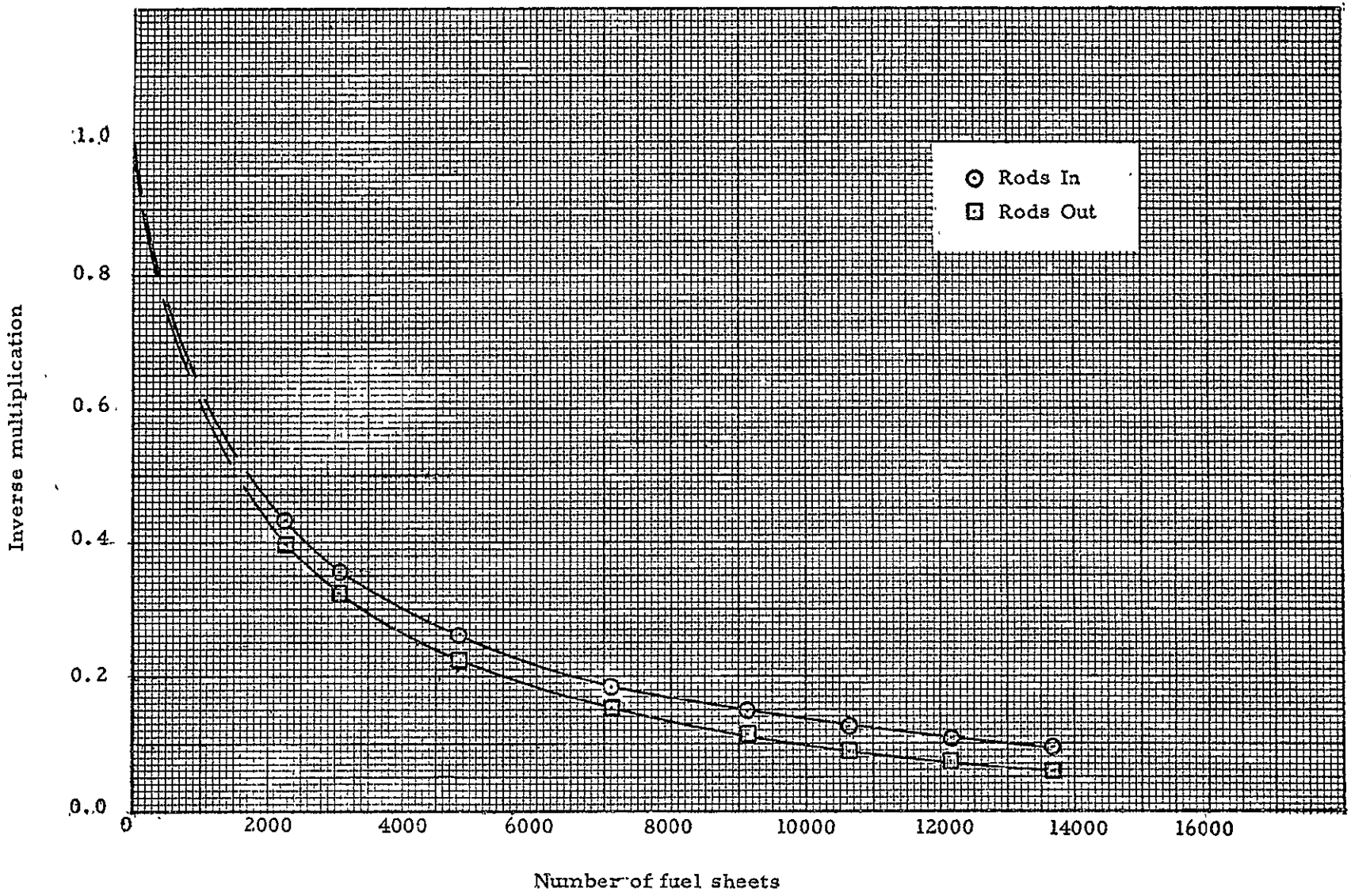

Fig. 5.1 Inverse multiplication - average of three count rate channels

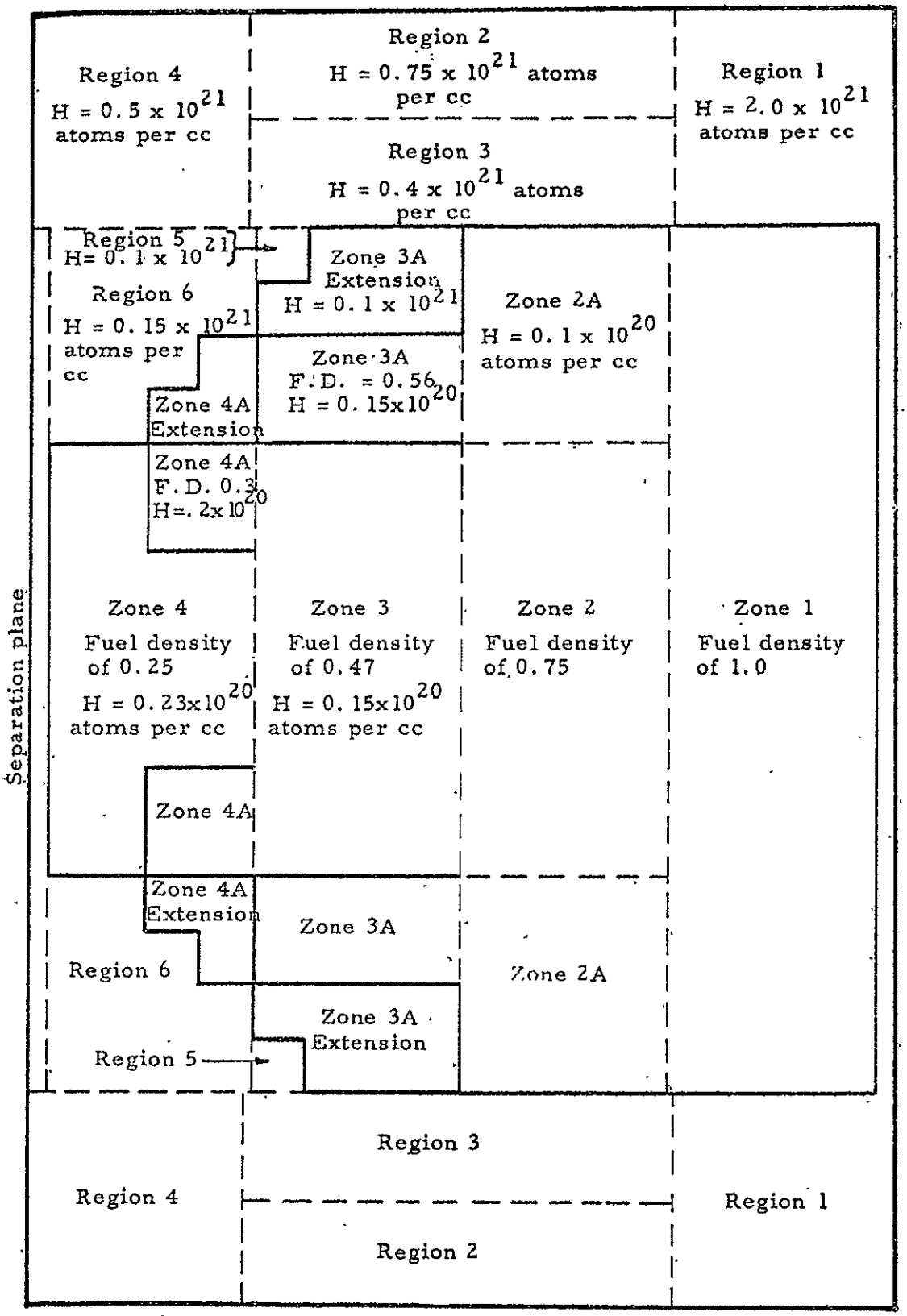

Fuel densities (F.D.) are relative to Zone 1. All zones contain fuel.

Fig. 5.2 Hydrogen and fuel density as loaded for the modified variable hydrogen, variable fuel density core; k = 1.0037 with the exhaust nozzle plugged

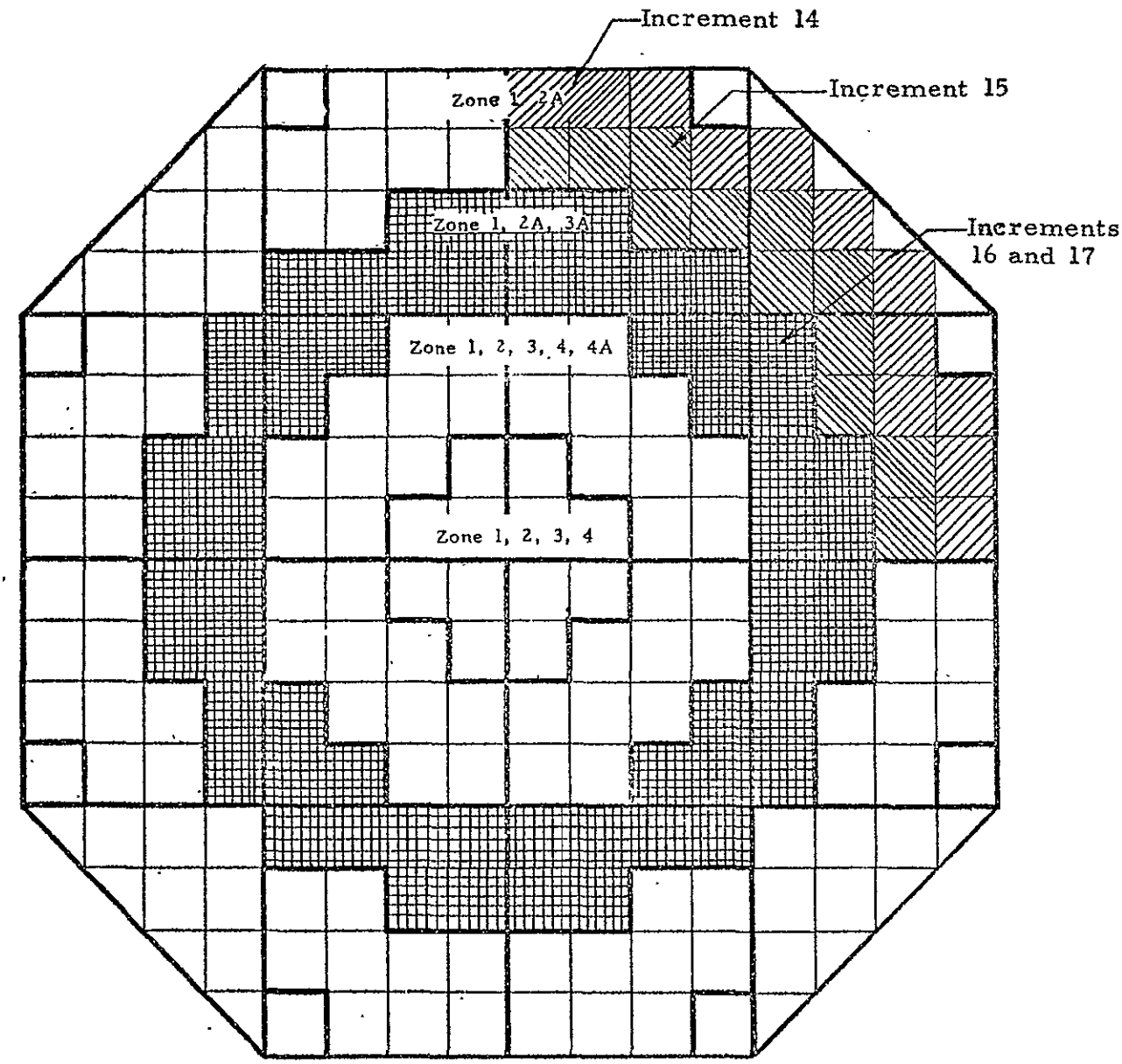

Fig. 5.3 Cross-section view of core at separation plane showing addition of fuel to Zone 3A and 4A extensions

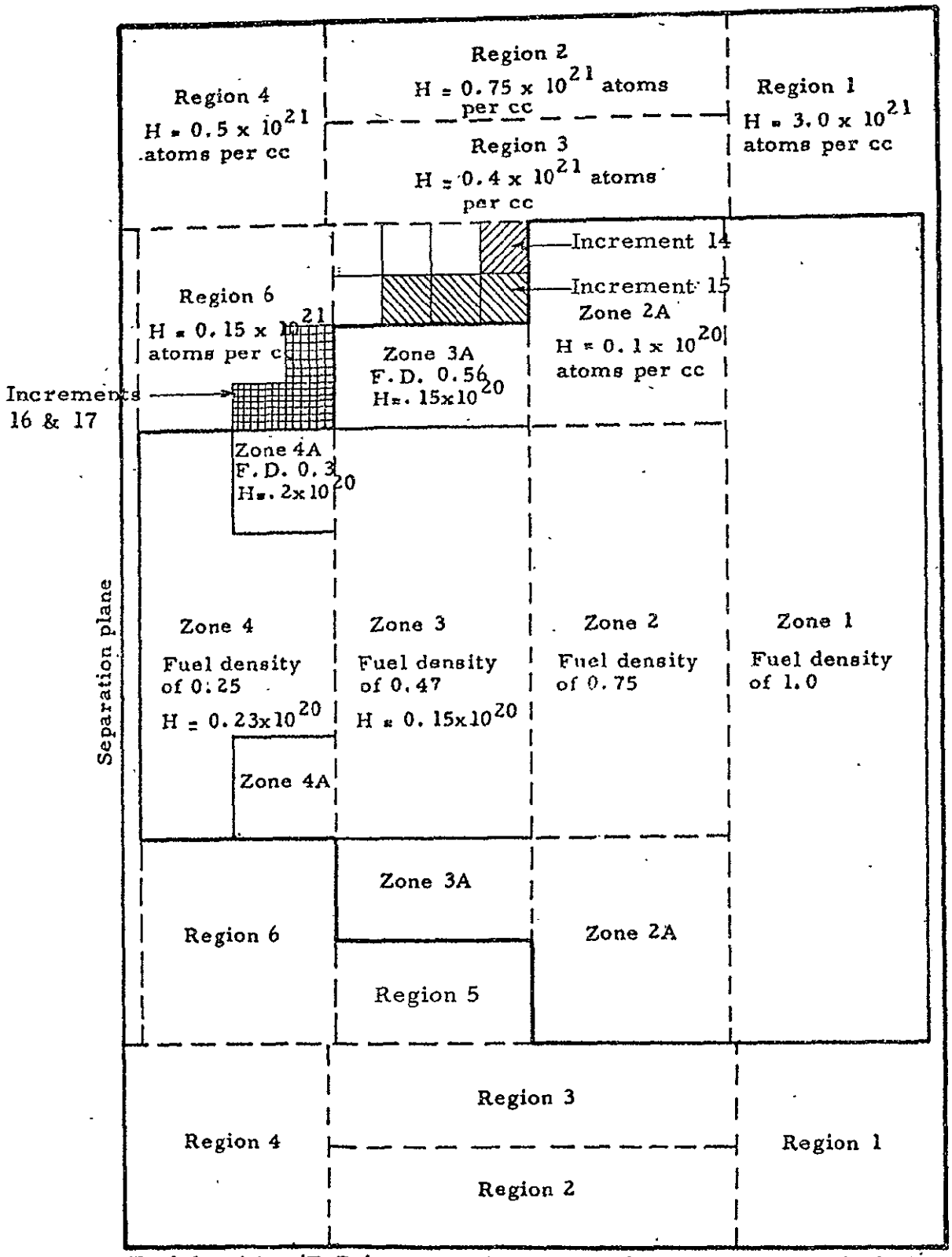

Fig. 5.4 Hydrogen and fuel density specification plus the extensions to Zones 3A and 4A

TYPE 1 fuel element

1	2	3	4	5	6	7	8	9	10	11	12	13	14	15	16	
1	2	3	1	2	3	1	2	3	1	2	3	1	2	3	1	Stage number
1	2	3	1	2	3	1	2	3	1	2	3	1	2	3	1	Fuel orientation
9	9	9	9	7	7	7	7	5	5	5	0	0	0	0	0	Number of fuel sheets per stage

TYPE 2 fuel element

1	2	3	4	5	6	7	8	9	10	11	12	13	14	15	16	
2	3	1	2	3	1	2	3	1	2	3	1	2	3	1	2	Stage number
9	9	9	9	7	7	7	6	4	5	5	0	0	0	0	0	Fuel orientation
																Number of fuel sheets per stage

TYPE 3 fuel element

1	2	3	4	5	6	7	8	9	10	11	12	13	14	15	16	
3	1	2	3	1	2	3	1	2	3	1	2	3	1	2	3	Stage number
8	8	8	9	6	6	6	6	5	5	5	0	0	0	0	0	Fuel orientation
																Number of fuel sheets per stage

Zone 1 — Zone 2A — Zone 3A Extension — Reg. 5 — Region 6

The following number and types of fuel elements will be required of the above loading:

Zones	Type 1	Type 2	Type 3	Totals
1, 2A, 3A	14	17	17	48

Fig. 5.5 Fuel element loading recipe for Zones 1, 2A, and 3A extension (outer ring)

TYPE 1 fuel element

1	2	3	4	5	6	7	8	9	10	11	12	13	14	15	16	Stage number
1	2	3	1	2	3	1	2	3	1	2	3	1	2	3	1	Fuel orientation
9	9	9	9	7	7	7	7	5	5	5	5	0	0	0	0	Number of fuel sheets per stage

TYPE 2 fuel element

1	2	3	4	5	6	7	8	9	10	11	12	13	14	15	16	Stage number
2	3	1	2	3	1	2	3	1	2	3	1	2	3	1	2	Fuel orientation
9	9	9	9	7	7	7	6	4	5	5	5	0	0	0	0	Number of fuel sheets per stage

TYPE 3 fuel element

1	2	3	4	5	6	7	8	9	10	11	12	13	14	15	16	Stage number
3	1	2	3	1	2	3	1	2	3	1	2	3	1	2	3	Fuel orientation
8	8	8	9	6	6	6	6	5	5	5	5	0	0	0	0	Number of fuel sheets per stage

Zone 1 — Zone 2A — Zone 3A Extension — Region 6

The following number and types of fuel elements will be required of the above loading:

Zones	Type 1	Type 2	Type 3	Totals
1, 2A, 3A	18	15	15	48

Fig. 5.6 Fuel element loading recipe for Zones 1, 2A, and 3A extension (inner ring)

TYPE 1 fuel element

1	2	3	4	5	6	7	8	9	10	11	12	13	14	15	16	Stage number
1	2	3	1	2	3	1	2	3	1	2	3	1	2	3	1	Fuel orientation
9	9	9	9	7	7	7	7	5	5	5	5	3	0	0	0	Number of fuel sheets per stage

TYPE 2 fuel element

1	2	3	4	5	6	7	8	9	10	11	12	13	14	15	16	Stage number
2	3	1	2	3	1	2	3	1	2	3	1	2	3	1	2	Fuel orientation
9	9	9	9	7	7	7	6	4	5	5	5	3	0	0	0	Number of fuel sheets per stage

TYPE 3 fuel element

1	2	3	4	5	6	7	8	9	10	11	12	13	14	15	16	Stage number
3	1	2	3	1	2	3	1	2	3	1	2	3	1	2	3	Fuel orientation
8	8	8	9	6	6	6	6	5	5	5	5	2	0	0	0	Number of fuel sheets per stage

Zone 1 — Zone 2A — Zone 3A — Zone 4A Extension — Region 6

The following number and types of fuel elements will be required of the above loading:

Zone	Type 1	Type 2	Type 3	Totals
1, 2A, 3A, 4A	8	13	11	32

Fig. 5.7 Fuel element loading recipe for Zones 1, 2A, 3A, and 4A extension (outer ring)

TYPE 1 fuel element

1	2	3	4	5	6	7	8	9	10	11	12	13	14	15	16	Stage number
1	2	3	1	2	3	1	2	3	1	2	3	1	2	3	1	Fuel orientation
9	9	9	9	7	7	7	7	5	5	5	5	3	3	0	0	Number of fuel sheets per stage

TYPE 2 fuel element

1	2	3	4	5	6	7	8	9	10	11	12	13	14	15	16	Stage number
2	3	1	2	3	1	2	3	1	2	3	1	2	3	1	2	Fuel orientation
9	9	9	9	7	7	7	6	4	5	5	5	3	3	0	0	Number of fuel sheets per stage

TYPE 3 fuel element

1	2	3	4	5	6	7	8	9	10	11	12	13	14	15	16	Stage number
3	1	2	3	1	2	3	1	2	3	1	2	3	1	2	3	Fuel orientation
8	8	8	9	6	6	6	6	5	5	5	5	2	2	0	0	Number of fuel sheets per stage

Zone 1 — Zone 2A — Zone 3A — Zone 4A Extension — Region 6

The following number and types of fuel elements will be required of the above loading:

Zone	Type 1	Type 2	Type 3	Totals
1, 2A, 3A, 4A	12	7	9	28

Fig. 5.8 Fuel element loading recipe for Zones 1, 2A, 3A, and 4A extension (inner ring)

6.0 REACTIVITY MEASUREMENTS

6.1 Rod Worth Data

Shortly after the reactor was critical, a single rod worth measurement was made to determine the control system worth. The seven actuators containing 21 control rods were worth -4.23%Δk. Four measurements of the worth of Actuators 3 and 6 (6 rods) gave -1.416 ± 0.007%Δk.

6.2 Material Worths

The worth of uranium was measured in each of the active core zones by slightly increasing the fuel density in a 1/8 or 1/4 sector of each zone and the resulting increase in k-excess was measured as shown in Table 6.1. The average worth in each zone was then weighted by its fuel fraction, giving a resulting weighted core average of 0.250 ± 0.017%Δk/kg U.

After the fuel worth data were obtained and the reactor had been power mapped, the exhaust nozzle tank was removed from the reactor. Based on the loss of excess reactivity and the amount the reactor was subcritical, the plug was worth 0.456%Δk. This compares with 0.459%Δk reported in Section 13.2.1 of Reference 1 when inserting the tank during the core rounding measurements.

In order to restore the reactor to a critical assembly after removing the exhaust nozzle tank, the fuel density in Zone 3 was increased to that of Zone 3A by adding 174 sheets of fuel (455.9 grams). The exact loading change as to location of the additional fuel sheets can be determined by comparing the fuel element loadings for Zones 3 and 3A as seen from Figures 3.4, 3.5, and 5.6. The fuel elements over Zone 3 were simply changed to be the same as for Zone 3A. The difference in multiplication caused by the increase in fuel gave a fuel worth of 0.163%Δk/kg. This value would be expected to have an uncertainty of about 10% being based on subcritical data. Prior to any addition of fuel to Zone 3, the worth of uranium in this zone was 0.210 ± 0.026%Δk/kg. The uranium worth would be expected to decrease as the loading increased, which agrees with the results.

The next modification was to increase the fuel loading in the portion of Zone 2A which was directly in line with the original Zone 3A. This affected 60 fuel elements over Zone 2A and the fuel loading was increased by 340 fuel sheets (890.8 grams of uranium). The fuel concentration in each stage was increased to 8 sheets per stage whereas they originally contained either 6 or 7 sheets per stage as shown in Figure 5.5. The reactor was critical at this point with 0.0624 ± 0.0050%Δk excess reactivity. Prior to making this final addition of fuel, the reactor was estimated to be 0.036 ± 0.004%Δk subcritical. This plus the excess reactivity after the change should represent the worth of the increase in fuel loading or 0.0984 ± 0.0064%Δk. This results in a fuel worth of 0.110 ± 0.007%Δk/kg which appears to be too low compared to the average for Zones 2 and 2A of 0.196 ± 0.013%Δk/kg prior to removing the exhaust nozzle plug and changing the fuel loading. The portion of Zone 2A where the fuel loading increase occurred was over the region where the local fuel worth value was approximately equal to the average fuel worth over Zones 2, 2A. The 22% increase in fuel density in this local region ostensibly created a 44% decrease in fuel worth.

The 20% increase in fuel loading in Zone 3 reduced the fuel worth 22%, or nearly a linear relationship. The core spectrum in the specific zones is an important factor and Zone 3 is at the center of the core, surrounded by fueled zones. The portion of Zone 2A containing the increased loading was near the outer surface of the active core. Therefore, the neutron spectrum would be much harder in Zone 3A than in 2A. There would naturally be a greater change in fuel worth in the softer spectrum than the harder spectrum due to increasing the fuel density which could account for the above fuel worths.

In order to obtain further spatial detail for the fuel worth in Zone 2, the fuel was removed from the center 12 fuel elements over this zone. The uranium was worth $0.127 \pm 0.008\%\Delta k/kg$, which is higher than over the portion of Zone 2A where the fuel density was increased. This measurement, however, represented an infinite decrease in fuel density in these 12 fuel elements. Note, that a better comparison with the above results would have been obtained if fuel had been added rather than removed in making this latter measurement.

The removal of the exhaust nozzle tank was followed by a subsequent increase in fuel density in Zones 3 and 2A, as noted above, to simulate a possible shift in fuel density due to both temperature distribution and mixing effects in the power reactor.

After the exhaust nozzle plug was removed, several reactivity measurements were made to determine polyethylene (CH_2) and polystyrene (CH) worth within the cavity. Table 6.2 contains these data. In Zones 3 and 4 specific radial positions were measured to produce curves of worth as a function of radius. These points are shown in Figure 6.1. The worth in Zone 3 is positive from the core center to 35 cm at which point it turns negative. This was not the case in Zone 4 where polyethylene worth was negative both at the center of the core and at the outer boundary of this zone. Zone 4 is on the end of the core near the exhaust nozzle where the thermal flux is high, and the fuel density in the zone was quite low. These two factors would tend to cause the absorption effect to override the moderating properties of polyethylene.

It will be noted from Table 6.2 that the worth of carbon was measured at the average radial position of the polystyrene and polyethylene surrounding the active core. Compared to the average polyethylene worth across this region, carbon represents about 2% of the CH_2 worth and 4% of the CH worth. Assuming this to be true of other positions in the reactor it is a simple matter to reduce the CH and CH_2 data to hydrogen worth as shown in Table 6.3. Both materials were evaluated in Regions 5 and 6, where there was no fuel, with resulting hydrogen worths of $-5.076\%\Delta k/kg$ and $-5.093\%\Delta k/kg$ for CH and CH_2, respectively. Within the experimental error, these values are the same. Previous results reported in Reference 2, p. 88, showed CH to give higher hydrogen worths by 34% than did CH_2. The difference was attributed to molecular binding differences. The reason for excellent correlation on this assembly is not known. There was a substantial difference in the hydrogen atom density in the two cases (2×10^{21}/cc in Reference 2 case vs 0.15×10^{21}/cc in the present case). Further measurements on CH vs CH_2 effects will be needed to resolve this apparent discrepancy.

TABLE 6.1

Fuel Worth Measurements

Mockup of Flowing Gas Reactor

Location	Mass (grams)	Sector	Worth (%Δk)	Worth/kg (%Δk/kg)
Zone 4	167.7	1/4	0.1282 ± 0.007	0.764 ± 0.042
Zone 4 (repeat)	167.7	1/4	0.1245 ± 0.007	0.742 ± 0.042
Zone 4A	220.0	1/4	0.1173 ± 0.007	0.533 ± 0.032
Zone 3	272.5	1/4	0.0571 ± 0.007	0.210 ± 0.026
Zone 3A	372.0	1/4	0.1413 ± 0.007	0.380 ± 0.019
Zone 2, 2A	545.0	1/8	0.1068 ± 0.007	0.196 ± 0.013
Zone 1	545.0	1/8	0.1061 ± 0.007	0.195 ± 0.013
			Weighted Average (fuel fraction wt factors)	0.250 ± 0.017

NOTE: The change in reactivity was generally obtained from period differences with only slight movement of Actuators 3 and 6. Therefore, the estimated error per measurement was set at 0.007%Δk as noted in the table.

TABLE 6.2

Polyethylene, Polystyrene, and Carbon Reactivity Worths

Mockup of Flowing Gas Reactor

Material	Location	Mass (grams)	Reactivity Change(1) (%Δk)	Material Worth (%Δk/kg)
Polystyrene	Regions 5 and 6 (avg.) Zones 3A and 4A extensions	604	-0.1952	-0.323
Polystyrene	Regions 5 and 6 (avg.) Zones 3A and 4A extensions	604	-0.2319	-0.384
Polyethylene	Zones 3A and 4A Extensions (avg.)	23.7	-0.0203	-0.638
Polyethylene	Zone 2A (avg.)	256.3	-0.0609	-0.238
Polyethylene	Zone 3, 9.8 cm from core center	153.0	+0.0280	+0.183
Polyethylene	Zone 3, 27.7 cm from core center	256.3	+0.0185	+0.0722
Polyethylene	Zone 3, 43.0 cm from core center	311.3	-0.0365	-0.117
Polystyrene	Regions 5 and 6 not occupied by fuel	779	-0.318	-0.408
Polyethylene	Zone 3A, 61.0 cm from core center	143.5	-0.0955	-0.666
Polyethylene	Zone 4, 9.8 cm from core center	157.0	-0.0271	-0.173
Polyethylene	Zones 4 and 4A, 27.7 cm from core center	261.0	-0.0843	-0.323
Polyethylene	Zone 4A extension, 42.1 cm from core center	142	-0.0578	-0.407
Polyethylene	Outer edge of core	238.0	-0.1751	-0.736
Polyethylene	Average over regions 5 and 6	129.5	-0.0965	-0.745
Polyethylene	Cavity wall	238.0	-0.0628	-0.264
Carbon	Mid position between core and cavity wall	3898	-0.0424	-0.0109

(1) The standard error on the reactivity data is estimated to be ±.007%Δk or less.

TABLE 6.3

Hydrogen Worth from CH_2 and CH Worths

Assume Carbon to be 2% of CH_2 Worth and 4% of CH Worth

Location	CH_2-C Worth (%Δk/kg)	CH-C Worth (%Δk/kg)	Hydrogen Worth %Δk/kg
Regions 5 and 6 Zones 3A and 4A ext.		-0.311	-4.017
Regions 5 and 6 Zones 3A and 4A ext.		-0.370	-4.779
Zones 3A and 4A ext.	-0.627		-4.363
Zone 2A avg.	-0.234		-1.628
Zone 3 9.8 cm from core center	+0.180		+1.252
Zone 3 27.7 cm from core center	+0.0710		+0.494
Zone 3 43.0 cm from core center	-0.115		-0.0139
Regions 5 and 6 not occupied by fuel		-0.393	-5.076
Zone 3A, 61.0 cm from core center	-0.655		-4.557
Zone 4, 9.8 cm from core center	-0.170		-1.183
Zone 4 and 4A, 27.7 cm from core center	-0.317		-2.206
Zone 4A ext. 42.1 cm from core center	-0.400		-2.783
Outer edge of core	-0.723		-5.031
Avg. over regions 5 and 6 with no fuel	-0.732		-5.093
Cavity wall	-0.259		-1.802

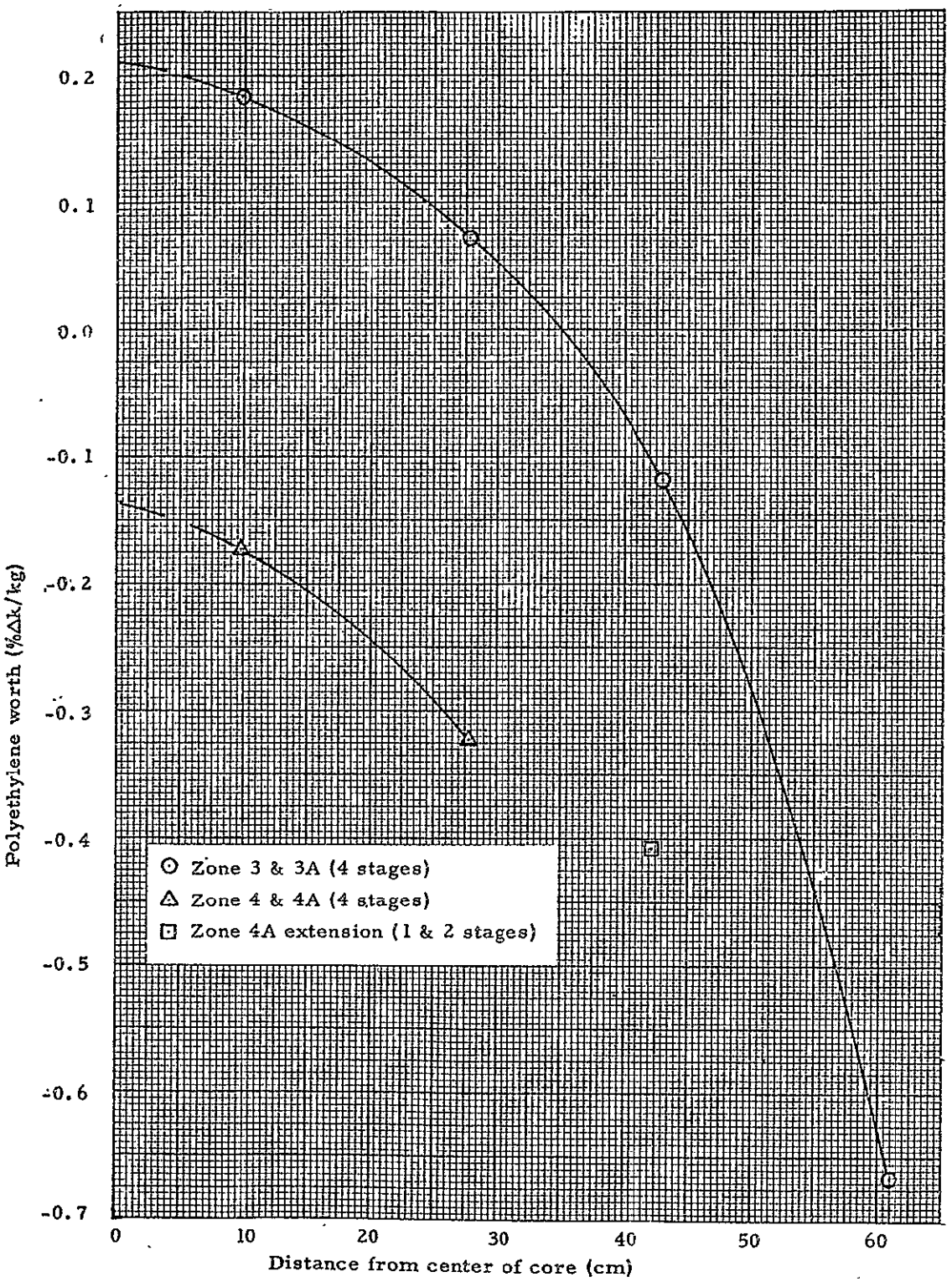

Fig. 6.1 Radial distribution of polyethylene worth in Zones 3, 3A, 4, and 4A. Exhaust nozzle tank removed from reactor.

7.0 POWER DISTRIBUTION MEASUREMENTS

7.1 Bare Catcher Foils - Exhaust Nozzle Plug in Reactor

The cavity region of the reactor was power mapped using both bare and cadmium covered catcher foils with the exhaust nozzle plug in the reactor. Actuators 1, 2, and 3 were fully withdrawn. The average temperature during the measurements was 20.3°C and the control rods on Actuators 4, 5, 6, and 7 were 40.6 cm withdrawn. The data are contained in Table 7.1. Eight axial traverses were measured at different radial locations from the center of the core to the outer portion of the cavity region and these data are shown in Figure 7.1 normalized to the axial and radial center of the core. The effects of the heavy concentration of both fuel and hydrogen at the inlet end of the core (opposite the exhaust nozzle end) are clearly evident. The polyethylene and polystyrene used to mockup hydrogen act as a flux trap which enhances the flux in the hydrogenous material but inhibits the neutrons from reaching the fueled region. This, coupled with the variable fuel loading in the active core, causes the power to be tilted, high at the separation plane and low at the other end of the core.

Each of the axial profiles was averaged and the axially-averaged specific power distribution is plotted as shown in Figure 7.2. Although this curve is smooth and quite typical of a radial profile for a uniform core, this core was not loaded uniformally. In order to obtain the core power developed in each zone, it was necessary to volume weight the radial distribution for each zone. These axially weighted profiles are shown in Figure 7.3. These radial profiles were then volume weighted and averaged over each zone and the values are recorded in the figure. Finally, the portion of the total core power generated by each of the zones, as well as the fuel annulus in the radial reflector, is given in Table 7.2. The average power density (power per unit volume) is also given in this table.

7.2 Catcher Foil Cadmium Ratios - Exhaust Nozzle in Reactor

The cadmium ratios obtained from catcher foils are given near the end of Table 7.1. Five axial profiles were measured across the core as shown in Figure 7.4. The highest cadmium ratio (40.26) was located on the cavity wall near the end of the core containing the heavy concentration of hydrogen and uranium, This decreased rapidly along the cavity wall to about 24 at the axial center of the core on the entrance end of the cavity. Near the radial center of the core, the cadmium ratios followed the general profile of the power distribution with the minimum of 2.92 occurring at an axial position of about 120 cm from the axial reference point or 30 cm from the end of the cavity. This is the end of Zone 1 and the beginning of Zone 2.

7.3 Bare Catcher Foils - Exhaust Nozzle Removed from Reactor

After removing the exhaust nozzle and adjusting the fuel loading in Zones 3 and 2A, the power distribution measurements were repeated with foils. The core temperature averaged 20.8°C and Actuators 4, 5, 6, and 7 were 53.3 cm withdrawn. The rods on Actuators 1, 2, and 3 were fully withdrawn. Table 7.3 contains these data and Figure 7.5

shows the nine axial profiles measured from the bare foils. Each of the axial curves was averaged and compared to the case with the exhaust nozzle tank in the reactor. A slight average increase of 1.2 ± 3.6% was indicated for the axial profiles with the nozzle removed. This increase appears primarily over the axial profiles out to about 38 cm from the center of the core which would normally be expected based on earlier measurements of the effects of removing the exhaust nozzle plug (Reference 4, p. 165).

The axial curves were also averaged by zones, as was done with the exhaust nozzle tank in the reactor, and the results as given in Figure 7.6. A comparison in Zones 4 and 4A, which were closest to the exhaust nozzle and where no changes were made in fuel loading, showed that the volume weighted averages increased considerably when removing the plug. Zone 4 increased 24% and 4A increased 7%. The volume weighted average on the other end of the core (Zone 1) where no fuel changes were made decreased about 2%.

Zones 2 and 2A indicated very little change due to the increased loading in Zone 2A as would be seen if one overlayed the two curves. It will be noted from Figure 7.6 that the curve for Zone 2 and 2A is continuous. However, the power density in Zone 2A where the fuel loading was increased would decrease compared to the earlier configuration.

7.4 Catcher Foil Cadmium Ratios - Exhaust Nozzle Removed

The cadmium ratio measurements were also repeated after removing the exhaust nozzle tank and increasing the fuel loading in Zones 2A and 3. Table 7.3 contains these values and they are shown graphically in Figure 7.7. A direct comparison on a point by point basis (Table 7.4) showed an overall average increase of 4.5 ± 10.0% in cadmium ratio due to removing the plug and increasing the fuel loading over Zones 2A and 3. The 10% standard deviation does not represent experimental uncertainty of that amount. It is mostly indicative of the variations in cadmium ratios from the plug-in to the plug-out configurations. Some Zones experienced greater changes than others and some were positive while others were negative changes. Because the reactor experienced two alterations, it is difficult to differentiate between the two. Removing the plug should have increased the cadmium ratio at the separation plane over the central part of the core. This effect which is generally substantiated by the data. There weren't sufficiently detailed data to identify for certain the specific changes in Zone 3 or the inner portion of Zone 2A where the fuel density was increased. The increased fuel density should have resulted in a slight decrease in cadmium ratio in these zones.

TABLE 7.1

Catcher Foil Data

Mockup of Flowing Gas Reactor

Exhaust Nozzle Plug In Reactor

Foil No.	Type	Location Radial (cm)	Location Axial (cm)	Normalized Counts	Local to Foil (X)
Run 1158					
1	Bare	0	93.3	34263	2.096
2	Bare	0	105.3	14526	0.889
3	Bare	0	120.6	11018	0.674
4	Bare	0	135.8	12079	0.739
5	Bare	0	151.1	16344	1.000
6	Bare	0	166.3	24463	1.497
7	Bare	0	181.6	37539	2.297
8	Bare	0	196.8	31518	3.140
9	Bare	0	208.8	66205	4.050
10	Bare	15.2	93.3	46700	2.245
11	Bare	15.2	105.3	15538	0.951
12	Bare	15.2	120.6	11925	0.730
13	Bare	15.2	135.8	13960	0.854
14	Bare	15.2	151.1	17971	1.099
15	Bare	15.2	166.3	24542	1.501
16	Bare	15.2	181.6	39099	2.392
17	Bare	15.2	196.8	49194	3.010
18	Bare	15.2	208.8	66492	4.068
19	Bare	30.5	93.3	41781	2.556
20	Bare	30.5	105.3	15727	0.962
21	Bare	30.5	120.6	15588	0.954
22	Bare	30.5	135.8	17593	1.076
23	Bare	30.5	151.1	22949	1.404
24	Bare	30.5	166.3	29965	1.833
25	Bare	30.5	181.6	49627	3.036
26	Bare	30.5	189.2	60194	3.683
27	Bare	30.5	196.8	70372	4.305
28	Bare	30.5	204.4	79561	4.868
29	Bare	30.5	208.8	81966	5.015
30	Bare	38.1	93.3	41573	2.543
31	Bare	38.1	105.3	24131	1.476
32	Bare	38.1	120.6	16396	1.003
33	Bare	38.1	135.8	21051	1.288
34	Bare	38.1	151.1	25842	1.581
35	Bare	38.1	166.3	28982	1.773
36	Bare	38.1	181.6	49653	3.038

TABLE 7.1

(Continued)

Foil No.	Type	Location Radial (cm)	Location Axial (cm)	Normalized Counts	Local to Foil (%)
Run 1158 (Cont'd)					
37	Bare	38.1	189.2	70319	4.302
38	Bare	38.1	196.8	85114	5.207
39	Bare	38.1	204.4	90750	5.552
40	Bare	38.1	208.8	92597	5.665
41	Bare	45.7	93.3	40683	2.489
42	Bare	45.7	105.3	24116	1.475
43	Bare	45.7	120.6	21925	1.341
44	Bare	45.7	135.8	26352	1.612
45	Bare	45.7	151.1	33243	2.034
46	Bare	45.7	166.3	39062	2.390
47	Bare	45.7	181.6	69999	4.283
48	Bare	45.7	189.2	78283	4.789
49	Bare	45.7	196.8	87674	5.364
50	Bare	45.7	208.8	100300	6.136
51	Bare	53.3	93.3	55331	3.385
52	Bare	53.3	105.3	35949	2.199
53	Bare	53.3	120.6	31696	1.939
54	Bare	53.3	135.8	32367	1.980
55	Bare	53.3	151.1	45749	2.799
56	Bare	53.3	166.3	52769	3.228
57	Bare	53.3	173.9	63357	3.876
58	Bare	53.3	181.6	84620	5.177
59	Bare	53.3	196.8	94938	5.808
60	Bare	53.3	208.8	111355	6.813
61	Bare	61.0	93.3	75892	4.643
62	Bare	61.0	105.3	58794	3.597
63	Bare	61.0	120.6	59901	3.665
64	Bare	61.0	135.8	66512	4.069
65	Bare	61.0	151.1	67691	4.141
66	Bare	61.0	166.3	77309	4.730
67	Bare	61.0	173.9	81468	4.984
68	Bare	61.0	181.6	93023	5.691
69	Bare	61.0	196.8	102103	6.247
70	Bare	61.0	208.8	108591	6.644
71	Bare	76.2	93.3	146826	8.893
72	Bare	76.2	105.3	144617	8.848
73	Bare	76.2	120.6	122830	7.515
74	Bare	76.2	135.8	116467	7.125
75	Bare	76.2	151.1	117922	7.214
76	Bare	76.2	166.3	123496	7.555
77	Bare	76.2	181.6	121004	7.403

TABLE 7.1

(Continued)

Foil No.	Type	Location Radial (cm)	Location Axial (cm)	Normalized Counts	Local to Foil (X)
Run 1158 (Cont'd)					
78	Bare	76.2	196.8	132391	8.100
79	Bare	76.2	208.8	121009	7.403
80	Bare	91.4	93.3	172586	10.56
81	Bare	91.4	105.3	175783	10.75
82	Bare	91.4	120.6	152049	9.302
83	Bare	91.4	135.8	124835	7.637
84	Bare	91.4	151.1	126920	7.765
85	Bare	91.4	166.3	119626	7.319
86	Bare	91.4	181.6	123912	7.581
87	Bare	91.4	196.8	123870	7.578
88	Bare	91.4	208.8	125781	7.695
Run 1159					Cadmium Ratios
1	Cd	61.0	93.3	4729	16.05
2	Cd	61.0	105.3	4488	13.10
3	Cd	61.0	120.6	4732	12.66
4	Cd	61.0	151.1	4581	14.78
5	Cd	61.0	181.6	4819	19.30
6	Cd	61.0	208.8	4469	24.30
7	Cd	91.4	93.3	4287	40.26
8	Cd	91.4	105.3	4907	35.82
9	Cd	91.4	120.6	5389	28.21
10	Cd	91.4	151.1	5286	24.01
11	Cd	91.4	181.6	4678	26.49
12	Cd	91.4	208.8	4066	30.93
Run 1160					
1	Cd	30.5	93.3	4603	9.08
2	Cd	30.5	105.3	3636	4.33
3	Cd	30.5	120.6	3671	4.23
4	Cd	30.5	151.1	4019	5.71
5	Cd	30.5	181.6	4208	11.79
6	Cd	30.5	208.8	4683	17.50
Run 1161					
1	Cd	0	93.3	4248	8.07
2	Cd	0	105.3	3770	3.85
3	Cd	0	120.6	3774	2.92

TABLE 7. 1

(Continued)

Foil No.	Type	Location Radial (cm)	Location Axial (cm)	Normalized Counts	Cadmium Ratio
Run 1161	(Cont'd)				
4	Cd	0	151.1	3565	4.58
5	Cd	0	181.6	4280	8.77
6	Cd	0	208.8	4743	13.96
7	Cd	76.2	93.3	4930	29.78
8	Cd	76.2	105.3	4755	30.43
9	Cd	76.2	120.6	5281	23.26
10	Cd	76.2	151.1	5251	22.46
11	Cd	76.2	181.6	4464	27.11
12	Cd	76.2	208.8	4189	28.89
Run 1162					Local to Foil (X)
1	Bare	111.7	128.2	251323	15.38
2	Bare	111.1	128.2	258174	15.80
3	Bare	111.7	151.1	265556	16.25
4	Bare	111.1	151.1	251080	15.36
5	Bare	111.7	174.0	231566	14.17
6	Bare	111.1	174.0	233505	14.29

TABLE 7.2

Power Fractions in the Core of the Mockup of the Flowing Gas Reactor Exhaust Nozzle in the Reactor

Zone No.	U Mass (kg)	Fuel Fraction	Fraction of Total Power	Relative Power Density	Ratio of Power to Fuel Fraction
1	19.07	0.417	0.327	1.00	0.786
2 and 2A	14.34	0.313	0.238	0.726	0.760
3	2.22	0.048	0.036	0.440	0.542
3A	7.41	0.162	0.209	2.216	1.290
4 (inner 12 elements)	0.262	0.006	0.008	0.424	1.333
4 (outer 40 elements)	0.456	0.010	0.017	0.527	1.700
4A	1.17	0.026	0.035	1.163	1.346
Fuel Annulus	0.823(U^{235}) (1)	0.018	0.129	--	7.167

(1) Equivalent Oralloy would be 883 grams.

TABLE 7.3

Catcher Foil Data

Mockup of Flowing Gas Reactor

End Plug Removed

Foil No.	Type	Location Radial (cm)	Location Axial (cm)	Normalized Counts	Local to Foil (X)
Run 1163					
1	Bare	111.1	128.2	267652	16.431
2	Bare	111.7	128.2	254521	15.625
3	Bare	111.1	151.1	241657	14.836
4	Bare	111.7	151.1	243383	14.942
5	Bare	111.1	174.0	238143	14.620
6	Bare	111.7	174.0	224397	13.776
Run 1164					Cadmium Ratio
1	Cd	0	93.3	4086	9.354
2	Cd	0	105.3	3578	4.337
3	Cd	0	120.6	3421	3.394
4	Cd	0	151.1	3619	4.501
5	Cd	0	181.6	3813	9.609
6	Cd	0	208.8	4067	18.955
7	Cd	76.2	93.3	4438	32.133
8	Cd	76.2	105.3	4587	30.289
9	Cd	76.2	120.6	4933	26.953
10	Cd	76.2	151.1	5120	22.583
11	Cd	76.2	181.6	4513	27.611
12	Cd	76.2	208.8	4713	24.552
Run 1165					Local to Foil (X)
1	Bare	0	93.3	38222	2.346
2	Bare	0	105.3	15516	0.953
3	Bare	0	120.6	11610	0.713
4	Bare	0	135.8	12275	0.754
5	Bare	0	151.1	16289	1.000 (X)
6	Bare	0	166.3	22221	1.364
7	Bare	0	181.6	36639	2.249
8	Bare	0	196.8	51546	3.164
9	Bare	0	208.8	77092	4.733
10	Bare	15.2	93.3	37335	2.292
11	Bare	15.2	105.3	14808	0.909
12	Bare	15.2	120.6	11434	0.702

TABLE 7.3

(Continued)

Foil No.	Type	Location Radial (cm)	Location Axial (cm)	Normalized Counts	Local to Foil (X)
Run 1165	(Cont'd)				
13	Bare	15.2	135.8	11999	0.737
14	Bare	15.2	151.1	16364	1.003
15	Bare	15.2	166.3	22584	1.386
16	Bare	15.2	181.6	40648	2.495
17	Bare	15.2	196.8	55087	3.382
18	Bare	15.2	208.8	70488	4.327
19	Bare	30.5	93.3	38288	2.351
20	Bare	30.5	105.3	17785	1.092
21	Bare	30.5	120.6	14671	0.901
22	Bare	30.5	135.8	16169	0.993
23	Bare	30.5	151.1	21076	1.294
24	Bare	30.5	166.3	29915	1.836
25	Bare	30.5	181.6	47347	2.907
26	Bare	30.5	189.2	56781	3.486
27	Bare	30.5	196.8	67454	4.141
28	Bare	30.5	204.5	81684	5.015
29	Bare	30.5	208.8	83226	5.109
30	Bare	38.1	93.3	40023	2.457
31	Bare	38.1	105.3	19577	1.202
32	Bare	38.1	120.6	15918	0.977
33	Bare	38.1	135.8	15746	0.967
34	Bare	38.1	151.1	24979	1.533
35	Bare	38.1	158.7	30362	1.864
36	Bare	38.1	166.3	32195	1.976
37	Bare	38.1	174.0	43062	2.644
38	Bare	38.1	181.6	52941	3.250
39	Bare	38.1	196.8	82513	5.065
40	Bare	38.1	208.8	92658	5.688
41	Bare	45.7	93.3	43954	2.698
42	Bare	45.7	105.3	24545	1.507
43	Bare	45.7	120.6	23639	1.451
44	Bare	45.7	135.8	25005	1.535
45	Bare	45.7	151.1	29533	1.813
46	Bare	45.7	158.7	36032	2.212
47	Bare	45.7	166.3	35766	2.196
48	Bare	45.7	174.0	45167	2.773
49	Bare	45.7	181.6	70771	4.345
50	Bare	45.7	196.8	87993	5.402
51	Bare	45.7	208.8	93828	5.760
52	Bare	53.3	93.3	52509	3.224
53	Bare	53.3	105.3	32145	1.973

TABLE 7.3

(continued)

Foil No.	Type	Location Radial (cm)	Location Axial (cm)	Normalized Counts	Local to Foil (X)
Run 1165 (Cont'd)					
54	Bare	53.3	120.6	26584	1.632
55	Bare	53.3	135.8	38002	2.333
56	Bare	53.3	151.1	44727	2.746
57	Bare	53.3	158.7	47196	2.897
58	Bare	53.3	166.3	51420	3.157
59	Bare	53.3	174.0	62695	3.849
60	Bare	53.3	181.6	81330	4.993
61	Bare	53.3	196.8	96047	5.896
62	Bare	53.3	208.8	102896	6.317
63	Bare	61.0	93.3	76803	4.715
64	Bare	61.0	105.3	61867	3.798
65	Bare	61.0	120.6	53705	3.297
66	Bare	61.0	135.8	67282	4.130
67	Bare	61.0	151.1	65322	4.010
68	Bare	61.0	158.7	66845	4.104
69	Bare	61.0	166.3	79814	4.900
70	Bare	61.0	174.0	88955	5.461
71	Bare	61.0	181.6	98179	6.027
72	Bare	61.0	196.8	103683	6.365
73	Bare	61.0	208.8	105067	6.450
74	Bare	76.2	93.3	142607	8.755
75	Bare	76.2	105.3	138934	8.529
76	Bare	76.2	120.6	132960	8.162
77	Bare	76.2	135.8	109656	6.732
78	Bare	76.2	151.1	115626	7.098
79	Bare	76.2	166.3	109395	6.716
80	Bare	76.2	181.6	124609	7.650
81	Bare	76.2	196.8	116680	7.163
82	Bare	76.2	208.8	115715	7.104
83	Bare	91.4	93.3	161253	9.899
84	Bare	91.4	105.3	162221	9.959
85	Bare	91.4	120.6	138710	8.515
86	Bare	91.4	135.8	132014	8.104
87	Bare	91.4	151.1	126488	7.765
88	Bare	91.4	166.3	123083	7.556
89	Bare	91.4	181.6	127172	7.807
90	Bare	91.4	196.8	123878	7.605
91	Bare	91.4	208.8	128833	7.909

TABLE 7.3

(Continued)

Foil No.	Type	Location Radial (cm)	Location Axial (cm)	Normalized Counts	Cadmium Ratio
Run 1166					
1	Cd	61.0	93.3	4470	17.182
2	Cd	61.0	105.3	4494	13.767
3	Cd	61.0	120.6	4397	12.214
4	Cd	61.0	151.1	4255	15.352
5	Cd	61.0	181.6	4301	22.827
6	Cd	61.0	208.8	4335	24.237
7	Cd	91.4	93.3	4382	36.799
8	Cd	91.4	105.3	4893	33.154
9	Cd	91.4	120.6	5042	27.511
10	Cd	91.4	151.1	5081	24.894
11	Cd	91.4	181.6	4333	29.350
12	Cd	91.4	208.8	4167	30.917
Run 1167					
1	Cd	30.5	93.3	4350	8.802
2	Cd	30.5	105.3	3801	4.679
3	Cd	30.5	120.6	3543	4.141
4	Cd	30.5	151.1	3699	5.698
5	Cd	30.5	181.6	3931	12.045
6	Cd	30.5	208.8	4534	18.356

TABLE 7.4

Comparison of Catcher Foil Cadmium Ratios Before and After Removing the Exhaust Nozzle Plug

Location		Cadmium Ratios		Ratio of
Radial (cm)	Axial (cm)	Before Plug Removal	After Plug Removal	Plug Out to Plug In
0	93.3	8.07	9.35	1.159
0	105.3	3.85	4.34	1.127
0	120.6	2.92	3.39	1.161
0	151.1	4.58	4.50	0.983
0	181.6	8.77	9.61	1.096
0	208.8	13.96	18.96	1.358
30.5	93.3	9.08	8.80	0.969
30.5	105.3	4.33	4.68	1.081
30.5	120.6	4.23	4.14	0.979
30.5	151.1	5.71	5.70	0.998
30.5	181.6	11.79	12.04	1.021
30.5	208.8	17.50	18.36	1.049
61.0	93.3	16.05	17.18	1.070
61.0	105.3	13.10	13.77	1.051
61.0	120.6	12.66	12.21	0.964
61.0	151.1	14.78	15.35	1.039
61.0	181.6	19.20	22.83	1.183
61.0	208.8	24.30	24.24	0.998
76.2	93.3	29.78	32.13	1.079
76.2	105.3	30.43	30.29	0.995
76.2	120.6	23.26	26.95	1.159
76.2	151.1	22.46	22.58	1.005
76.2	181.6	27.11	27.61	1.018
76.2	208.8	28.89	24.55	0.850
91.4	93.3	40.26	36.80	0.914
91.4	105.3	35.82	33.15	0.925
91.4	120.6	28.21	27.51	0.975
91.4	151.1	24.01	24.89	1.037
91.4	181.6	26.49	29.35	1.108
91.4	208.8	30.93	30.92	1.000
				1.045 ± 0.100
				1.034 ± 0.082

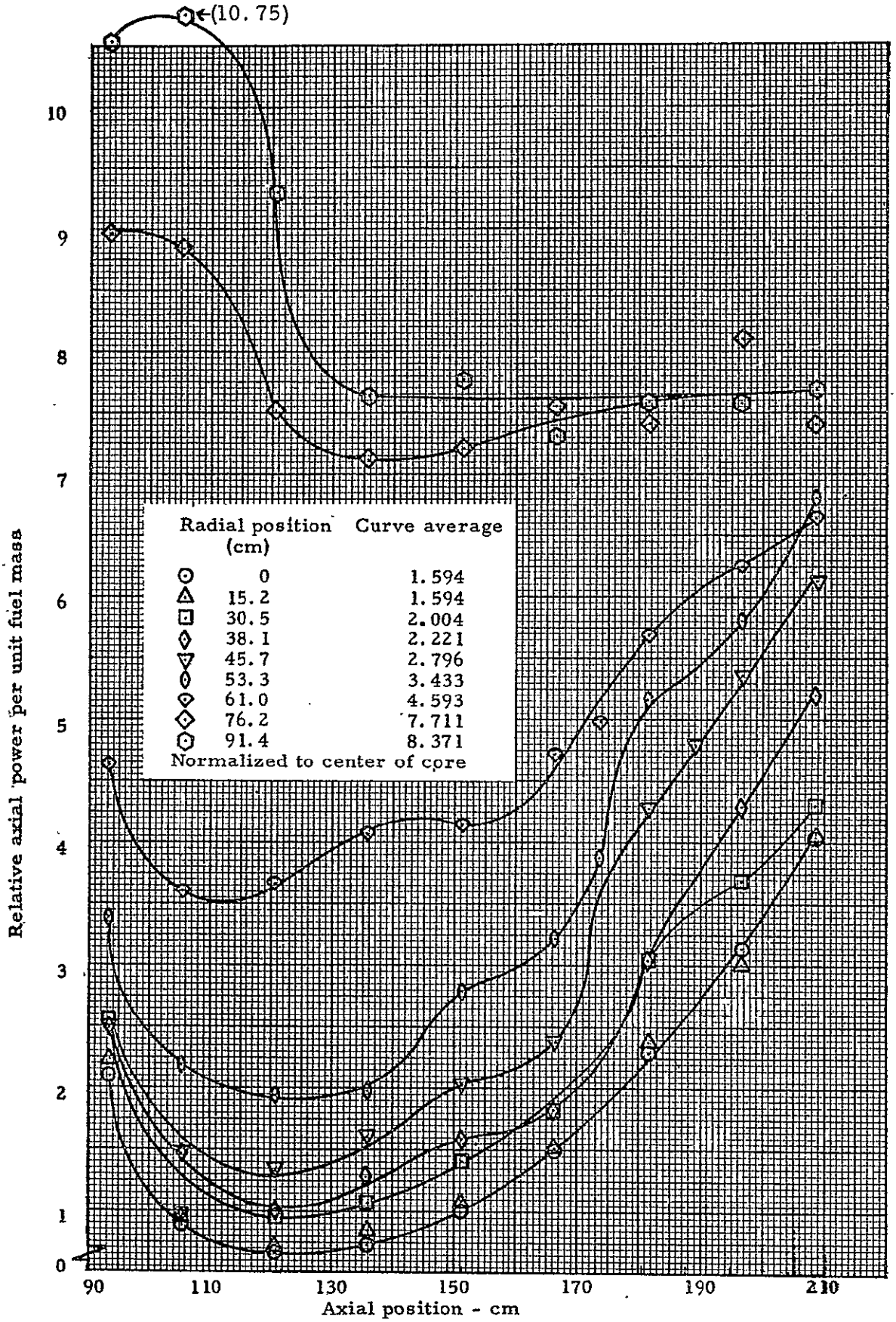

Fig. 7.1 Relative axial power distribution in the cavity region with exhaust nozzle tank in the reactor.

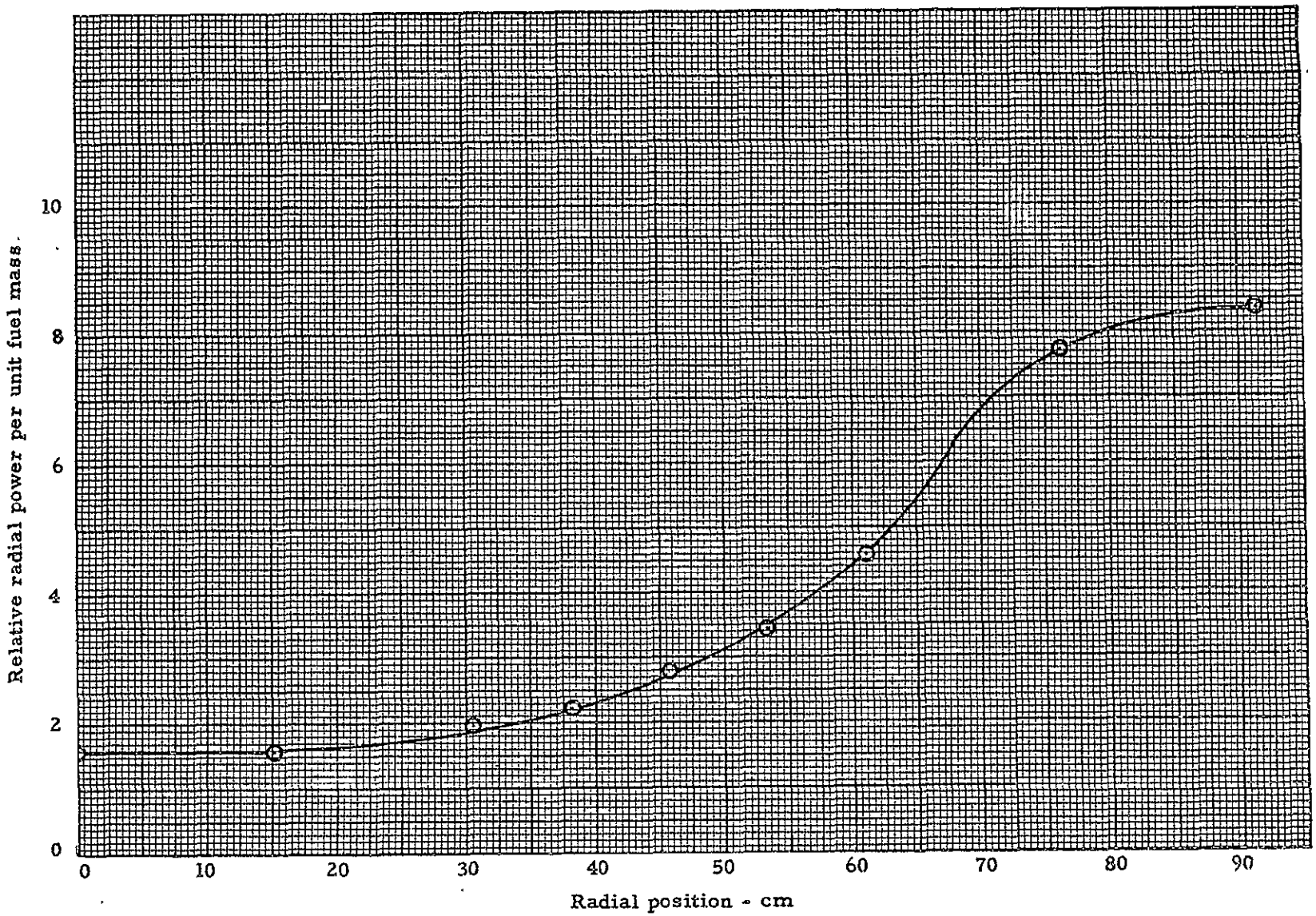

Fig. 7.2 Relative radial power distribution from average axial profile with exhaust nozzle tank in the reactor.

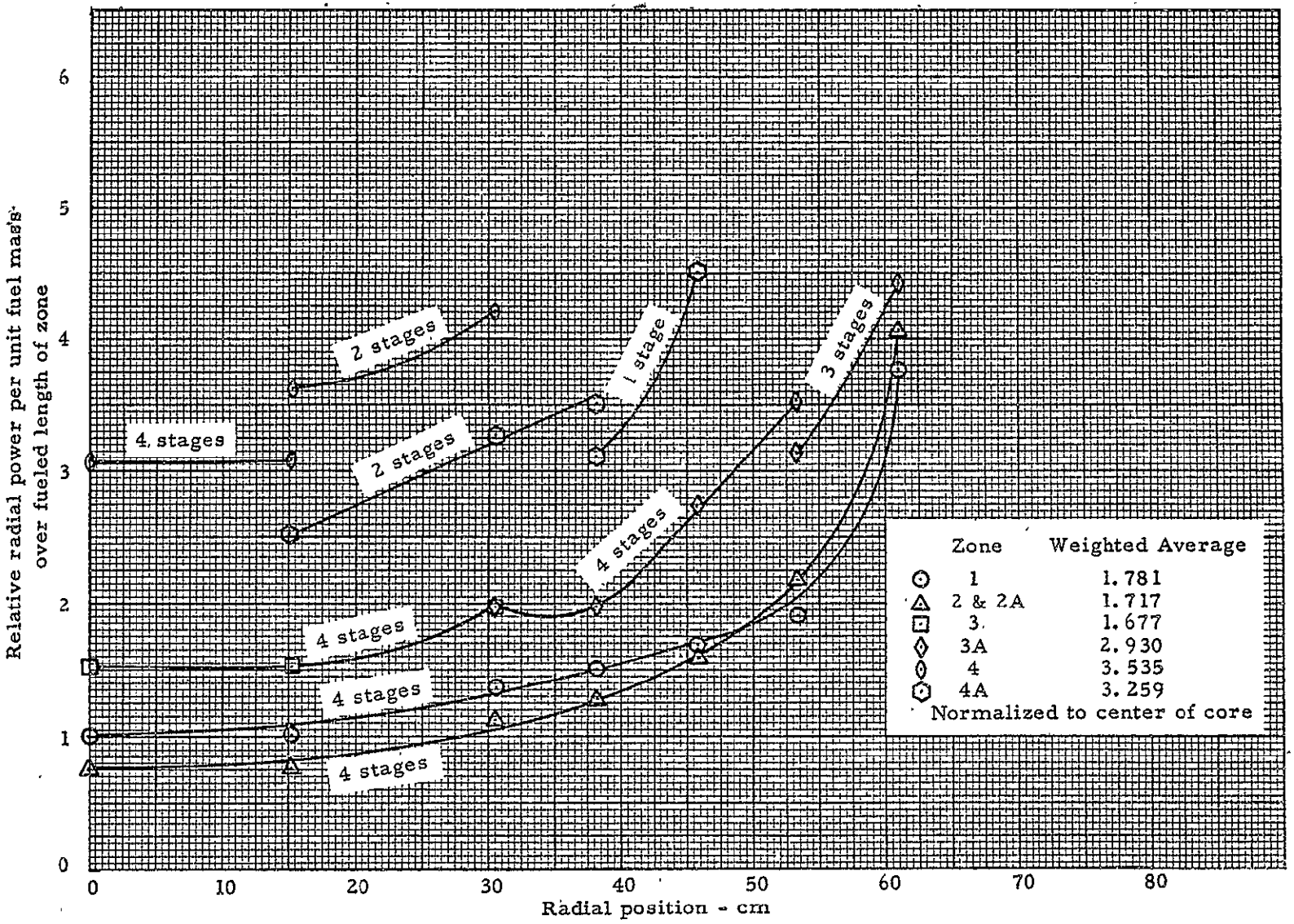

Fig. 7.3 Relative radial power distribution from axial averages over fueled zones with exhaust nozzle in the reactor.

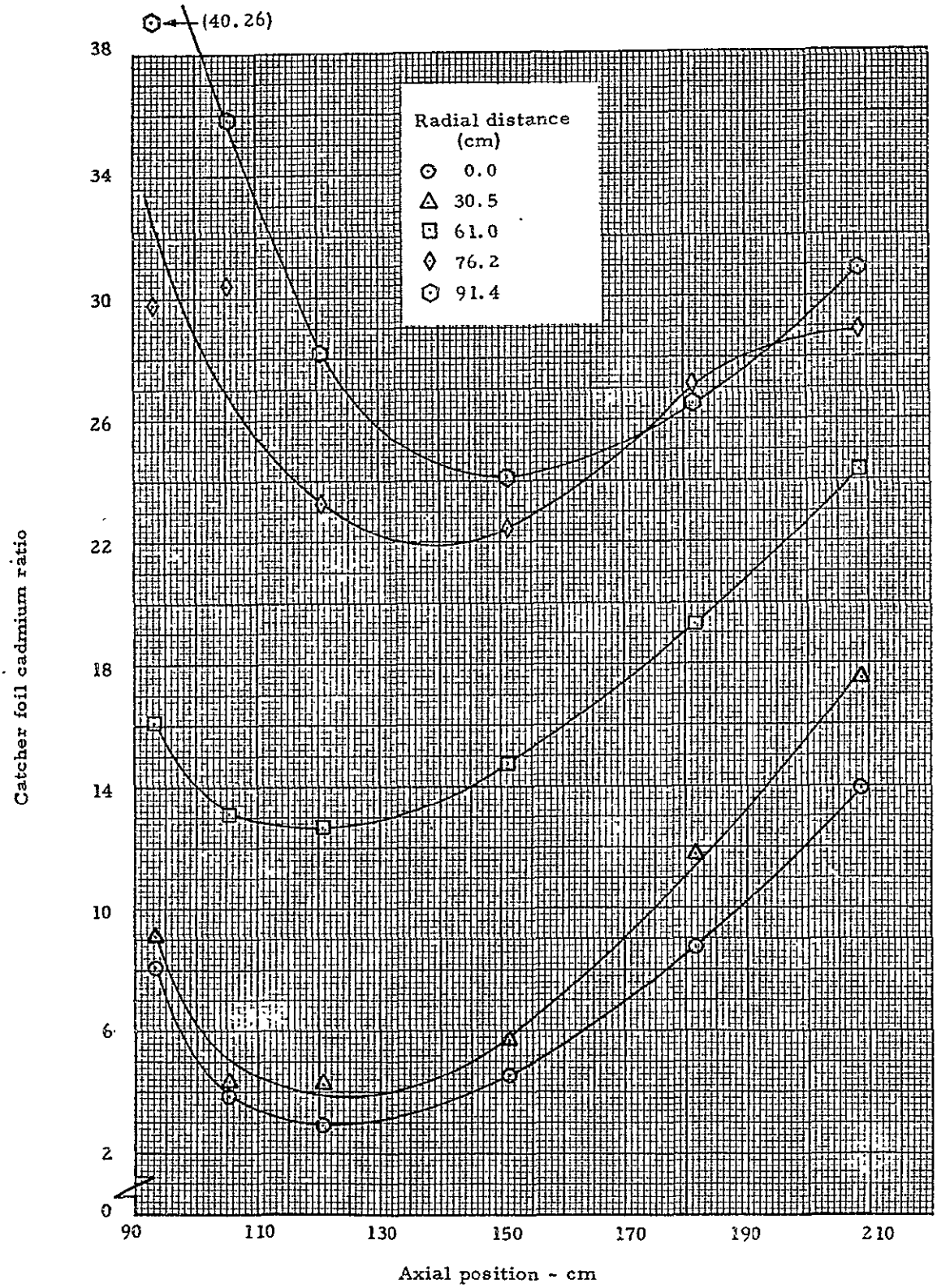

Fig. 7.4 Axial distribution of catcher foil cadmium ratios with exhaust nozzle tank in the reactor.

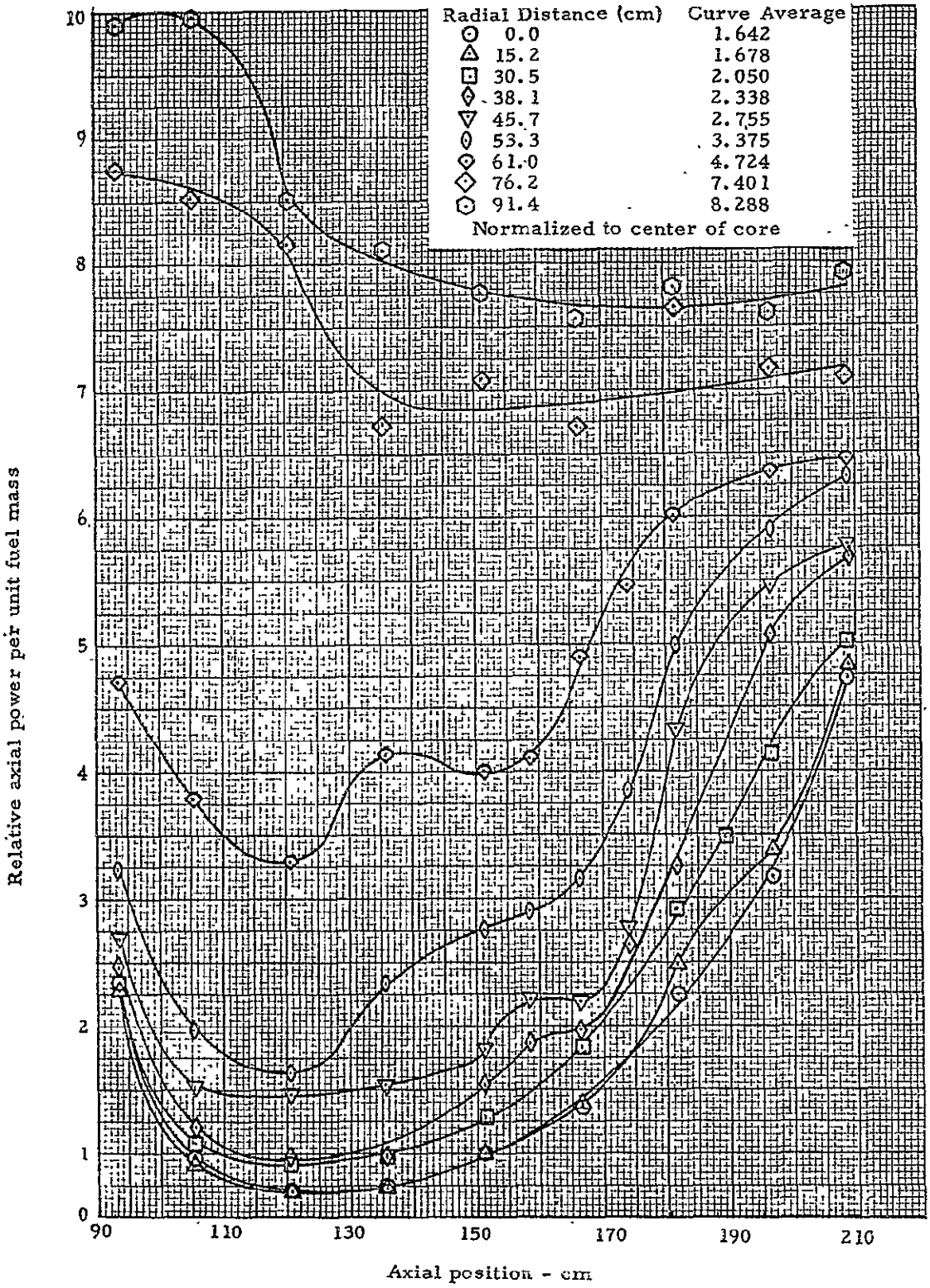

Fig. 7.5 Relative axial power distribution in the cavity region with exhaust nozzle tank removed.

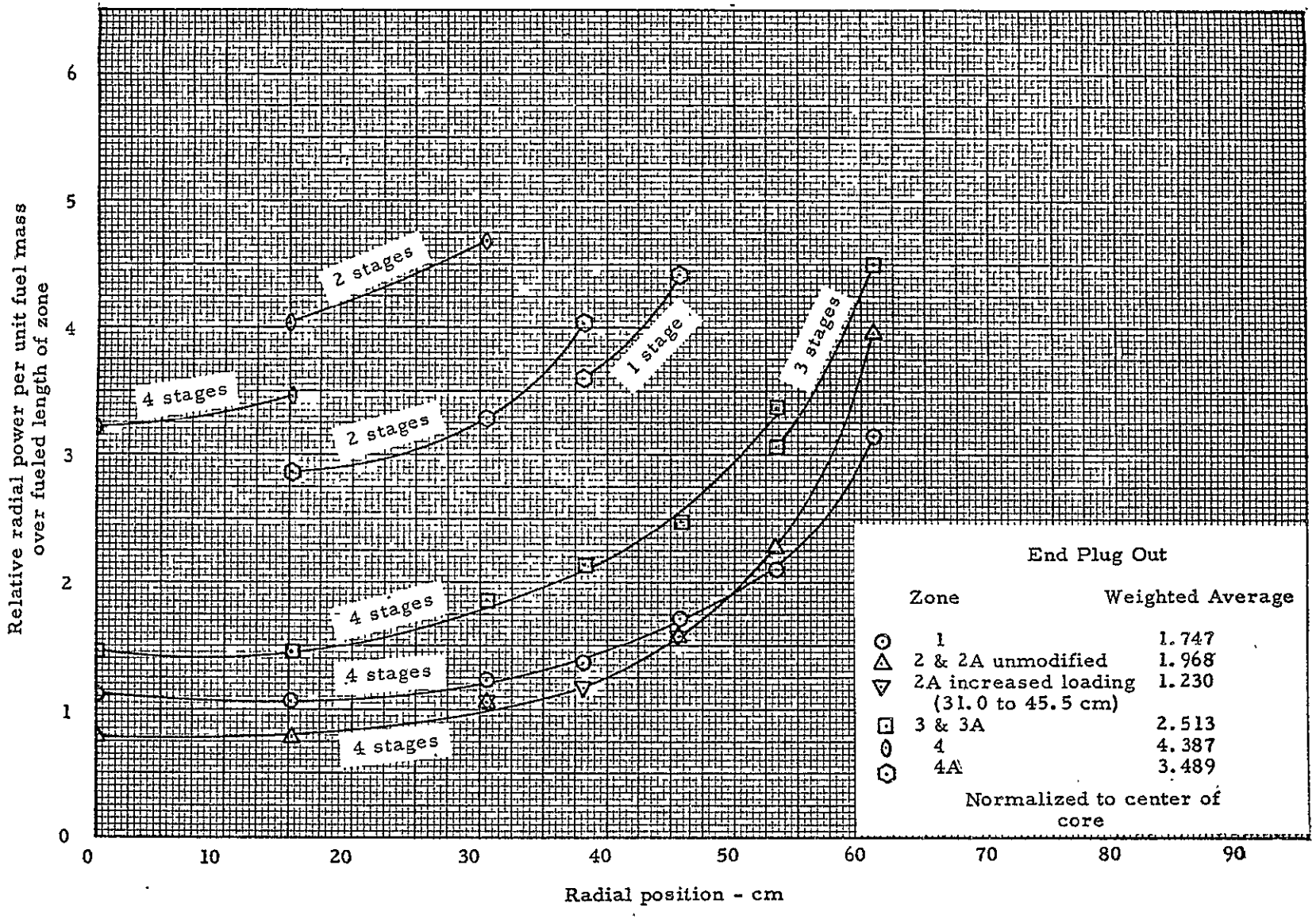

Fig. 7.6 Relative radial power distribution from axial averages over fueled zones with exhaust nozzle removed.

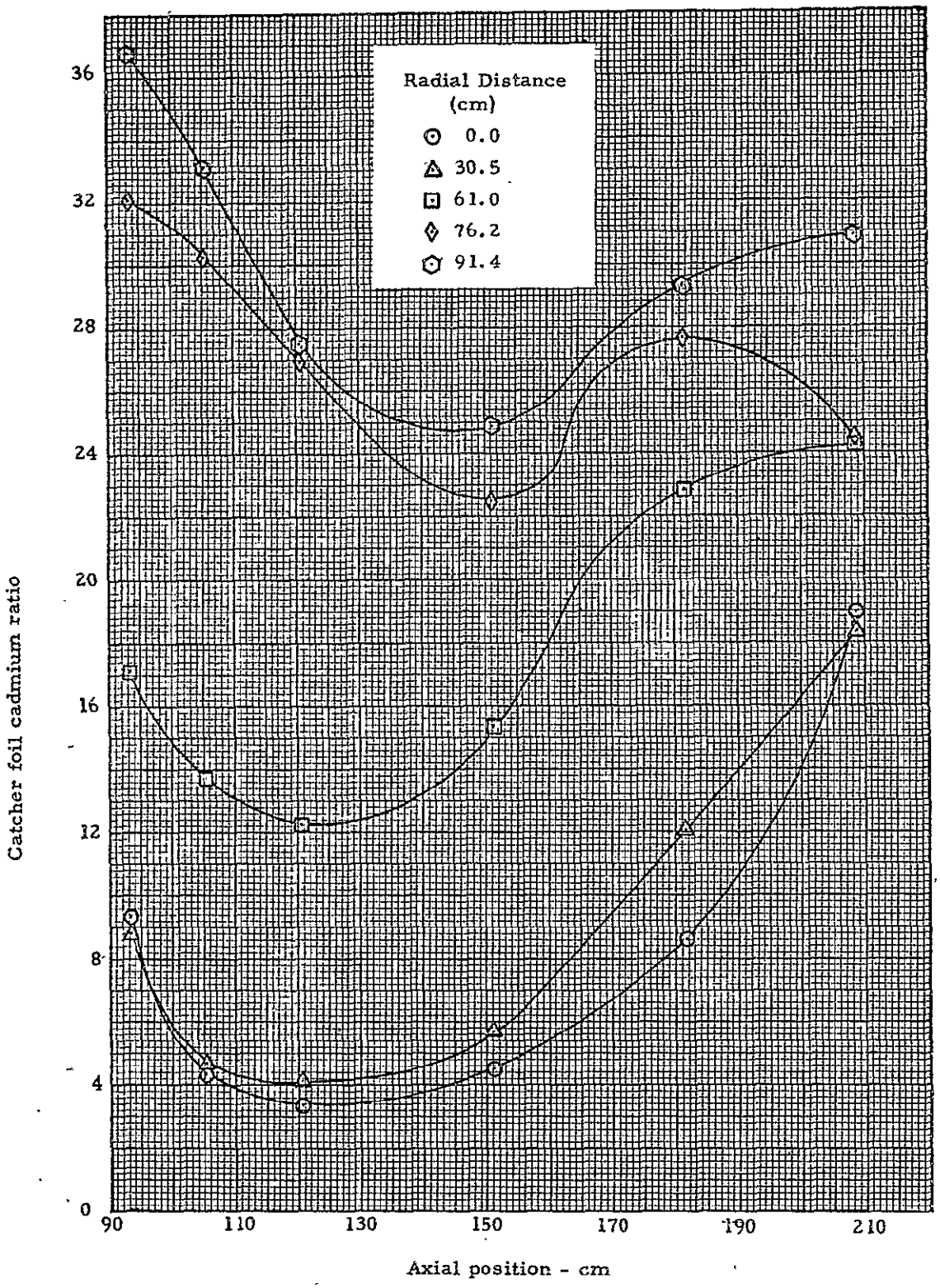

Fig. 7.7 Axial distribution of catcher foil cadmium ratios in the cavity region with the exhaust nozzle tank in the reactor.

8.0 RESONANCE DETECTORS

8.1 Bare Gold Foil (0.0005 cm thick) Data - Exhaust Nozzle in Reactor

Gold foils were exposed in the cavity region at essentially the same locations as catcher foils. In addition, measurements were made in the radial and end reflectors. Each foil exposure run included power normalizer catcher foils which were mounted between the two reactor tanks about midway into the radial reflector. These foils were used to correct the gold data for differences in power levels from run to run. These power normalization data are given in Table 8.1. There was a scram on Run 1158 after about 9 minutes of operation, so the normalization factor was obtained by comparing the bare gold data in the radial and end reflectors and forcing a fit to a smooth curve. Run 1162 was deliberately shortened to 10 minutes because it involved the exposure of bare catcher foils on the fuel annulus in the radial reflector and only relative values were needed. This table covers the foil exposure runs for both reactor configurations discussed in this report.

Table 8.2 contains the gold foil data with the exhaust nozzle in the reactor. The bare foils in the cavity were normalized to the point at the center of the core and the relative activity was plotted in Figure 8.1 to show the axial distribution at eight radial positions across the core. Each of the axial profiles was averaged as noted in Figure 8.1 and these averages were then plotted to show the relative radial profile across the cavity region as noted in Figure 8.2. The data appear to be similar to the power distribution (catcher foil data) with the irregular core boundary causing fluctuations in the points where the boundary changes.

The bare and cadmium gold foil results from the radial and end reflectors are given in Figures 8.3 and 8.4, respectively. Except for the point at 22.9 cm from the cavity wall in the end reflector, all of the points fall on or very near a smooth curve.

8.2 Gold Foil Cadmium Ratios - Exhaust Nozzle in Reactor

The gold foil cadmium ratios were measured at several locations in both the cavity and reflector regions. The activity on the bare and cadmium covered foils was converted to infinitely dilute activity as outlined in Section 4.4 of Reference 4, and then the ratio of the bare to cadmium covered foils was taken. These data are given in Table 8.3 and are also shown graphically in Figures 8.5 and 8.6. Within the cavity, the minimum cadmium ratio was around 1.5 and occurred at the radial center of the reactor near the end of the core opposite the separation plane.

The gold foil cadmium ratios in the reflectors were very much the same as has been observed before with a uniform core (Reference 1). The difference between the two reflectors is caused by the annulus of uranium in the radial reflector, the proximity of the core to the end reflector and the hydrogen in the cavity along the radial reflector. The first two effects tend to harden the flux, whereas the last tends to make the flux more thermal.

8.3 Bare Gold Foil (0.0005 cm thick) Data - Exhaust Nozzle Removed From Reactor

The gold foil data in the cavity region was not as extensive with the exhaust nozzle tank removed as with the tank in the reactor but sufficient data were taken to make some comparisons. Table 8.4 contains the foil data and Figure 8.7 shows the axial profiles at six radial positions. The averages from these axial profiles (plotted in Figure 8.8) compared to the configuration with the exhaust nozzle tank in the reactor shows that within the core there was an average decrease in the curve averages of 4.6 ± 0.8% while the averages in the hydrogen increased only slightly, about 1.0%. The addition of fuel (1.35 kg) to Zones 2A and 3 seems to be the main cause of the decrease in the core although part of this could also have been due to any data uncertainty associated with the foils near the core center to which the data were normalized. The ratio of the specific foil activities for these normalizer foils (plug out to plug in) was 0.955. The reduction in foil activity near the core center due to the increased fuel loading would be expected but conversely, an increase would normally have been expected from removing the exhaust nozzle plug. The fact that the value to which the foils were normalized was lower for the modified core with the exhaust nozzle plug removed than with the unmodified core and yet the curve averages were lower after the modification shows that there were measureable changes in the core fluxes due to the modifications.

The relative gold foil activity distributions in the end and radial reflectors are shown in Figures 8.9 and 8.10, respectively. A point by point comparison of these data and those from the unmodified core is given in Table 8.5. On the average, the modified core resulted in lower gold foil activities in the reflectors by 10.2 ± 4.7%. Such a decrease in reflector flux was noted in an earlier experiment (Reference 4, p. 167) when removing the exhaust nozzle plug. The decrease is considered to be due primarily to the exhaust nozzle tank and not the change in fuel loading. Removal of the tank allows more reflector flux to stream into the core, raising the core flux relative to the reflector flux, or conversely, giving lower reflector flux for the same core flux.

8.4 Gold Flux Cadmium Ratios - Exhaust Nozzle Removed from Reactor

Table 8.6 contains the gold foil cadmium ratios (infinitely dilute) which were measured with the exhaust nozzle tank removed and the increased fuel loading. Also given in the table are the calculated infinitely dilute foil activities. These cadmium ratios are plotted in Figures 8.11 and 8.12. In comparing these data with the same results prior to the plug removal and core modification (Table 8.6), it was found that the core center experienced a general decrease in cadmium ratio of around 4%, on the average. From a radius of 30.5 cm to the outer edge of the fuel (61.0 cm), the cadmium ratios increased slightly, about 4%. In the hydrogen and on the cavity wall, there was also an increase, amounting to about 7%. The central region of the core where the flux is "hardest" was even more so with the plug removed, principally because of the higher fuel loading. The outer portion of the core and hydrogen regions reflect the increase in thermal neutron flux due to the exhaust nozzle plug removal which allows these additional thermal neutrons to stream back into the reactor.

The reflector regions both experienced a decrease in cadmium ratio, showing an overall hardening of the neutron flux (cadmium ratio decreased by about 20%), which is consistent with earlier measurements (Reference 4, p. 167). Thus, the exhaust nozzle hole created extra streaming of thermal flux out of the reflector and into the cavity.

TABLE 8.1

Power Normalization Data

Run	Time	Decay Time (min)	Decay Factor	Activity (CPM)	Corrected Activity (CPM)	Normalization Factor
1157	1527.85	41.50	0.809	321148	259809	
	1529.85	43.50	0.852	304661	259571	
	1531.85	45.50	0.897	290317	260414	
				Avg.	259931	1.073
1158	Scrammed after about 9 minutes					1.173
1159	1536.35	44.50	0.874	319616	279344	
	1538.35	46.50	0.919	303256	278692	
	1540.35	48.50	0.965	288967	278853	
				Avg.	278963	1.000
1160	1225.47	61.00	1.258	219887	276618	
	1227.47	63.00	1.312	210706	276446	
	1229.46	65.00	1.366	202726	276924	
				Avg.	276663	1.008
1161	1508.27	63.50	1.326	204157	270712	
	1510.27	65.50	1.380	196889	271707	
	1513.27	68.50	1.460	188380	275035	
				Avg.	272485	1.024
1162	Short 10 minute run					
1163	1344.25	54.50	1.107	251911	278865	
	1346.75	57.00	1.169	239120	279531	
	1348.25	58.50	1.207	231702	279664	
					279353	0.999
1164	1545.25	36.50	0.705	394803	278336	
	1547.25	38.50	0.746	373132	278356	
	1549.25	40.50	0.788	352844	278041	
					278244	1.003
1165	1057.54	46.50	0.919	300206	275889	
	1059.04	48.00	0.953	289471	275866	
	1100.54	49.50	0.988	278480	275138	
					275631	1.012
1166	1414.62	70.00	1.500	184082	276123	
	1416.12	71.50	1.540	179290	276107	
	1417.62	73.00	1.580	174762	276124	
					276118	1.010
1167	1543.44	33.50	0.645	428310	276260	
	1545.44	35.50	0.685	404104	276811	
	1547.44	37.50	0.725	381110	276305	
					276459	1.009

TABLE 8.2

Gold Foil Data

Mockup of Flowing Gas Reactor

Foil Thickness 0.0005 cm

Exhaust Nozzle in Reactor

Foil No.	Type	Location Radial (cm)	Location Axial (cm)	Foil Weight	Specific Activity d/m/gm x 10^{-6}	Local to Foil (X)
Run 1157						
1	Bare	0	82.5	0.0194	5.783	
2	Bare	0	67.2	0.0205	7.222	
3	Bare	0	52.0	0.0164	5.923	
4	Bare	101.1	151.1	0.0153	7.598	
5	Bare	115.4	151.1	0.0167	7.203	
6	Bare	130.6	151.1	0.0167	5.316	
7	Bare	0	93.3	0.0192	2.058	1.254
8	Bare	0	105.3	0.0211	1.574	0.959
9	Bare	0	120.6	0.0193	1.422	0.867
10	Bare	0	135.8	0.0160	1.538	0.937
11	Bare	0	151.1	0.0178	1.641	1.000 (X)
12	Bare	0	166.3	0.01835	1.829	1.115
13	Bare	0	181.6	0.0158	2.320	1.414
14	Bare	0	196.8	0.01835	2.691	1.640
15	Bare	0	208.8	0.0171	3.159	1.925
16	Bare	30.5	93.3	0.0177	2.394	1.459
17	Bare	30.5	105.3	0.0202	1.583	0.965
18	Bare	30.5	120.6	0.0152	1.569	0.956
19	Bare	30.5	135.8	0.0177	1.675	1.021
20	Bare	30.5	151.1	0.0164	1.807	1.101
21	Bare	30.5	166.3	0.0193	1.920	1.170
22	Bare	30.5	181.6	0.0161	2.562	1.561
23	Bare	30.5	196.8	0.0161	3.150	1.920
24	Bare	30.5	208.8	0.0165	3.544	2.160
25	Bare	38.1	93.3	0.0156	2.416	1.472
26	Bare	38.1	105.3	0.0194	1.792	1.092
27	Bare	38.1	120.6	0.0206	1.590	0.969
28	Bare	38.1	135.8	0.0156	1.751	1.067
29	Bare	38.1	151.1	0.0154	1.944	1.185
30	Bare	38.1	166.3	0.0163	2.086	1.271
31	Bare	38.1	181.6	0.0146	2.374	1.447
32	Bare	38.1	196.8	0.01965	3.286	2.002
33	Bare	38.1	208.8	0.0164	3.691	2.249
34	Bare	45.7	93.3	0.0157	2.486	1.515

TABLE 8.2

(Continued)

Foil No.	Type	Location Radial (cm)	Location Axial (cm)	Foil Weight	Specific Activity d/m/gm x 10^{-6}	Local to Foil (X)
Run 1157						
35	Bare	45.7	105.3	0.0159	1.975	1.204
36	Bare	45.7	120.6	0.0152	1.871	1.140
37	Bare	45.7	135.8	0.0171	1.922	1.171
38	Bare	45.7	151.1	0.0134	2.161	1.317
39	Bare	45.7	166.3	0.0155	2.355	1.435
40	Bare	45.7	181.6	0.0143	3.013	1.836
41	Bare	45.7	196.8	0.0177	3.600	2.194
42	Bare	45.7	208.8	0.0163	3.841	2.341
43	Bare	53.3	93.3	0.0171	2.796	1.704
44	Bare	53.3	105.3	0.0193	2.045	1.246
45	Bare	53.3	120.6	0.0211	2.020	1.231
46	Bare	53.3	135.8	0.0142	2.173	1.324
47	Bare	53.3	151.1	0.0158	2.311	1.408
48	Bare	53.3	166.3	0.0153	5.010	3.053
49	Bare	53.3	181.6	0.0154	3.494	2.129
50	Bare	53.3	196.8	0.0182	3.695	2.252
51	Bare	53.3	208.8	0.0163	3.828	2.333
52	Bare	61.0	93.3	0.0171	3.179	1.937
53	Bare	61.0	105.3	0.0183	2.930	1.785
54	Bare	61.0	1206.	0.0200	2.692	1.640
55	Bare	61.0	135.8	0.0143	3.064	1.867
56	Bare	61.0	151.1	0.0162	3.195	1.947
57	Bare	61.0	166.3	0.0206	3.326	2.027
58	Bare	61.0	181.6	0.0161	3.629	2.211
59	Bare	61.0	196.8	0.0160	3.897	2.375
60	Bare	61.0	208.8	0.0197	3.857	2.350
61	Bare	76.2	93.3	0.0216	4.756	2.898
62	Bare	76.2	105.3	0.0200	4.570	2.785
63	Bare	76.2	120.6	0.0148	4.429	2.699
64	Bare	76.2	135.8	0.0178	4.300	2.620
65	Bare	76.2	151.1	0.0170	4.327	2.637
66	Bare	76.2	166.3	0.0147	4.335	2.642
67	Bare	76.2	181.6	0.0169	4.262	2.597
68	Bare	76.2	196.8	0.0166	4.163	2.537
69	Bare	76.2	208.8	0.0175	3.908	2.381
70	Bare	91.4	93.3	0.0187	5.474	3.336
71	Bare	91.4	105.3	0.01935	5.276	3.215
72	Bare	91.4	120.6	0.0202	4.685	2.855
73	Bare	91.4	135.8	0.0145	4.493	2.738
74	Bare	91.4	151.1	0.01555	4.795	2.922

TABLE 8.2

(Continued)

Foil No.	Type	Location Radial (cm)	Location Axial (cm)	Foil Weight	Specific Activity d/m/gm x 10^{-6}	Local to Foil (X)
Run 1157						
75	Bare	91.4	166.3	0.0162	4.509	2.748
76	Bare	91.4	181.6	0.0172	4.487	2.734
77	Bare	91.4	196.8	0.0178	4.304	2.623
78	Bare	91.4	208.8	0.0164	4.065	2.477
79	Cd	30.5	93.3	0.0137	1.566	
80	Cd	30.5	105.3	0.0146	1.416	
81	Cd	30.5	120.6	0.0156	1.343	
82	Cd	30.5	151.1	0.0147	1.441	
83	Cd	30.5	181.6	0.0161	1.487	
84	Cd	30.5	208.8	0.0164	1.689	
85	Cd	76.2	93.3	0.0147	1.700	
86	Cd	76.2	105.3	0.0162	1.869	
87	Cd	76.2	120.6	0.01735	1.873	
88	Cd	76.2	151.1	0.0198	1.754	
89	Cd	76.2	181.6	0.0163	1.749	
90	Cd	76.2	208.8	0.0204	1.487	
Run 1158						
1	Bare	0	89.4	0.0190	2.997	
2	Bare	0	74.9	0.0178	8.146	
3	Bare	0	59.6	0.0173	7.245	
4	Bare	0	44.4	0.0175	4.969	
5	Bare	0	29.1	0.0182	3.005	
6	Bare	0	13.9	0.0189	1.565	
7	Bare	0	0	0.0183	0.226	
8	Bare	93.2	151.1	0.0184	6.899	
9	Bare	107.7	151.1	0.0193	8.029	
10	Bare	123.0	151.1	0.0173	6.477	
11	Bare	138.2	151.1	0.0183	4.407	
12	Bare	153.5	151.1	0.0180	2.549	
13	Bare	168.7	151.1	0.0188	0.937	
14	Bare	183.9	151.1	0.0185	0.178	
15	Cd	61.0	93.3	0.0199	1.752	
16	Cd	61.0	105.3	0.0163	1.746	
17	Cd	61.0	120.6	0.01615	1.782	
18	Cd	61.0	151.1	0.0160	1.806	
19	Cd	61.0	181.6	0.0164	1.863	

TABLE 8.2

(Continued)

Foil No.	Type	Location Radial (cm)	Location Axial (cm)	Foil Weight	Specific Activity d/m/gm x 10^{-6}	Local to Foil (X)
Run 1158 (Cont'd)						
20	Cd	61.0	208.8	0.0169	1.844	
21	Cd	91.4	93.3	0.0161	1.805	
22	Cd	91.4	105.3	0.0141	2.083	
23	Cd	91.4	120.6	0.0153	2.164	
24	Cd	91.4	151.1	0.0174	2.042	
25	Cd	91.4	181.6	0.0153	1.961	
26	Cd	91.4	208.8	0.0187	1.506	
Run 1159						
1	Cd	0	89.4	0.0161	1.537	
2	Cd	0	59.6	0.0144	0.396	
3	Cd	0	29.1	0.0130	0.009	
4	Cd	93.2	151.1	0.0172	1.934	
5	Cd	123.0	151.1	0.0163	0.401	
6	Cd	153.5	151.1	0.0201	0.009	
Run 1160						
1	Cd	0	74.9	0.0184	1.574	
2	Cd	0	44.4	0.0174	0.084	
3	Cd	107.7	151.1	0.0184	1.339	
4	Cd	138.2	151.1	0.0221	0.076	
5	Cd	0	93.3	0.0172	1.422	
6	Cd	0	105.3	0.0182	1.198	
7	Cd	0	120.6	0.0169	1.174	
8	Cd	0	151.1	0.01975	1.224	
9	Cd	0	181.6	0.0167	1.394	
10	Cd	0	208.8	0.0136	1.683	

TABLE 8.3

Gold Foil Cadmium Ratios

Mockup of Flowing Gas Reactor

Exhaust Nozzle in Reactor

Location		Infinitely Dilute Foil Activity $d/m/gm \times 10^{-6}$		
Radial (cm)	Axial (cm)	Bare Foil	Cadmium Foil	Cadmium Ratio
0	93.3	3.220	2.530	1.272
0	105.3	2.611	2.174	1.201
0	120.6	2.377	2.076	1.145
0	151.1	2.657	2.286	1.163
0	181.6	3.360	2.465	1.363
0	208.8	4.370	2.772	1.577
30.5	93.3	3.540	2.585	1.370
30.5	105.3	2.701	2.386	1.132
30.5	120.6	2.527	2.312	1.093
30.5	151.1	2.850	2.433	1.171
30.5	181.6	3.662	2.587	1.416
30.5	208.8	4.815	2.957	1.628
61.0	93.3	4.617	3.280	1.406
61.0	105.3	4.302	3.051	1.410
61.0	120.6	4.142	3.105	1.334
61.0	151.1	4.532	3.136	1.445
61.0	181.6	5.016	3.262	1.538
61.0	208.8	5.370	3.261	1.647
76.2	93.3	6.138	2.870	2.138
76.2	105.3	6.091	3.259	1.869
76.2	120.6	5.796	3.343	1.734
76.2	151.1	5.755	3.278	1.756
76.2	181.6	5.590	3.056	1.829
76.2	208.8	5.148	2.809	1.832
91.4	93.3	6.900	3.141	2.197
91.4	105.3	6.874	3.470	1.981
91.4	120.6	6.420	3.702	1.734
91.4	151.1	6.320	3.648	1.733
91.4	181.6	5.956	3.355	1.775
91.4	208.8	5.248	2.758	1.903
0	98.7	4.219	2.674	1.578
0	74.9	9.420	2.867	3.286
0	59.6	7.537	0.664	11.35
0	44.4	5.035	0.150	33.56
0	29.1	3.012	0.015	206.1
93.2	151.1	8.451	3.441	2.456
107.7	151.1	9.151	2.439	3.752
123.0	151.1	6.785	0.701	9.684
138.2	151.1	4.474	0.148	30.26
153.5	151.1	2.557	0.017	151.2

TABLE 8.4

Gold Foil Data

Mockup of Flowing Gas Reactor

Foil Thickness 0.0005 cm

Exhaust Nozzle Removed

Foil No.	Type	Location Radial (cm)	Location Axial (cm)	Foil Weight	Specific Activity d/m/gm x 10^{-6}	Local to Foil (X)
Run 1163.						
1	Bare	0	82.5	0.0187	5.465	
2	Bare	0	67.2	0.0199	6.858	
3	Bare	0	52.0	0.0159	5.280	
4	Bare	101.1	151.1	0.0141	6.977	
5	Bare	115.4	151.1	0.0168	6.773	
6	Bare	130.6	151.1	0.01995	5.036	
7	Bare	0	93.3	0.0164	1.975	1.260
8	Bare	0	105.3	0.0208	1.432	0.914
9	Bare	0	120.6	0.0187	1.289	0.823
10	Bare	0	135.8	0.0185	1.367	0.872
11	Bare	0	151.1	0.0160	1.567	1.000 (X)
12	Bare	0	166.3	0.0169	1.699	1.084
13	Bare	0	181.6	0.0161	2.130	1.359
14	Bare	0	196.8	0.0212	2.328	1.486
15	Bare	0	208.8	0.0179	2.973	1.897
16	Bare	30.5	93.3	0.0186	2.137	1.364
17	Bare	30.5	105.3	0.0156	1.646	1.050
18	Bare	30.5	120.6	0.01395	1.549	0.989
19	Bare	30.5	135.8	0.0202	1.438	0.918
20	Bare	30.5	151.1	0.0189	1.584	1.011
21	Bare	30.5	166.3	0.0163	1.940	1.238
22	Bare	30.5	181.6	0.0158	2.359	1.505
23	Bare	30.5	196.8	0.0171	2.879	1.837
24	Bare	30.5	208.8	0.0134	3.452	2.203
25	Bare	45.7	93.3	0.0196	2.232	1.424
26	Bare	45.7	105.3	0.0178	1.817	1.160
27	Bare	45.7	120.6	0.0190	1.750	1.117
28	Bare	45.7	135.8	0.0180	1.768	1.128
29	Bare	45.7	151.1	0.01625	1.989	1.269
30	Bare	45.7	166.3	0.0205	2.167	1.383
31	Bare	45.7	181.6	0.0198	2.796	1.784
32	Bare	45.7	196.8	0.0149	3.445	2.198
33	Bare	45.7	208.8	0.0123	3.754	2.396
34	Bare	61.0	93.3	0.0203	2.987	1.906

TABLE 8.4

(Continued)

Foil No.	Type	Location Radial (cm)	Location Axial (cm	Foil Weight	Specific Activity d/m/gm x 10^{-6}	Local to Foil (X)
Run 1163 (Cont'd)						
35	Bare	61.0	105.3	0.0182	2.572	1.641
36	Bare	61.0	120.6	0.0163	2.614	1.668
37	Bare	61.0	135.8	0.0180	2.778	1.773
38	Bare	61.0	151.1	0.0200	2.755	1.771
39	Bare	61.0	166.3	0.0176	2.960	1.889
40	Bare	61.0	181.6	0.0146	3.474	2.217
41	Bare	61.0	196.8	0.0151	3.674	2.345
42	Bare	61.0	208.8	0.0162	3.685	2.352
43	Bare	76.2	93.3	0.0175	4.729	3.018
44	Bare	76.2	105.3	0.0176	4.587	2.927
45	Bare	76.2	120.6	0.0155	4.282	2.733
46	Bare	76.2	135.8	0.0175	4.136	2.639
47	Bare	76.2	151.1	0.0157	4.101	2.617
48	Bare	76.2	166.3	0.0193	3.884	2.479
49	Bare	76.2	181.6	0.0185	3.959	2.526
50	Bare	76.2	196.8	0.0155	4.092	2.611
51	Bare	76.2	208.8	0.0191	3.881	2.477
52	Bare	91.4	93.3	0.0184	5.058	3.228
53	Bare	91.4	105.3	0.0175	5.199	3.318
54	Bare	91.4	120.6	0.0164	4.827	3.080
55	Bare	91.4	135.8	0.0177	4.274	2.727
56	Bare	91.4	151.1	0.0148	4.418	2.819
57	Bare	91.4	166.3	0.0157	4.283	2.733
58	Bare	91.4	181.6	0.0185	4.225	2.696
59	Bare	91.4	196.8	0.0145	4.110	2.623
60	Bare	91.4	208.8	0.0163	4.064	2.593
61	Cd cov	30.5	93.3	0.0155	1.409	
62	Cd cov	30.5	105.3	0.0152	1.296	
63	Cd cov	30.5	120.6	0.0168	1.218	
64	Cd cov	30.5	151.1	0.0203	1.193	
65	Cd cov	30.5	181.6	0.0196	1.346	
66	Cd cov	30.5	208.8	0.0178	1.575	
67	Cd cov	76.2	93.3	0.0154	1.661	
68	Cd cov	76.2	105.3	0.0158	1.745	
69	Cd cov	76.2	120.6	0.0186	1.646	
70	Cd cov	76.2	151.1	0.0122	1.848	
71	Cd cov	76.2	181.6	0.0162	1.620	
72	Cd cov	76.2	208.8	0.0191	1.454	

TABLE 8.4

(Continued)

Foil No.	Type	Location Radial (cm)	Location Axial (cm)	Foil Weight	Specific Activity d/m/gm x 10^{-6}	Local to Foil (X)
Run 1165						
1	Bare	0	89.4	0.0133	2.838	
2	Bare	0	74.9	0.0139	6.965	
3	Bare	0	59.6	0.0131	6.098	
4	Bare	0	44.4	0.0143	4.465	
5	Bare	0	29.1	0.0129	2.810	
6	Bare	0	13.0	0.0210	1.397	
7	Bare	0	0	0.0189	0.204	
8	Bare	93.2	151.1	0.0179	5.329	
9	Bare	107.7	151.1	0.0175	6.998	
10	Bare	123.0	151.1	0.0204	5.778	
11	Bare	138.2	151.1	0.0152	3.929	
12	Bare	153.5	151.1	0.0211	2.221	
13	Bare	168.7	151.1	0.0171	0.913	
14	Bare	183.9	151.1	0.0171	0.146	
15	Cd cov	61.0	93.3	0.0136	1.584	
16	Cd cov	61.0	105.3	0.0210	1.368	
17	Cd cov	61.0	120.6	0.0142	1.555	
18	Cd cov	61.0	151.1	0.0133	1.591	
19	Cd cov	61.0	181.6	0.0163	1.541	
20	Cd cov	61.0	208.8	0.0165	1.541	
21	Cd cov	91.4	93.3	0.0182	1.479	
22	Cd cov	91.4	105.3	0.0166	1,687	
23	Cd cov	91.4	120.6	0.0156	1.784	
24	Cd cov	91.4	151.1	0.0206	1.625	
25	Cd cov	91.4	181.6	0.0158	1.617	
26	Cd cov	91.4	208.8	0.0176	1.272	
Run 1166						
1	Cd cov	0	89.4	0.0175	1.518	
2	Cd cov	0	59.6	0.0177	0.374	
3	Cd cov	0	29.1	0.0198	0.0103	
4	Cd cov	93.2	151.1	0.0172	1.803	
5	Cd cov	123.0	151.1	0.0153	0.467	
6	Cd cov	153.5	151.1	0.0189	0.0117	
Run 1167						
1	Cd cov	107.7	151.1	0.0136	1.465	
2	Cd cov	138.2	151.1	0.0159	0.088	
3	Cd cov	0	74.9	0.0174	1.683	

TABLE 8.4

(Continued)

Foil No.	Type	Location Radial (cm)	Location Axial (cm)	Foil Weight	Specific Activity d/m/gm x 10^{-6}	Local to Foil (X)
Run 1167 (Cont'd)						
4	Cd cov	0	44.4	0.0211	0.088	
5	Cd cov	0	93.3	0.0208	1.254	
6	Cd cov	0	105.3	0.0154	1.233	
7	Cd cov	0	120.6	0.0169	1.115	
8	Cd cov	0	151.1	0.0173	1.215	
9	Cd cov	0	181.6	0.0168	1.329	
10	Cd cov	0	208.8	0.0136	1.882	

TABLE 8.5

Comparison of Gold Foil Data

In Reflectors With the Exhaust Nozzle Plug In and Out of the Reactor

Location		Bare Gold Foil (0.0005 cm thick) Activity (d/m/g x 10^{-6})		Ratio Plug Out to Plug In
Radial (cm)	Axial (cm)	Plug In	Plug Out	
0	89.4	2.997	2.838	0.947
0	82.5	5.783	5.465	0.945
0	74.9	8.146	6.965	0.855
0	67.2	7.222	6.858	0.950
0	59.6	7.245	6.098	0.842
0	52.0	5.923	5.280	0.891
0	44.4	4.969	4.465	0.899
0	29.1	3.005	2.810	0.935
0	13.0	1.565	1.397	0.893
0	0	0.226	0.204	0.903
93.2	151.1	6.899	5.329	0.772
101.1	151.1	7.598	6.977	0.918
107.7	151.1	8.029	6.998	0.872
115.4	151.1	7.203	6.773	0.940
123.0	151.1	6.477	5.778	0.892
130.6	151.1	5.316	5.036	0.947
138.2	151.1	4.407	3.929	0.892
153.5	151.1	2.549	2.221	0.871
168.7	151.1	0.937	0.913	0.974
183.9	151.1	0.178	0.146	0.820
				0.898 ± 0.047

Gold Foil Cadmium Ratios

Mockup of Flowing Gas Reactor

Exhaust Nozzle Tank Removed from Reactor

Location		Infinitely Dilute Foil Activity d/m/gm x 10^{-6}			
Radial (cm)	Axial (cm)	Bare Foil	Cadmium Foil	Cadmium Ratio	Ratio Plug Out to Plug In
0	93.3	2.998	2.386	1.257	0.988
0	105.3	2.435	2.114	1.152	0.959
0	120.6	2.184	1.972	1.108	0.968
0	151.1	2.486	2.166	1.147	0.986
0	181.6	3.128	2.346	1.333	0.978
0	208.8	4.354	3.100	1.405	0.891
30.5	93.3	3.234	2.421	1.336	0.975
30.5	105.3	2.573	2.212	1.163	1.027
30.5	120.6	2.401	2.150	1.117	1.022
30.5	151.1	2.610	2.250	1.160	0.991
30.5	181.6	3.416	2.507	1.363	0.963
30.5	208.8	4.558	2.836	1.607	0.987
61.0	93.3	4.212	2.609	1.615	1.149
61.0	105.3	3.744	2.612	1.434	1.017
61.0	120.6	3.724	2.596	1.434	1.075
61.0	151.1	3.970	2.602	1.526	1.056
61.0	181.6	4.568	2.692	1.697	1.103
61.0	208.8	4.837	2.703	1.789	1.086
76.2	93.3	5.986	2.848	2.102	0.983
76.2	105.3	5.922	3.017	1.963	1.050
76.2	120.6	5.540	3.009	1.841	1.062
76.2	151.1	5.338	2.943	1.814	1.033
76.2	181.6	5.236	2.825	1.854	1.014
76.2	208.8	5.110	2.683	1.905	1.040
91.4	93.3	6.268	2.683	2.336	1.063
91.4	105.3	6.508	2.966	2.194	1.108
91.4	120.6	6.144	3.072	2.000	1.153
91.4	151.1	5.677	3.079	1.844	1.064
91.4	181.6	5.489	2.796	1.963	1.106
91.4	208.8	5.040	2.281	2.209	1.161
0	89.4	3.894	2.717	1.433	0.908
0	74.9	8.159	3.006	2.714	0.826
0	59.6	6.357	0.672	9.460	0.833
0	44.4	4.533	0.168	26.94	0.803
0	29.1	2.817	0.019	146.4	0.710
93.2	151.1	6.759	3.208	2.107	0.858
107.7	151.1	8.063	2.413	3.342	0.891
123.0	151.1	6.154	0.799	7.703	0.795
138.2	151.1	3.992	0.152	26.2	0.866
153.5	151.1	2.231	0.022	103.7	0.686

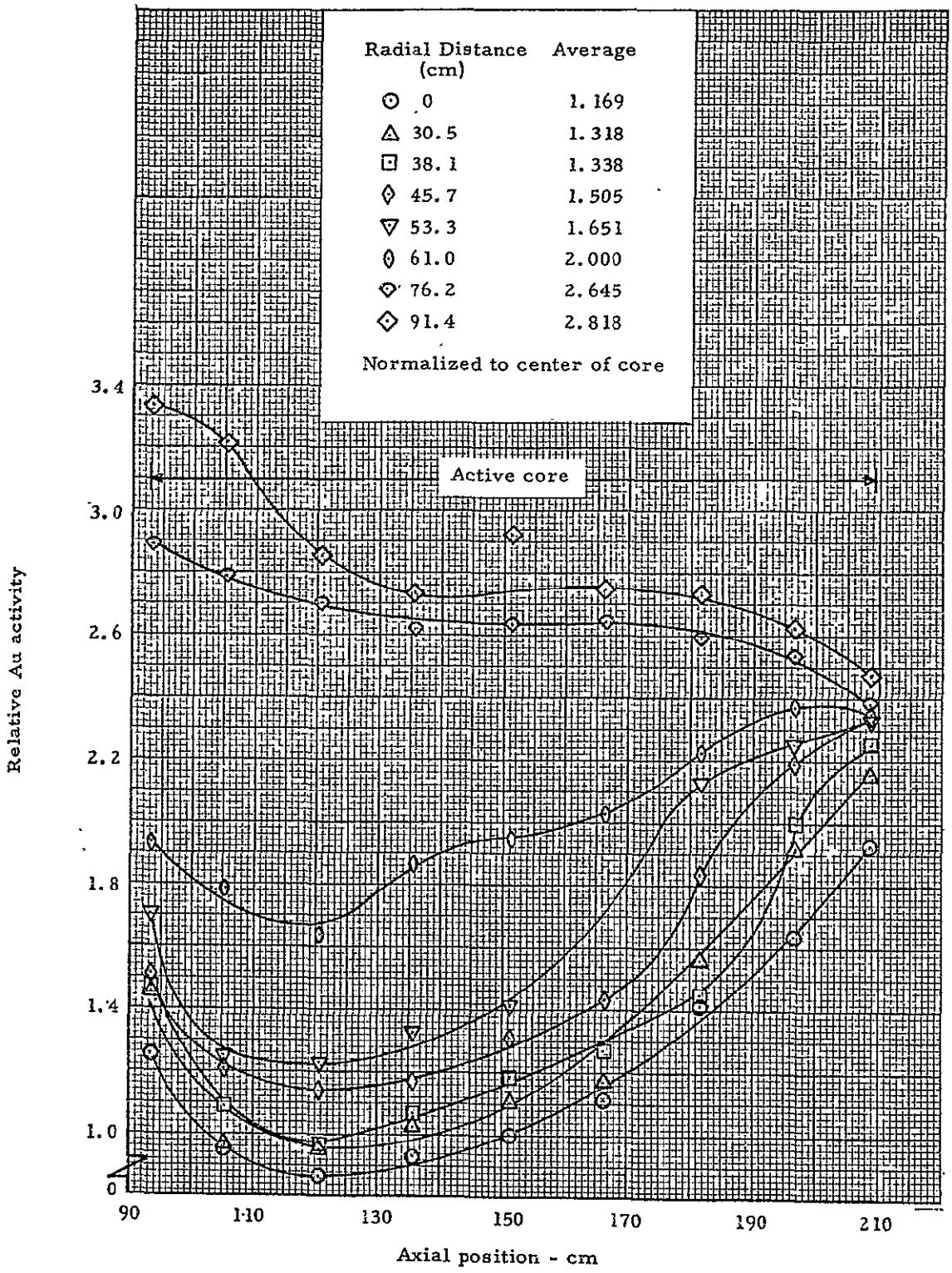

Fig. 8.1 Relative axial distribution of gold foil activity in the cavity region with the exhaust nozzle tank in the reactor.

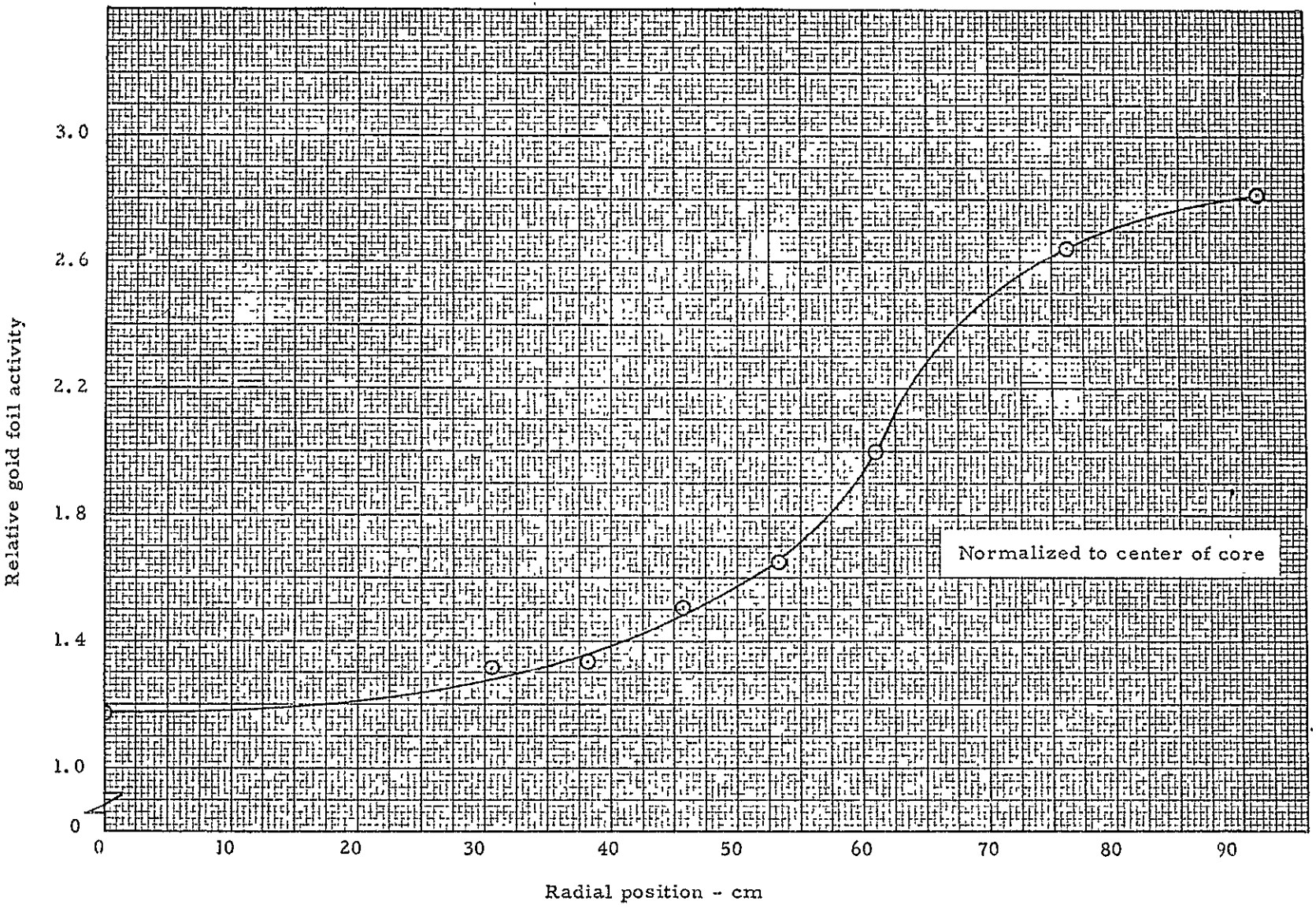

Fig. 8.2 Relative radial distribution of gold foil activity within the cavity region with the exhaust nozzle tank in the reactor.

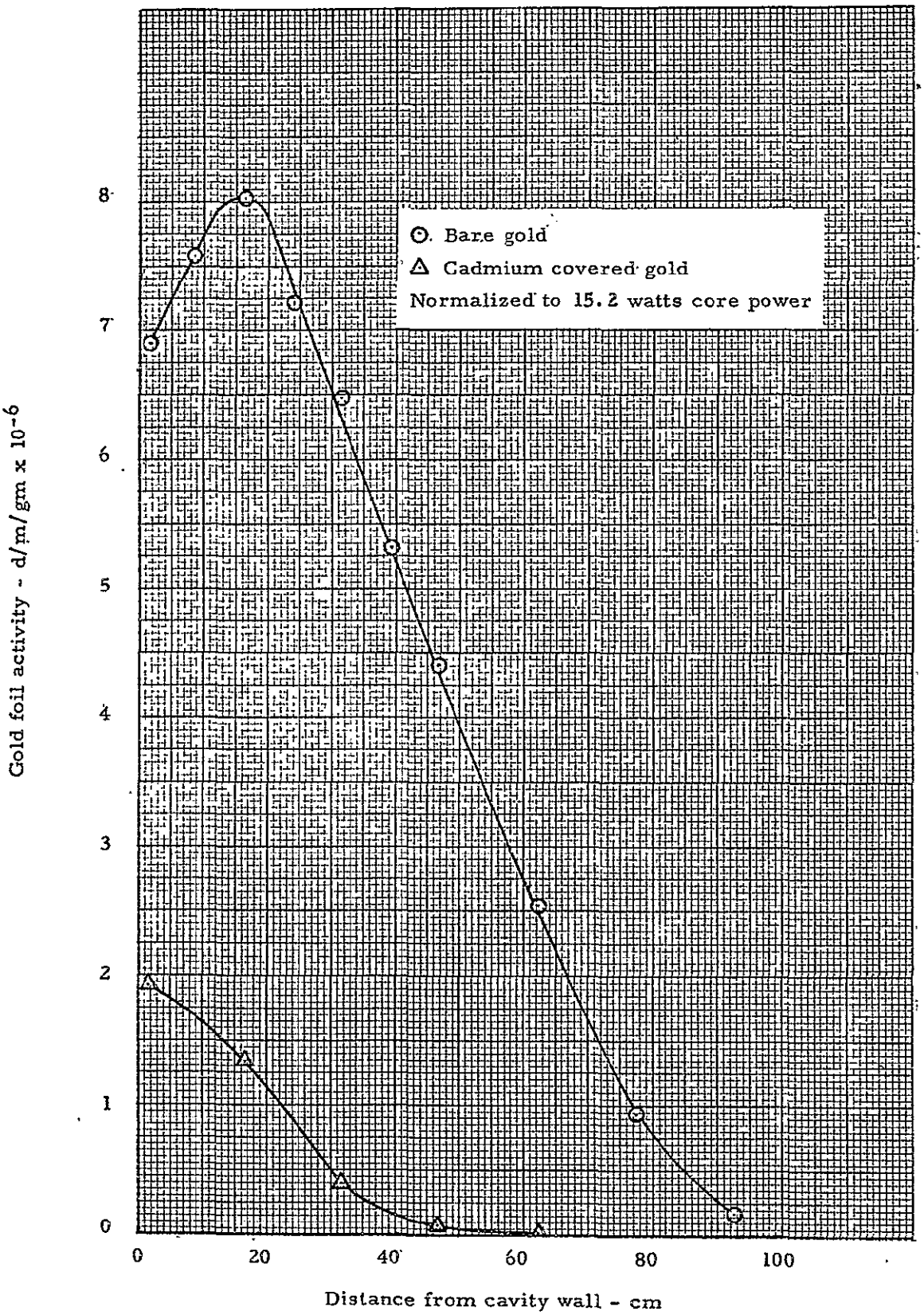

Fig. 8.3 Gold foil activity distribution in the radial reflector with the exhaust nozzle tank in the reactor.

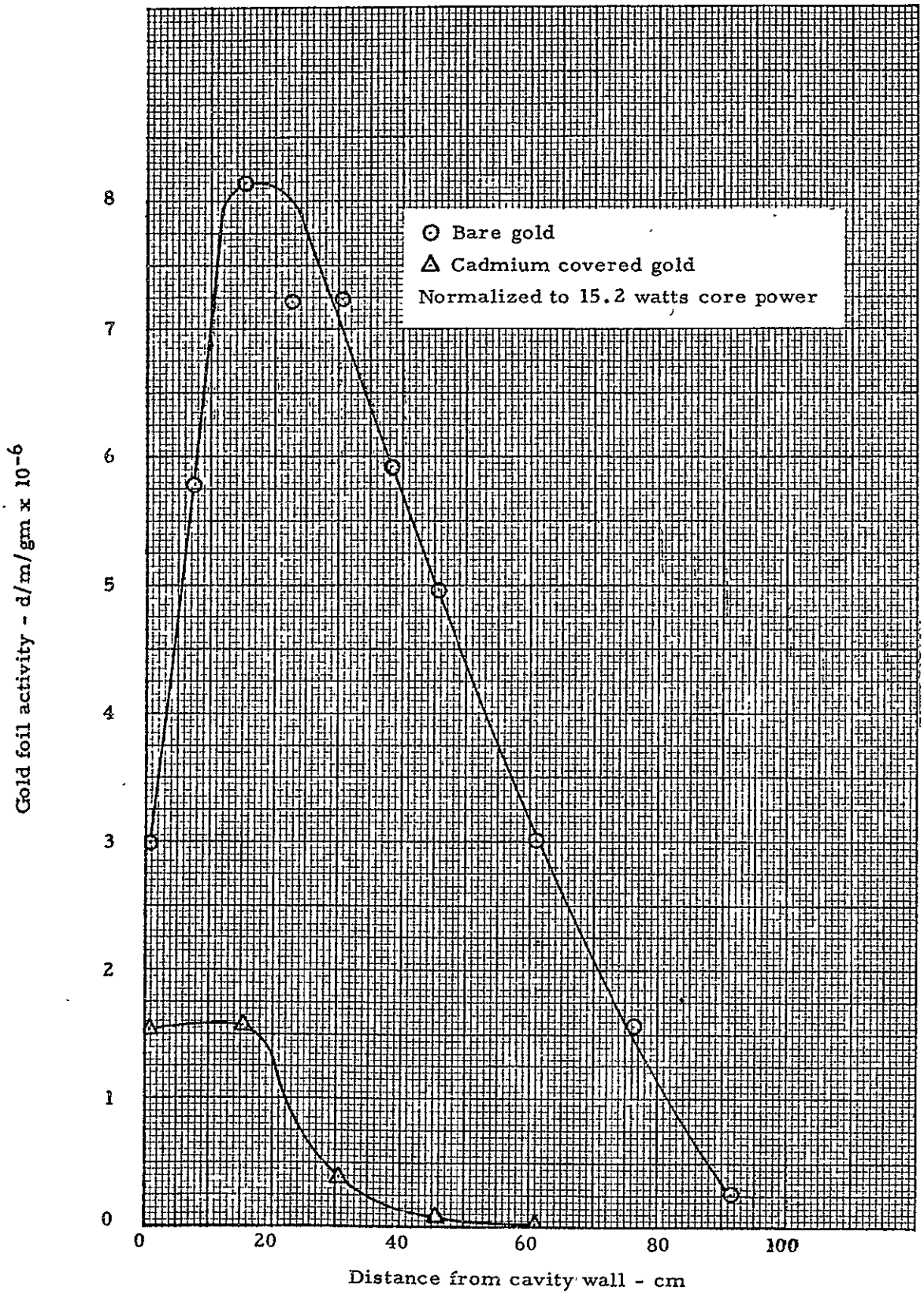

Fig. 8.4 Gold foil activity distribution in the end reflector with the exhaust nozzle tank in the reactor.

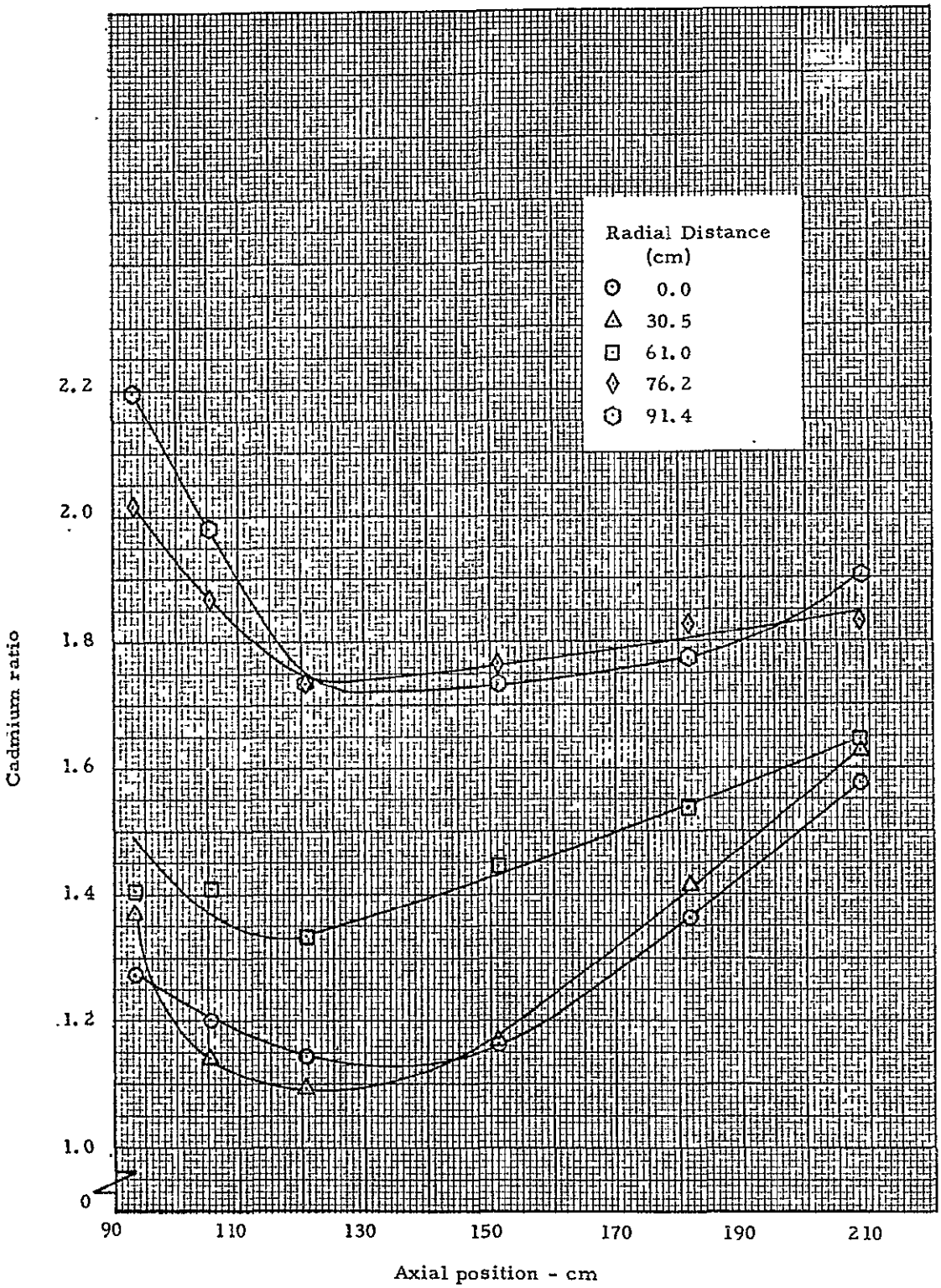

Fig. 8.5 Gold foil cadmium ratios in the cavity region with the exhaust nozzle tank in the reactor.

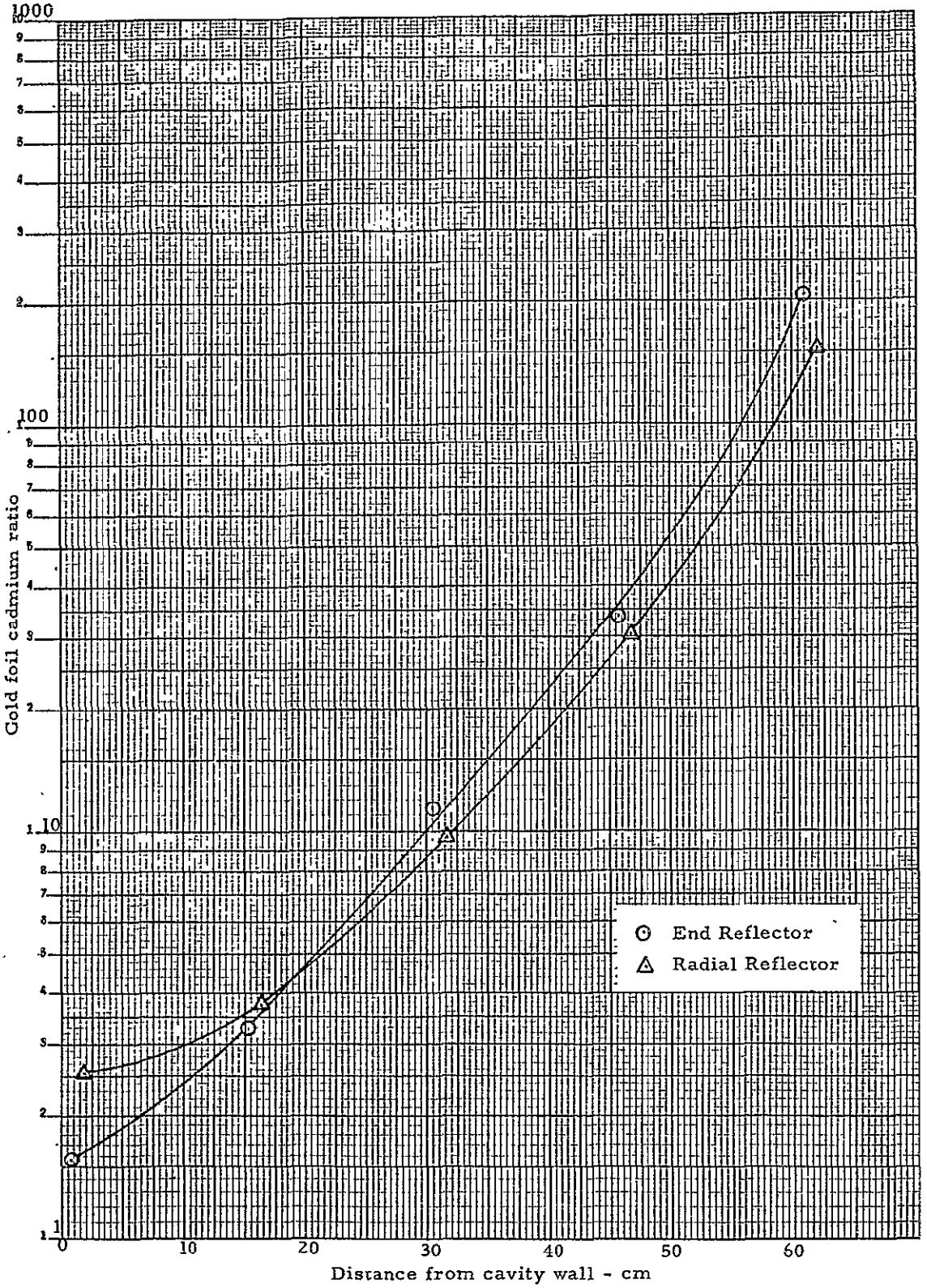

Fig. 8.6 Gold foil cadmium ratios in the reflector regions with the exhaust nozzle tank in the reactor.

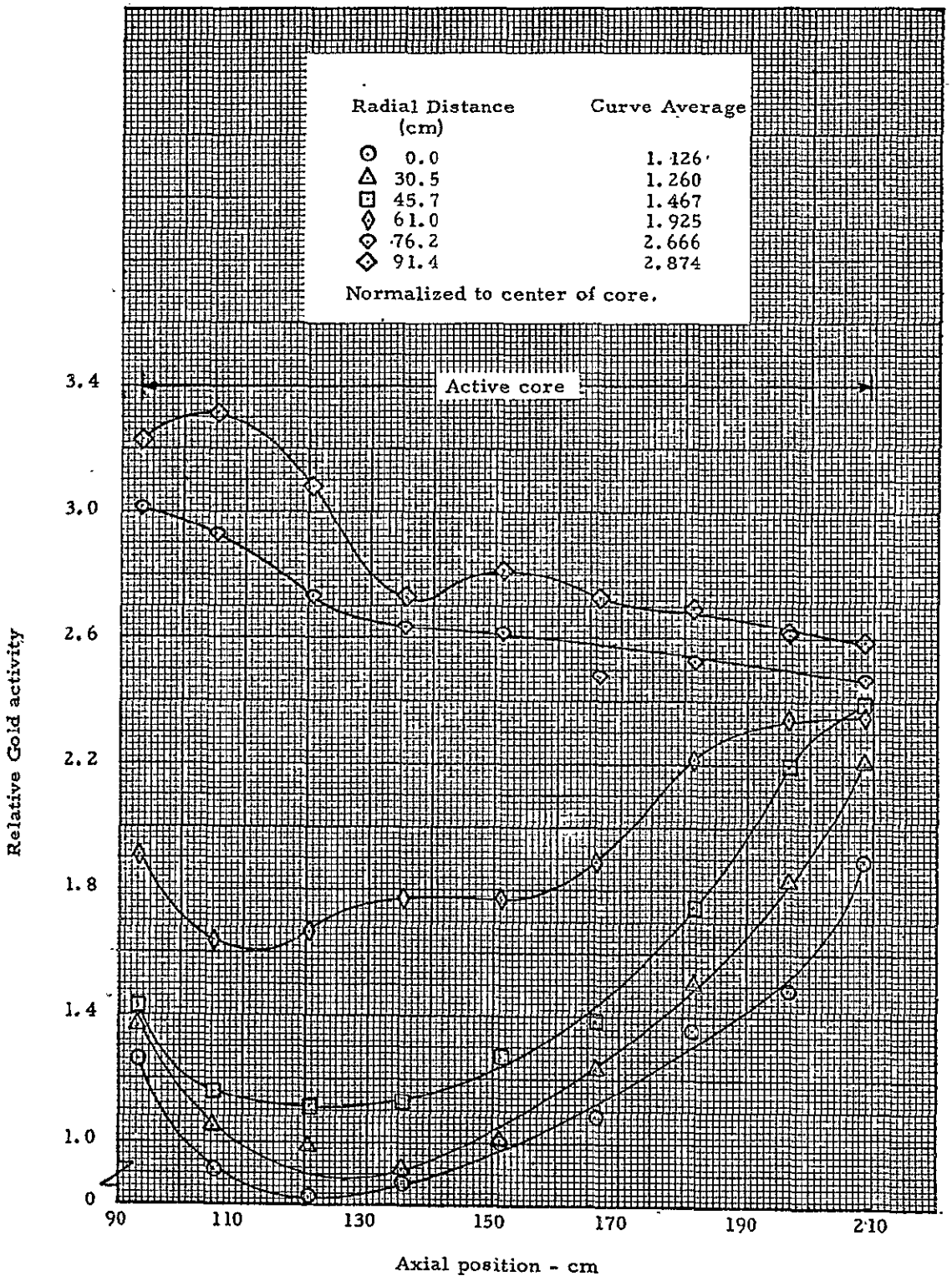

Fig. 8.7 Relative axial distribution of bare gold foil activities in the cavity region with the exhaust nozzle tank removed.

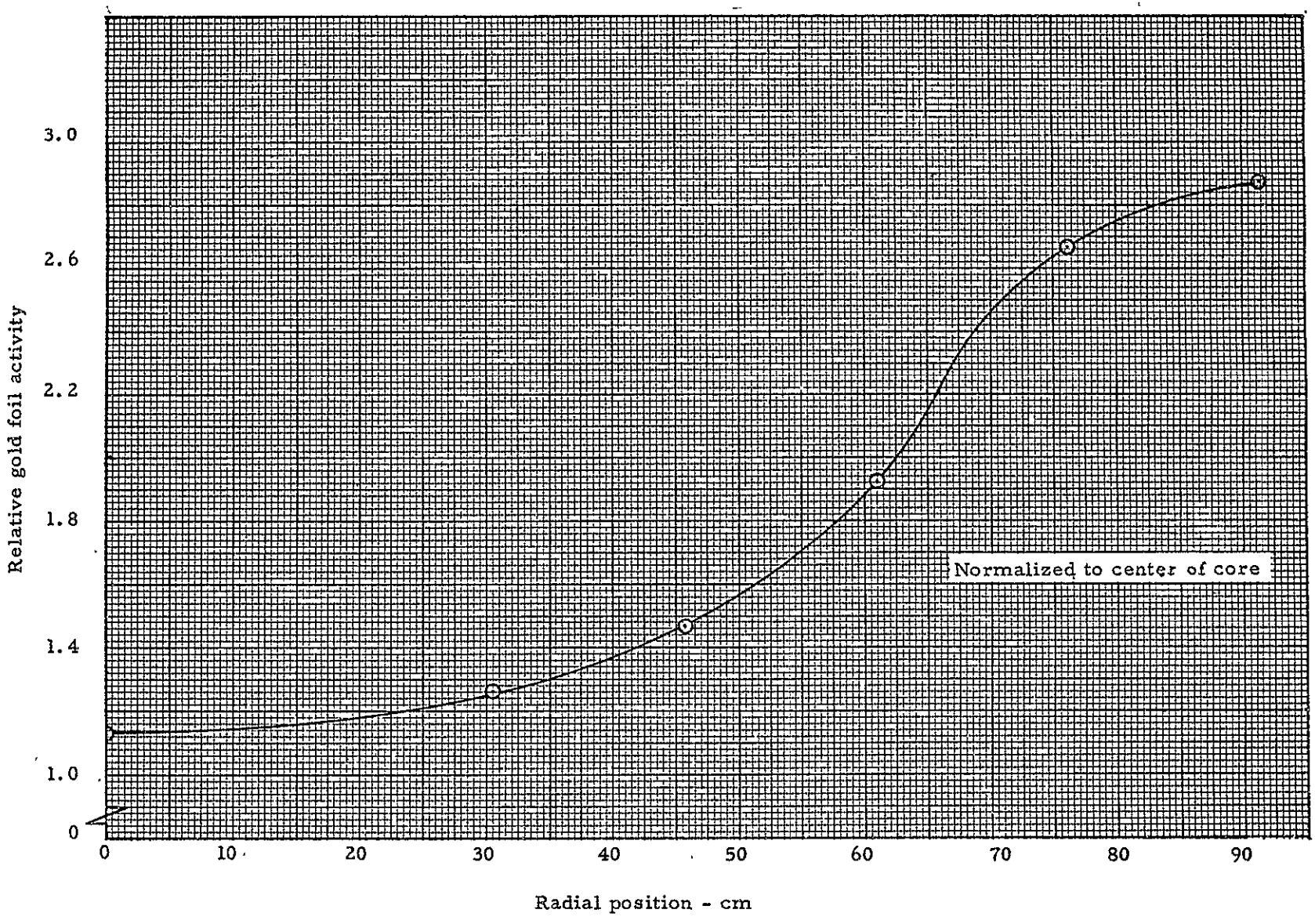

Fig. 8.8 Relative radial distribution of gold foil activity within the cavity region with the exhaust nozzle tank removed

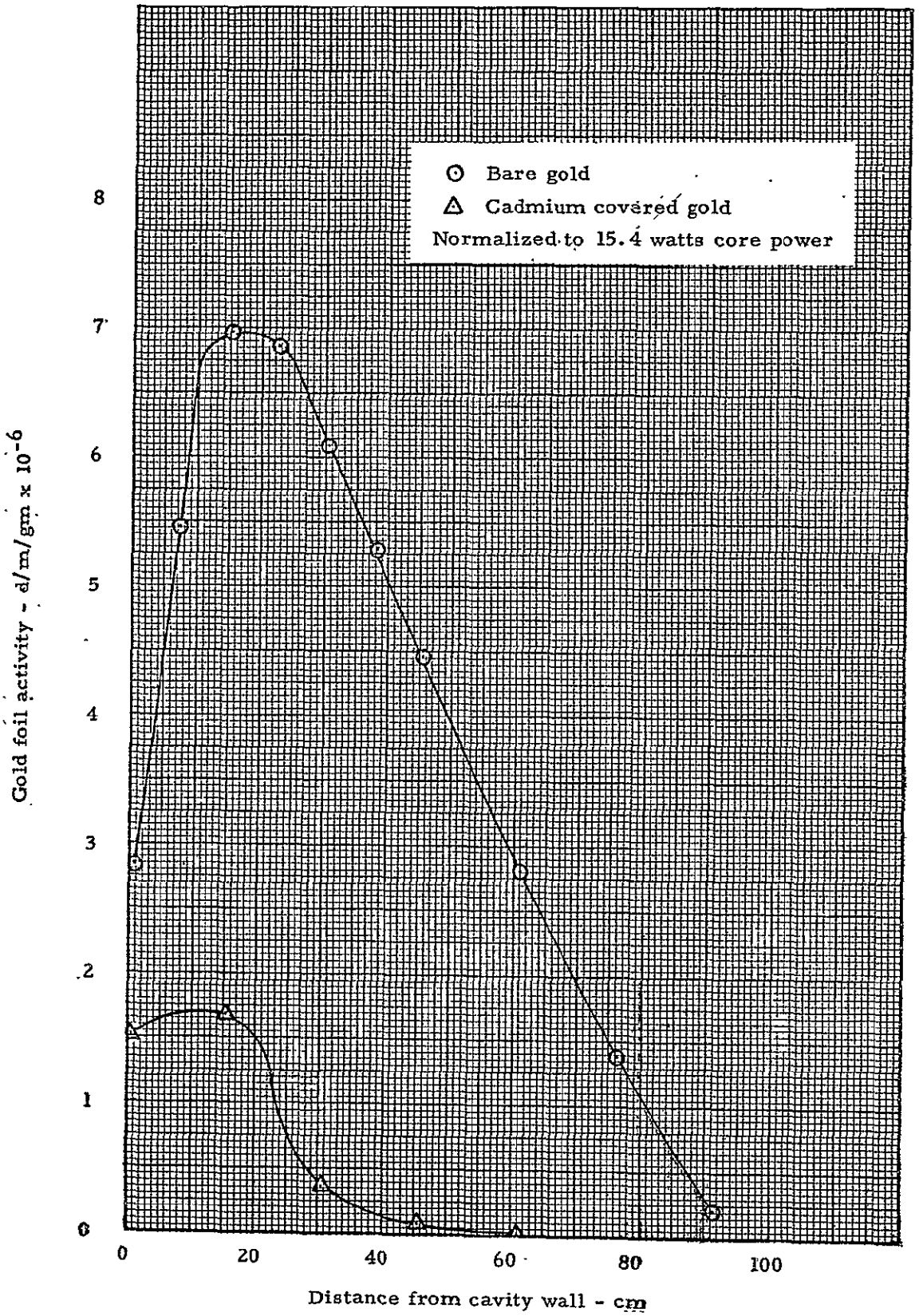

Fig. 8.9 Gold foil activity distribution in the end reflector with the exhaust nozzle tank removed

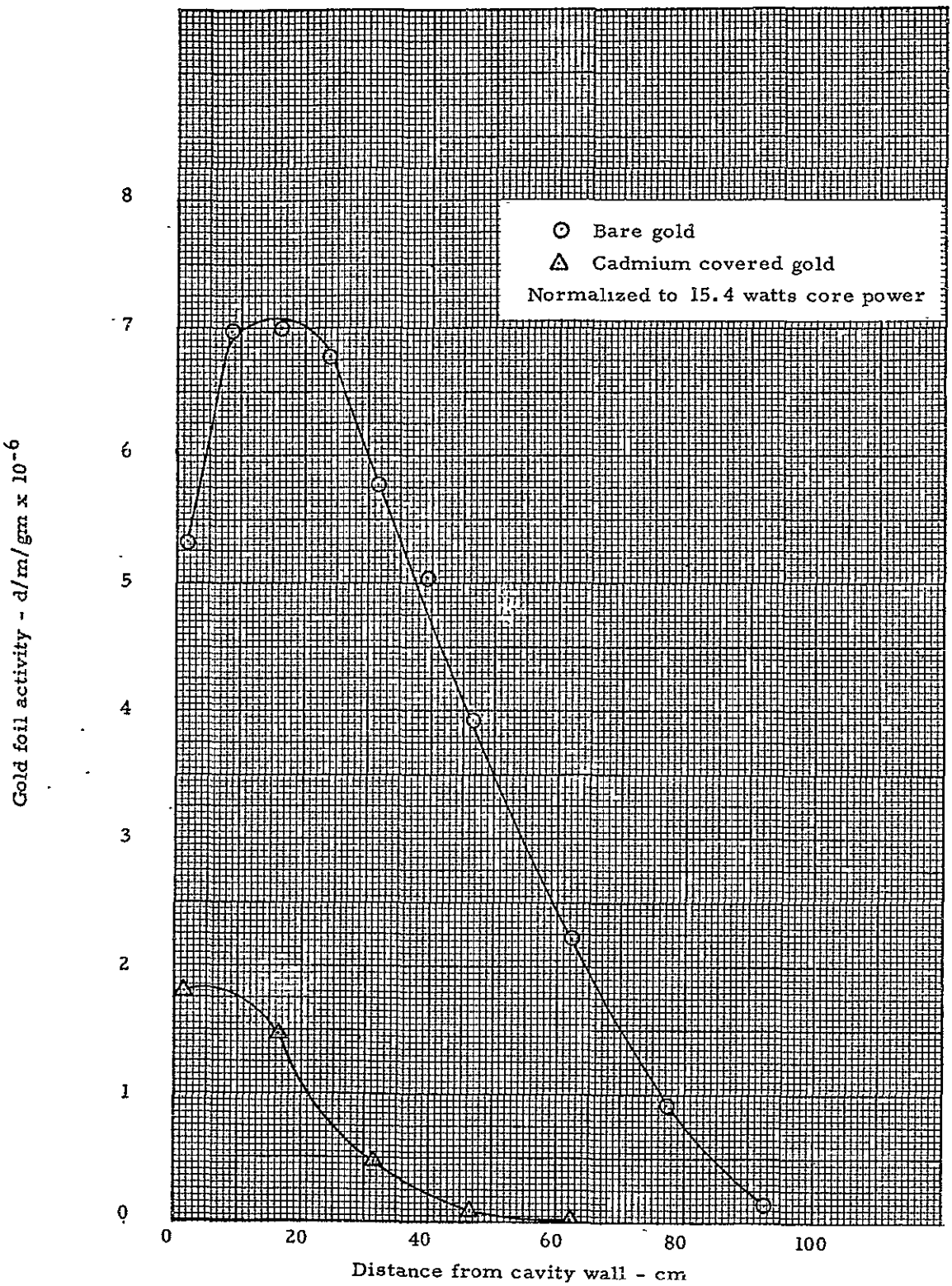

Fig. 8.10 Gold foil activity distribution in the radial reflector with the exhaust nozzle tank removed

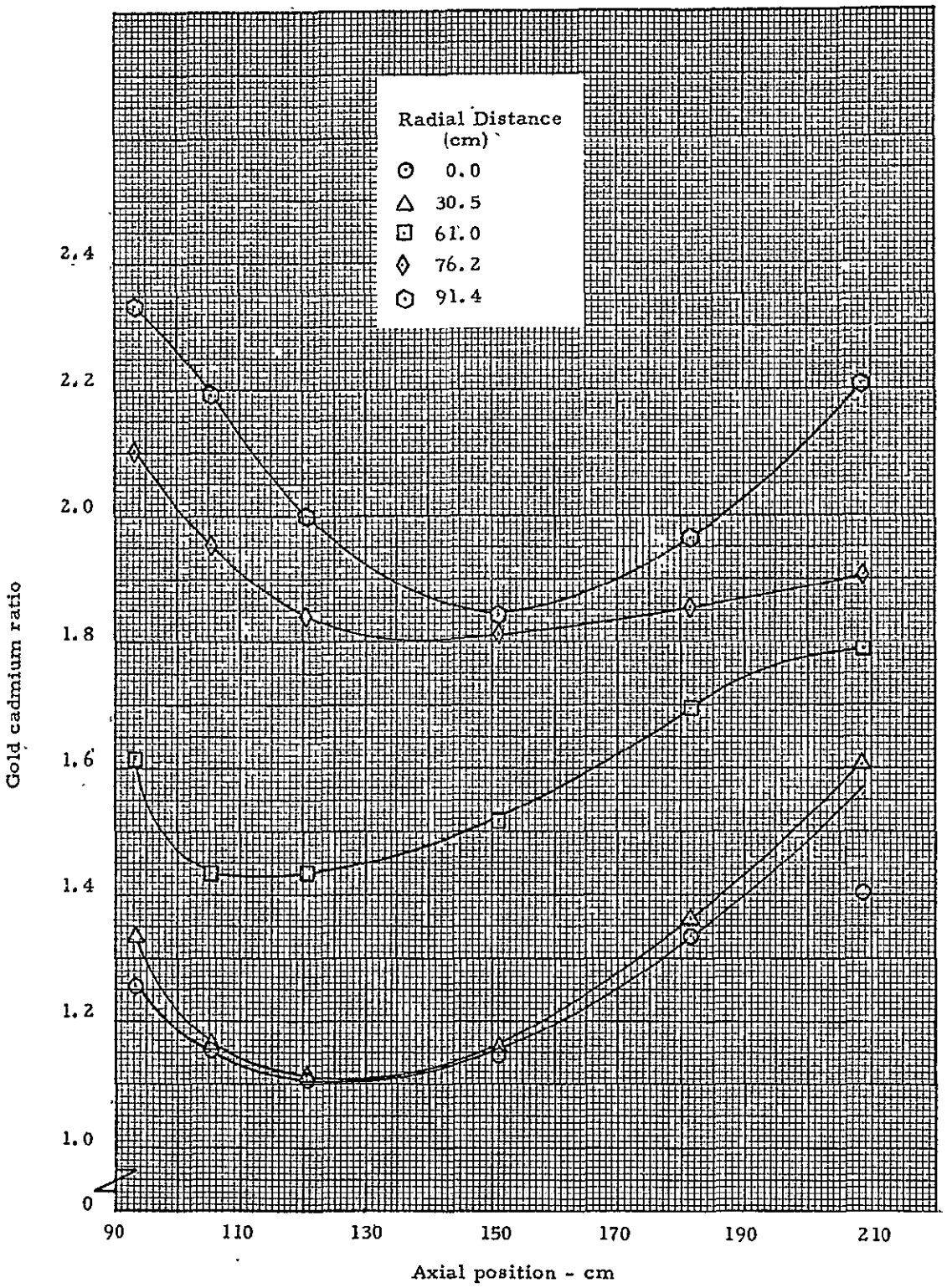

Fig. 8.11 Gold foil cadmium ratios in the cavity region with the exhaust nozzle tank removed

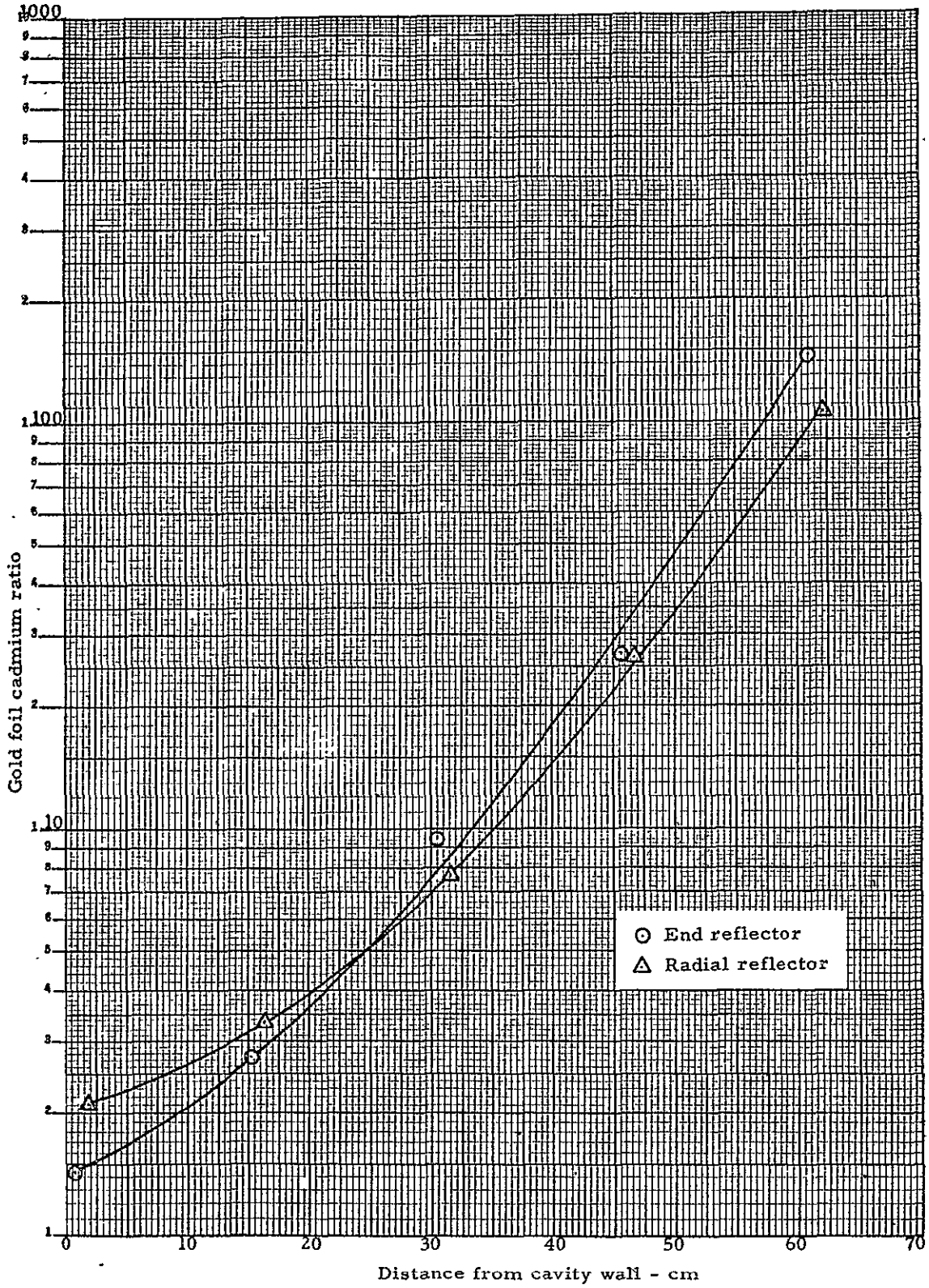

Fig. 8.12 Gold foil cadmium ratios in the reflector regions with the exhaust nozzle tank removed

9.0 THERMAL NEUTRON FLUX

9.1 Exhaust Nozzle in Reactor

Where both bare and cadmium covered gold foil data were available it was possible to calculate thermal neutron flux from the known gold cross section of 98.8 barns. The procedure used is outlined in Reference 4, p. 69 Table 9.1 gives the results of these calculations. The flux distribution within the cavity is shown in Figure 9.1. The fuel zones are 29.2 cm long beginning at an axial position of 92.6 cm from the reference point (the inner surface of the outer reflector containment tank). Therefore, the minimum flux near the radial center of the core occurs near the point where Zone 1 and Zone 2 meet.

The heavy hydrogen density over Region 1 clearly caused flux peaking over that portion of the cavity in the area between the active core and cavity wall. This is due to the flux trapping effect of the hydrogen, which tends to block the neutrons from entering the active core as they come from the reflector and scatters them back into the reflector. The neutron density is also enhanced at the ends of the reactor because of the neutrons coming from both end and radial reflectors which do not pass through the fueled region of the core.

The thermal neutron flux levels in the reflector regions are shown in Figures 9.2 and 9.3. Included in these plots are the radial and axial data through the core. Both curves show the peak to occur in the D_2O about 20 cm from the cavity wall and the flux distribution in the reflectors is similar to that in previous configurations (except for the first point on the radial reflector (Figure 9.2) which appears to be too high).

9.2 Exhaust Nozzle Tank Removed and Fuel Loading Increased

Table 9.2 gives the thermal neutron flux values which were calculated from the gold foil data after the exhaust nozzle tank was removed and the uranium was added to Zones 2A and 3. The data are plotted in Figures 9.4 to 9.6. These results were compared with the earlier data with the nozzle tank in the reactor and it was found that, on the average, there was a 17 ± 7% decrease in thermal flux in the reflector regions. This, of course, is consistent with the results of the bare foil data and cadmium ratios discussed earlier in this report. The axial traverse down the radial center of the core experienced a 30 ± 8% decrease in thermal flux which is attributed to the increased fuel loading in Zones 2A and 3. The thermal flux levels in the other portions of the cavity where measurements were made showed little or no measurable changes within ±5%.

TABLE 9.1

Thermal Neutron Flux

Mockup of Gas Flowing Reactor

Exhaust Nozzle Tank in the Reactor

Location Radial (cm)	Axial (cm)	Thermal Neutron Flux $n/cm^2/sec/watt$
0	93.3	0.705
0	105.3	0.447
0	120.6	0.308
0	151.1	0.380
0	181.6	0.914
0	208.8	1.633
30.5	93.3	0.976
30.5	105.3	0.323
30.5	120.6	0.219
30.5	151.1	0.426
30.5	181.6	1.099
30.5	208.8	1.899
61.0	93.3	1.361
61.0	105.3	1.279
61.0	120.6	1.059
61.0	151.1	1.427
61.0	181.6	1.793
61.0	208.8	2.155
76.2	93.3	3.340
76.2	105.3	2.895
76.2	120.6	2.508
76.2	151.1	2.532
76.2	181.6	2.590
76.2	208.8	2.390
91.4	93.3	3.842
91.4	105.3	3.479
91.4	120.6	2.778
91.4	151.1	2.731
91.4	181.6	2.659
91.4	208.8	2.544
0	89.4	1.579
0	74.9	6.698
0	59.6	7.024
0	44.4	4.993
0	29.1	3.063
93.2	151.1	5.120
107.7	151.1	6.860
123.0	151.1	6.218
138.2	151.1	4.421
153.5	151.1	2.596

TABLE 9.2.

Thermal Neutron Flux

Mockup of Flowing Gas Reactor

Exhaust Nozzle Tank Removed from Reactor

Location		
Radial (cm)	Axial (cm)	Thermal Neutron Flux $n/cm^2/sec/watt$
0	93.3	0.618
0	105.3	0.324
0	120.6	0.214
0	151.1	0.322
0	181.6	0.789
0	208.8	1.266
30.5	93.3	0.820
30.5	105.3	0.364
30.5	120.6	0.253
30.5	151.1	0.363
30.5	181.6	0.917
30.5	208.8	1.737
61.0	93.3	1.618
61.0	105.3	1.142
61.0	120.6	1.138
61.0	151.1	1.380
61.0	181.6	1.892
61.0	208.8	2.152
76.2	93.3	3.165
76.2	105.3	2.930
76.2	120.6	2.553
76.2	151.1	2.416
76.2	181.6	2.432
76.2	208.8	2.448
91.4	93.3	3.616
91.4	105.3	3.573
91.4	120.6	3.099
91.4	151.1	2.621
91.4	181.6	2.716
91.4	208.8	2.782
0	89.4	1.187
0	74.9	5.197
0	59.6	5.735
0	44.4	4.402
0	29.1	2.822
93.2	151.1	3.581
107.7	151.1	5.699
123.0	151.1	5.402
138.2	151.1	3.873
153.5	151.1	2.229

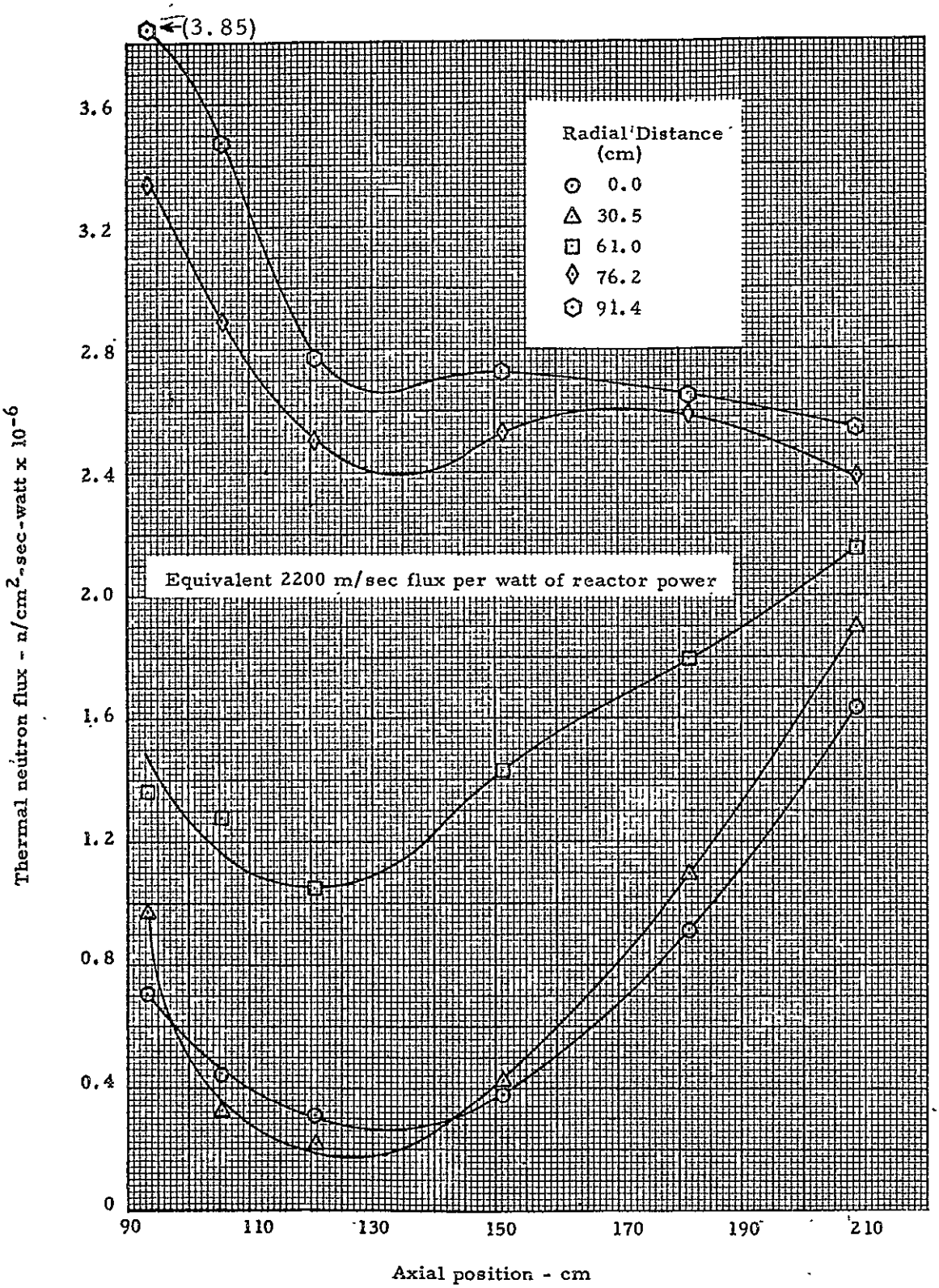

Fig. 9.1 Axial distribution of thermal neutron flux in the cavity region with the exhaust nozzle tank in the reactor.

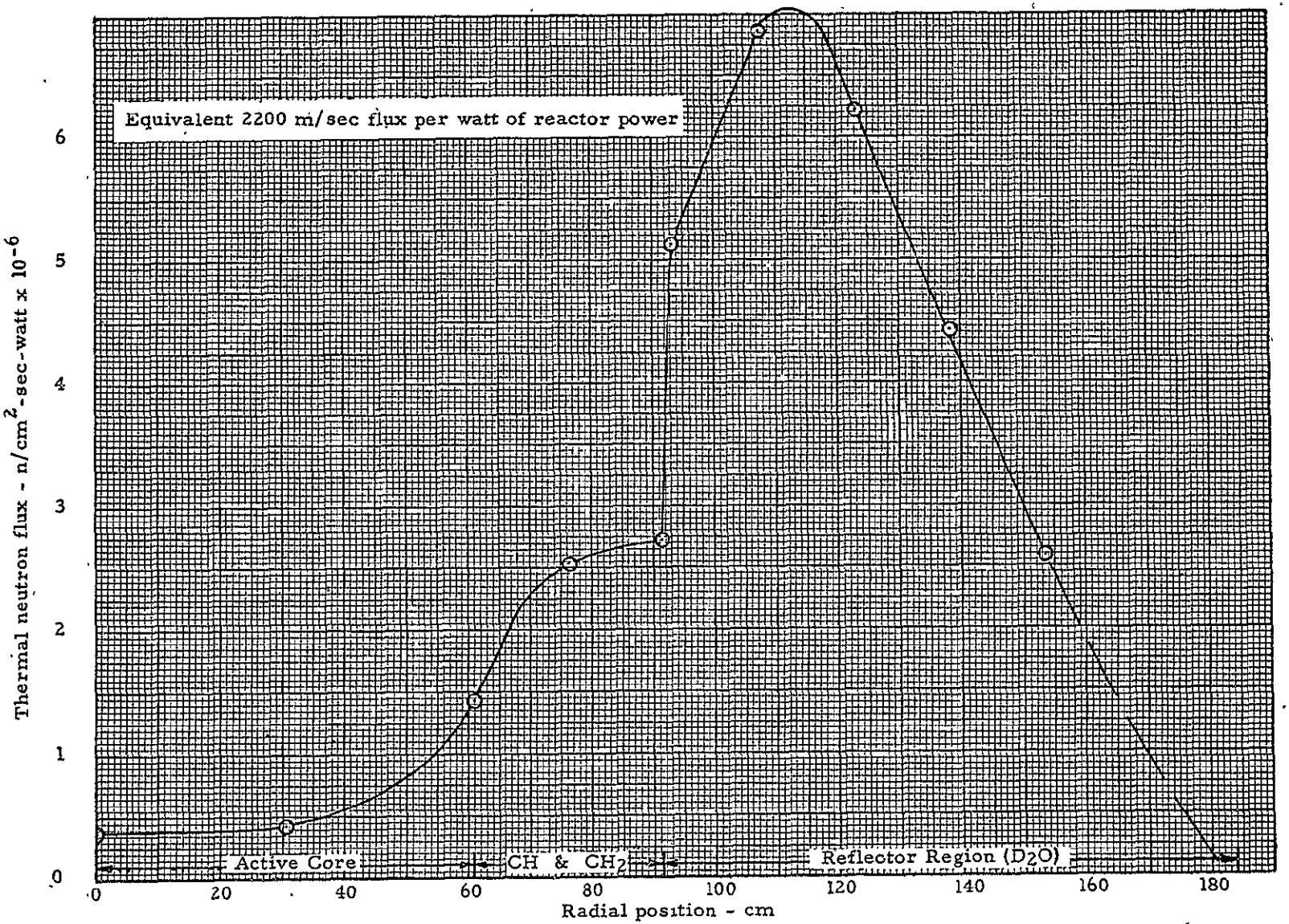

Fig. 9.2 Radial distribution of thermal neutron flux at the axial centerline with the exhaust nozzle tank in the reactor.

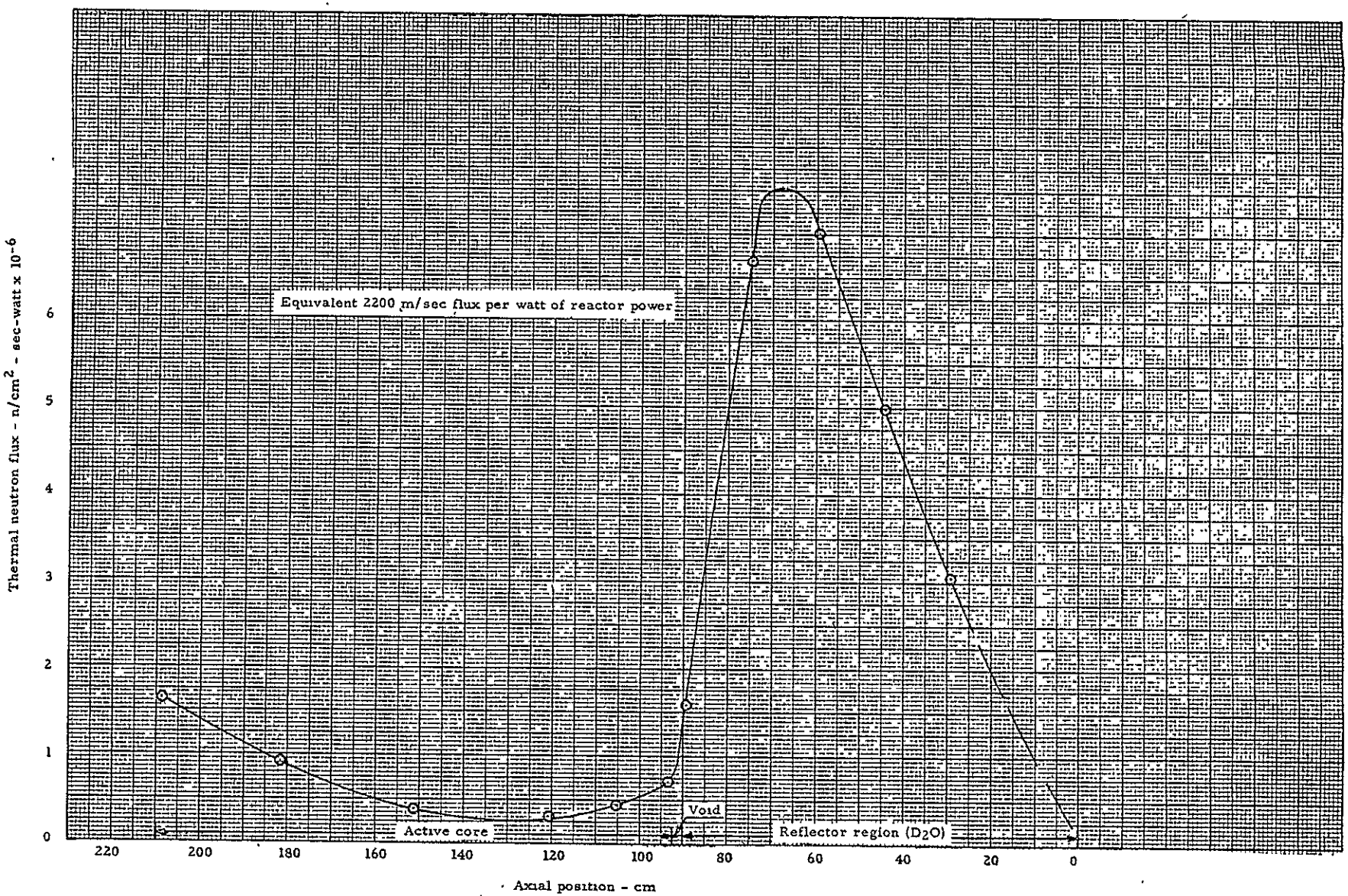

Fig. 9.3 Axial distribution of thermal neutron flux at the radial centerline with the exhaust nozzle tank in the reactor.

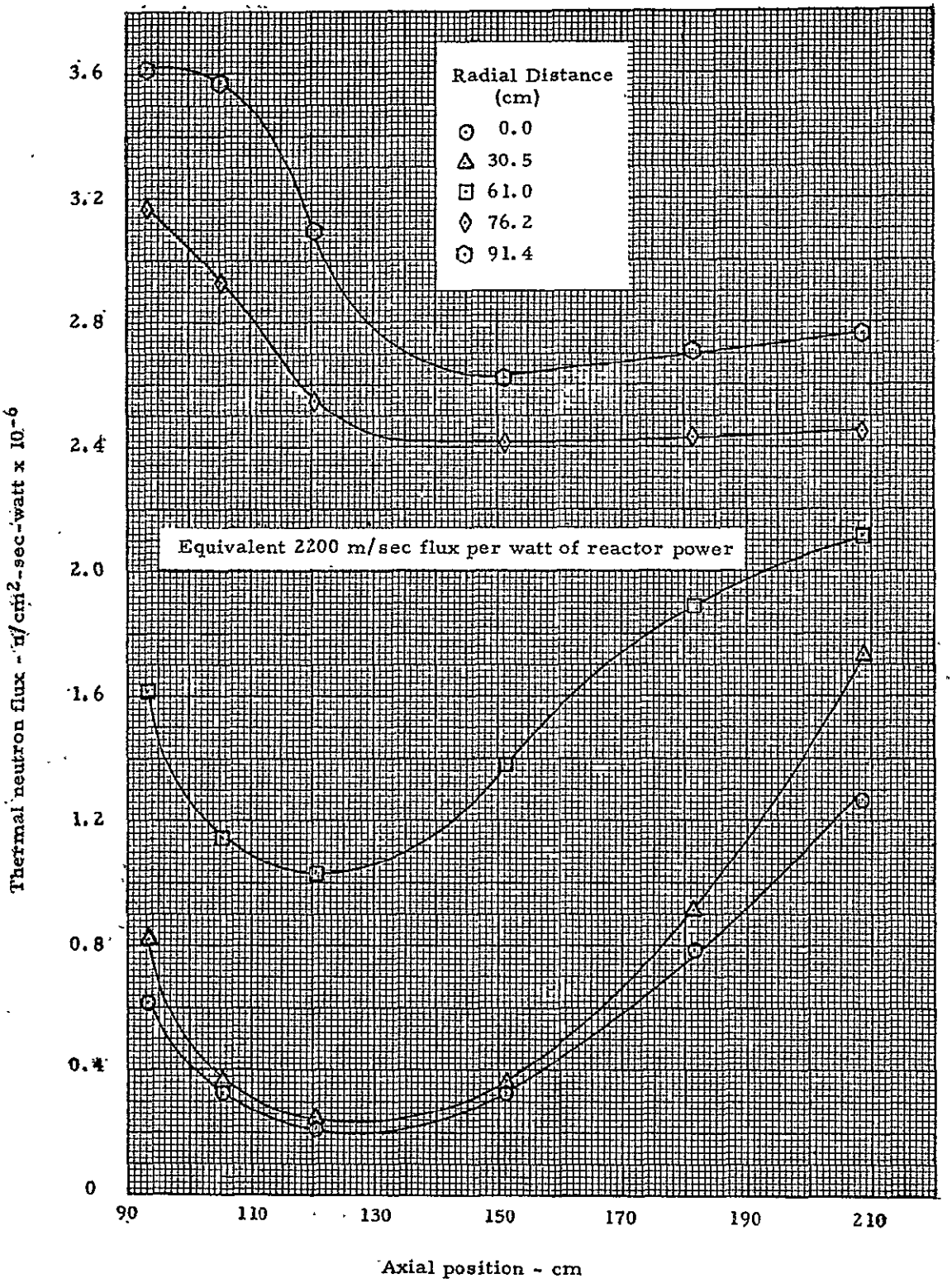

Fig. 9.4 Axial distribution of thermal neutron flux in the cavity region with the exhaust nozzle tank removed.

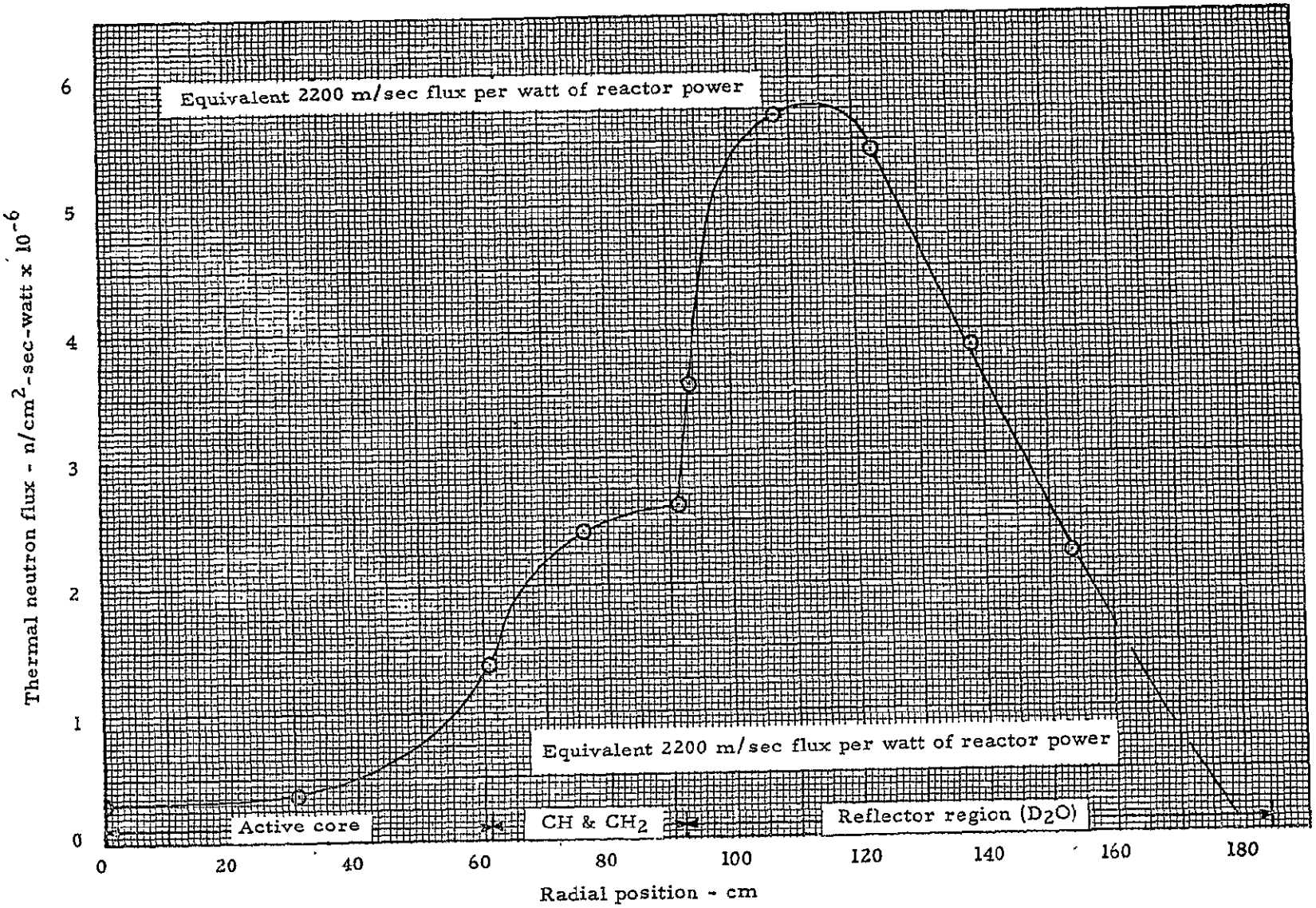

Fig. 9.5 Radial distribution of thermal neutron flux at the axial centerline with the exhaust nozzle tank removed.

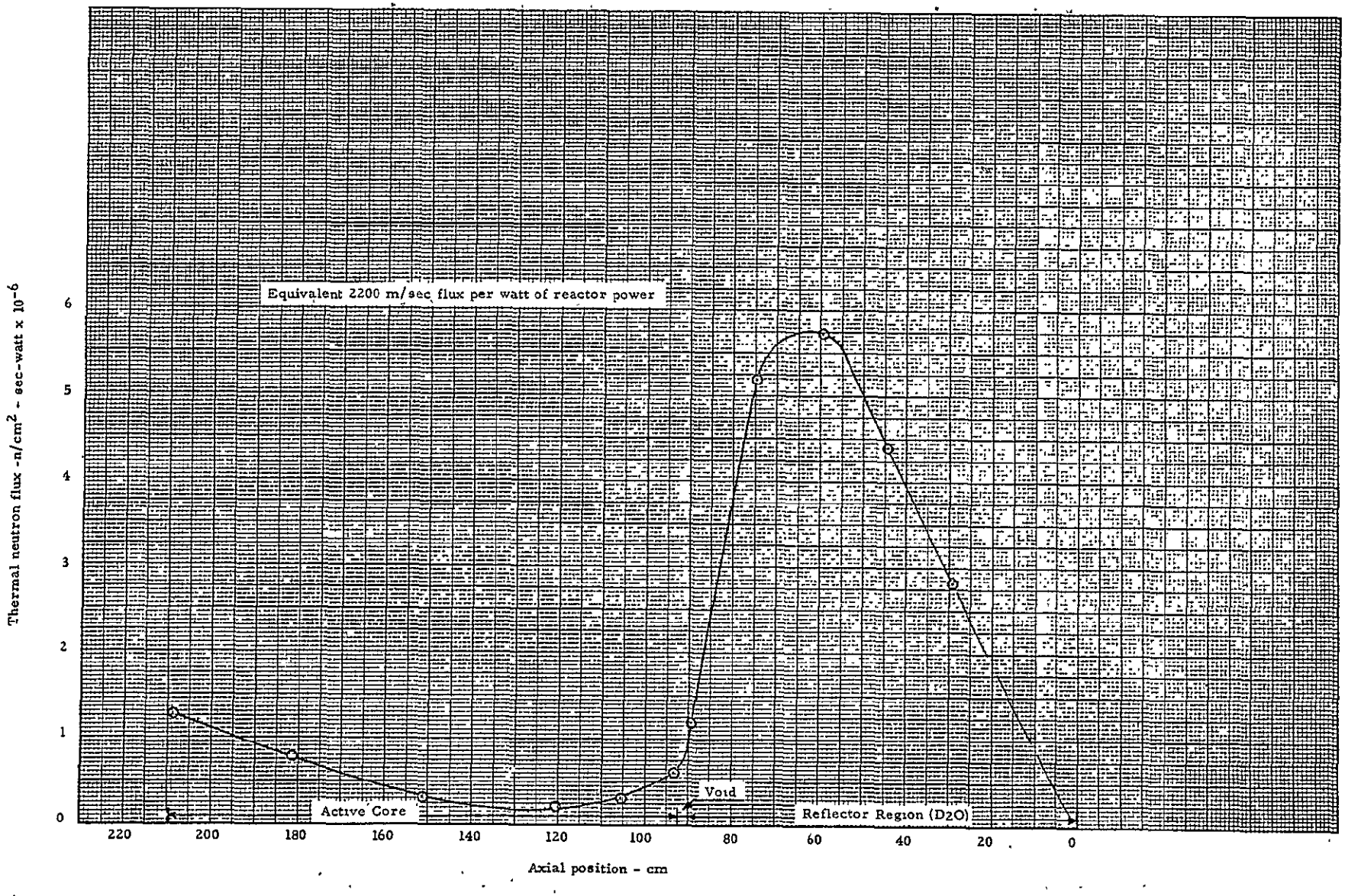

Fig. 9.6 Axial distribution of thermal neutron flux at the radial centerline with the exhaust nozzle tank removed.

10.0 CONCLUSIONS AND RECOMMENDATIONS

10.1 Critical Mass

In estimating the critical mass of the reactor, large extrapolations were made of experimental data from the uniformally loaded core to arrive at a loading for the core with both variable loading and a variable radius. Results showed an underestimation of the critical mass by about 13%. The error was due to uncertain fuel worths and uncertain effects of the reduced fuel radii in Zones 3 and 4. The core multiplication with the original core configuration (prior to modifications to Zones 3A and 4A) was 0.94 with a core loading of 40 kg of uranium. The effective core volume was 9.84×10^5 cm^3. Extending Zone 4A as shown in Figure 10.1, increased the fuel loading by 0.59 kg. The multiplication was then 0.95, as a result of this increase in fuel mass and effective core volume of 0.346×10^5 cm^3 (a 3.5% increase). The extension to Zone 3A, which added 4.34 kg of uranium, increased the multiplication to 0.99. There was an accompanying increase of 1.37×10^5 cm^3 (a 14% increase) in effective core volume.

The core was ultimately made critical by adjustments in the hydrogen loading. Despite the initial 13% error in estimated critical mass, the adjustments to achieve criticality were not unduly time consuming. Two dimensional computer calculations (using either diffusion theory or transport theory) were not within the scope of this work. Previous computer work on more uniform configurations was either relatively inaccurate (using few group diffusion theory) or extremely expensive (using multi-group transport theory).[5]

10.2 Power and Flux Distribution

The power distribution in the active core region generally showed small and insignificant changes due to removal of the exhaust nozzle except in the region of the nozzle where there was an overall increase in power. It had been observed in earlier experiments (Reference 4, p. 185), that removing the nozzle caused an increase in the radial power distribution near the separation plane in the region of the nozzle. This, however, was not observed in the present experiment as will be noted from Figure 10.2 and 10.3. Over the fueled portion of the end of the core next to the exhaust nozzle there was very little change in relative power distribution (though the net power was higher) with the nozzle removed on the variable loaded core. Beyond the active core (through the hydrogen region) there were major changes in relative flux distribution such that near the outer radius the specific power was the same. (Note, specific power distribution is meaningful only as a flux indicator since no fuel was present beyond 15 cm).

There was an inward streaming of thermal neutrons from the nozzle with the end plug removed, as the power over Zone 4 increased 24%. The fact that the fuel radius in Zone 4 at the separation plane was only 15 cm and the nozzle radius was also 15 cm could account for the unchanged shape of the power distribution out to about 35 cm for the variable core at the separation plane. On the uniform core without a cavity liner, the fueled radius was 61 cm and the space between the active core and the cavity wall was

void whereas this region in the variable core contained dilute hydrogen. The stainless steel liner was only 0.04 mean free absorption paths thick and hence had only a small effect on the flux with and without the exhaust nozzle tank in the reactor, but it appears that the relatively flat power distribution was a result of the small fuel radius and the dilute density. For this reason the characteristic hump observed in the previous experiments did not occur though the overall power density in the region was 24% higher with the nozzle plug removed.

After removing the exhaust nozzle, the core loading was also modified by adding 456 grams of uranium to Zone 3 and 891 grams to a portion of Zone 2A. This increased the fuel density 20% in Zone 3 and 22% in Zone 2A where the fuel was added. Power distribution comparisons before and after these changes showed the overall volume weighted average power per unit fuel mass to be 2.2% higher in Zones 2 and 2A and 3.3% lower in Zones 3 and 3A after making the changes. These are small changes and very close to the normal standard error for this type of measurement. If it is assumed that the exhaust nozzle had little effect on Zones 2, 2A, 3, and 3A, then it could be concluded that the change in fuel loading was of minor consequence as far as power distribution in the reactor is concerned. Thus movement of fuel within the active core region due to minor temperature and pressure changes will not cause large redistribution of power in the cavity reactor.

The hydrogen surrounding the active core region and acting as a coolant is a flux trap which not only absorbs neutrons but reflects them back into the D_2O. Figure 10.4 shows the flux distribution across the hydrogen in the heavy and light hydrogen density regions with the exhaust nozzle tank in the reactor. The high density region shows a much higher thermal flux at the cavity wall (91.4 cm radius) next to the D_2O than does the low density region. This relationship, however, reverses as the active core boundary is approached. Thus the power in the front or inlet end of the core will be suppressed where the hydrogen density is the highest.

10.3 Reactivity Effects

The core average worth of fuel was $0.250 \pm 0.017\% \Delta k/kg$ with 44.9 kg of uranium in the reactor. Earlier measurements on uniformly loaded cores yielded a fuel worth (interpolated to this loading) of about $0.31\% \Delta k/kg$. (Reference 3, p. 50). This difference is consistent with the error that occurred in estimating the critical mass, where it was assumed that fuel would be worth more than it was measured to be. The value of $\Delta k/k/\Delta m/m$ was 0.112 for this core.

The reactivity worths of polyethylene (CH_2) and polystyrene (CH), which were used to simulate hydrogen, were measured in Regions 5 and 6 where the hydrogen density was low (0.15×10^{21} atoms/cc). The hydrogen worth in the two materials was the same after subtracting off the worth of carbon. Previous measurements of this kind (Reference 2, p. 88) showed the hydrogen in CH to be worth 34% more than in CH_2. That difference was thought to be due to molecular binding effects. The close correlation on this experiment, however, shows a need for further investigation, even

though the density of materials involved in the two sets of measurements were substantially different (2×10^{21} H/cc when "molecular binding" effects were detected, and 0.15×10^{21} H/cc in this experiment).

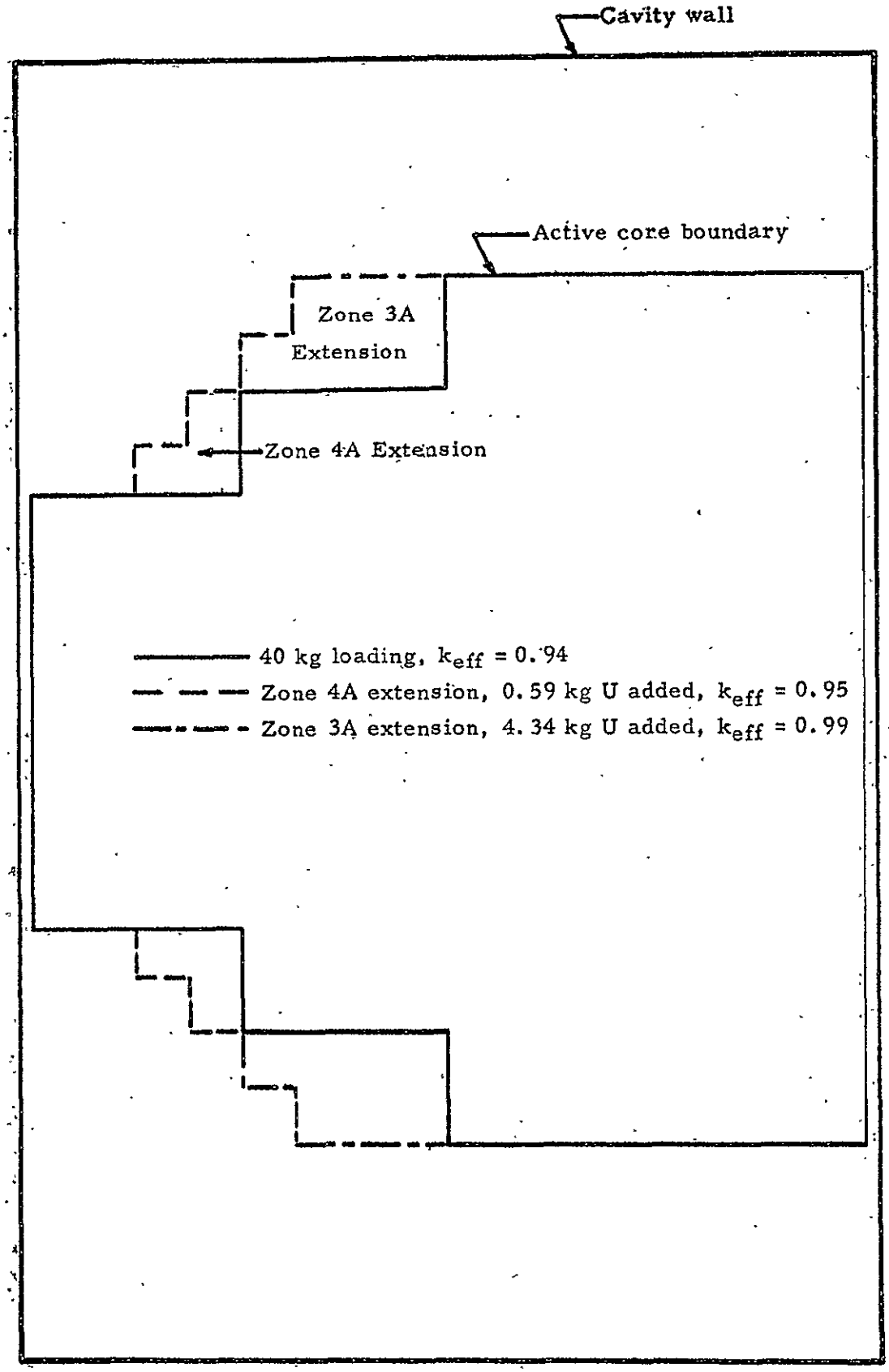

Fig. 10.1 Schematic layout of cavity region showing the base core and the extensions.

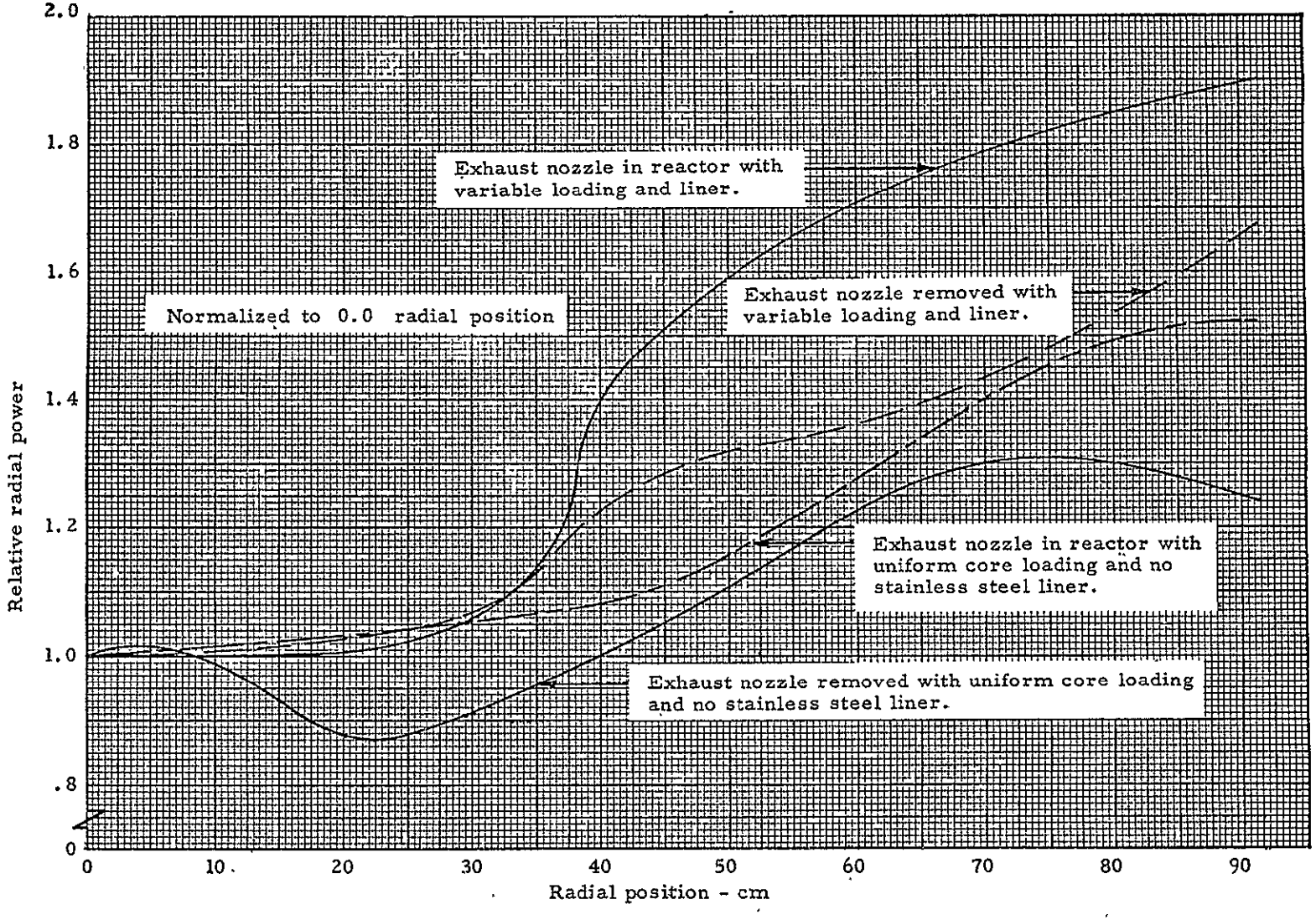

Fig. 10.2 Comparison of relative radial power distribution at the separation plane for the variable and uniform fuel loaded cores with and without the exhaust nozzle tank in the reactor.

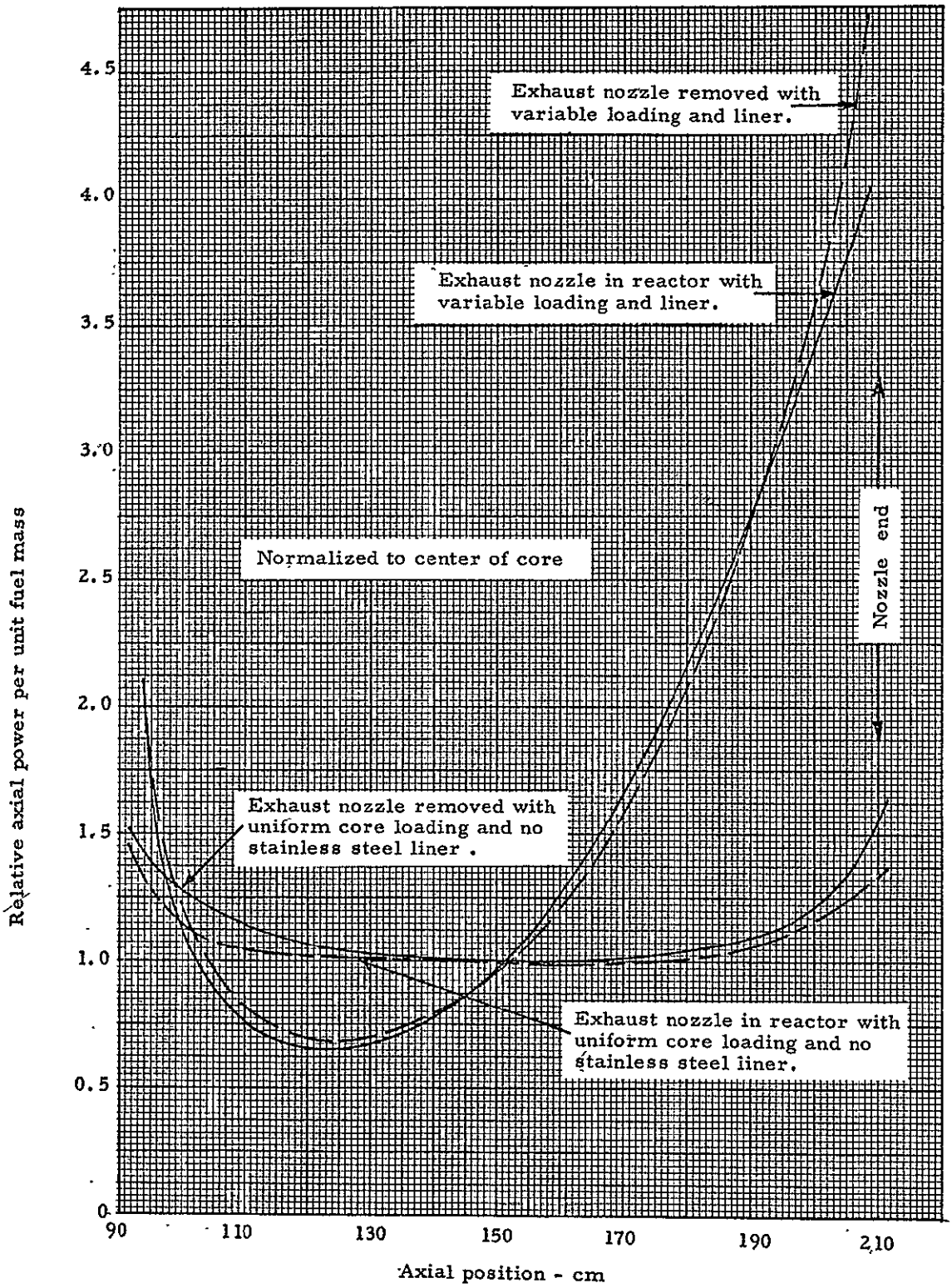

Fig. 10.3 Comparison of longitudinal (axial) power distributions showing effect of the end plug.

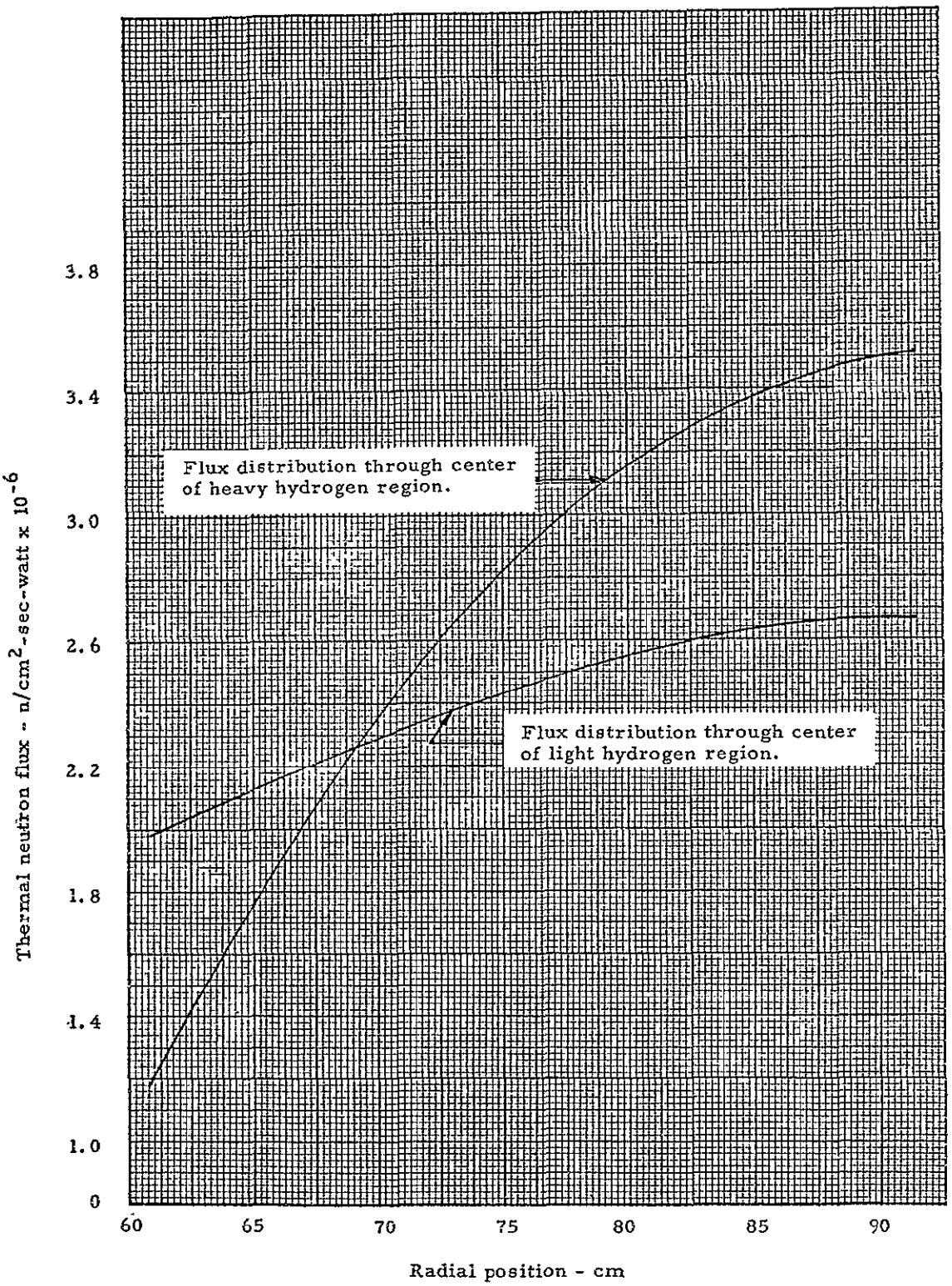

Fig. 10,4 Thermal neutron flux distribution through the hydrogen regions with the exhaust nozzle plug in the reactor.

REFERENCES

1. Pincock, G. D., Kunze, J. F., "Cavity Reactor Critical Experiment, Volume IV," General Electric Company, NSP-ITS, May 1969, (NASA CR-72550).

2. Pincock, G. D., Kunze, J. F., "Cavity Reactor Critical Experiment, Volume III," General Electric Company, NSP-ITS September 1968, (NASA-CR-72384).

3. Pincock, G. D., Kunze, J. F., "Cavity Reactor Critical Experiment, Volume II," General Electric Company, NSP-ITS, May 31, 1968, (NASA CR-72415).

4. Pincock, G. D., Kunze, J. F., "Cavity Reactor Critical Experiment, Volume I," General Electric Company, NMPO-ITS, September 6, 1967, (NASA CR-72234).

5. Henderson, W. B., Kunze, J. F., "Analysis of Cavity Reactor Experiments," NASA CR-72484 (January 1969).

INDEX

INDEX
(Cont'd)